Higher order corrections for precision observables

Thesis submitted in accordance with the requirements of
the University of Liverpool for the degree of Doctor in Philosophy
by

Maria Cerdà Sevilla

October 12, 2017

Declaration

I hereby declare that all work described in this thesis is the result of my own research unless reference to others is given. None of this material has previously been submitted to this or any other university. All work was carried out in the Theoretical Physics Division of the Department of Mathematical Sciences, University of Liverpool, UK, during the period of September 2013 until August 2017.

Author's note: This is a slightly updated version than that which was submitted to the University of Liverpool. Typos have been corrected, references have been added, and a few passages have been lightly edited.

Publication list

This thesis contains material that has appeared in the following publications by the author:

(1) **"Higher order effects in ε'/ε"**
M. Cerdá-Sevilla.
DOI:10.1088/1742-6596/770/1/012027
J. Phys. Conf. Ser. **770**, no. 1, 012027 (2016).

(2) **"Towards NNLO accuracy for ε'/ε"**
M. Cerdá-Sevilla, M. Gorbahn, S. Jäger and A. Kokulu.
arXiv:1611.08276 [hep-ph]
DOI:10.1088/1742-6596/800/1/012008
J. Phys. Conf. Ser. **800**, no. 1, 012008 (2017).

With love to my family,
"Una piña de cuatro piñones".

Abstract

Higher order corrections are a fundamental ingredient for the analysis of physical observables. They are essential to improve the precision of theory predictions within the Standard Model which then lead to an increased sensitivity of these observables to physics beyond the Standard Model. In this thesis we compute higher order QCD corrections to the effective Lagrangian for weak decays. We combine previous results for the Next-to-Next-to-Leading order in the five-flavour theory with new matching calculations. This allows us to determine the effective Lagrangian in the four- and in the three-flavour theory for current-current and QCD penguin operators. We discuss explicitly the relevant steps required for a proper matching calculation, in particular the cancellation of the ultra-violet and infra-red divergences. We also introduce a new formalism that leads to scale and scheme independent intermediate results. Moreover the scheme change for the electroweak penguin operators at the Next-to-Leading order is calculated, and the one-loop and two-loop anomalous dimensions for a general number of flavours in the modern basis is presented for the first time in this thesis. In addition we present an updated QCD×QED running. Here a detailed discussion is provided to explain the problem with the singularities when the eigenvalues of the anomalous dimension matrix differ by a factor $2\beta^s_{00}$. Finally we apply the result to the theory prediction of the CP-conserving hadronic kaon decays, and the ε'/ε observable, reducing the perturbative uncertainty by a factor 0.12 at NNLO level.

Acknowledgements

I would first like to thank the most important people in my life: Mum, Dad and Rita for their constant support and encouragement, for their patience and understanding, for their unconditional love, for that beautiful melody we have created together, which describes all those smiles, hugs, and special shared moments."*Per totes les experiències compartides, per donar-li sentit a la meva vida, per no deixar-me caure mai, us estime moltissim. Ho sou tot per mi*. A deep thanks goes to my three angels who are not here anymore, but will be always in my heart. Thanks also Nan for waiting long periods until being able to hug me again. I would also like to thanks my aunts, uncles, cousins and Sergio for caring about me. I love you and I am very lucky to have such a very nice family who is always next to me.

A big thank you goes to my best friend Paulina, for her constant support and marvellous friendship. No matter how far apart we are we always find a way to stay close to each other. I have enjoyed every second of the last ten years. Thank you for being such a very nice person and friend. I am very lucky to have met you. A special thanks also goes to Lotfi, Justo and Silva for their meaningful friendships. Thank you guys for your constant patience and for understanding those periods when I needed to disappear. I would also like to thank my friend Cristina for those talks and shared moments since we met ten years ago on the flight to the UK, and to Juan whom I miss very much. Thanks to Alessandro, Eduardo and Umberto for helping me to keep some perspective and for being very kind to me, and thanks to Andrea for his help with the preparation of my talk for the BEACH conference. I will never forget what you did for me.

Moreover, I would particularly like to thank all my friends that do not work in this field for all those moments we have spent together and that gave me strength to carry on with my dream, especially to Alba, Maria, Laura, Pilar, Antonio, Yoana and Soraya who were always there when I needed them, and to Andrea for those hugs and conversations. I am going to miss all of you.

Thanks to all the staff in the TP department at the University of Liverpool for making my time there particularly enjoyable. This is something I will keep for ever in my memories. Especially to my three favourite boys: Paul, Josh and Dave who became very important in my life, and who always did their best to make me laugh. Thanks for your support, for those Spanish hugs you learnt to give to make me feel close to

home, and of course thanks for all your help.

I would also like to thank Sebastian Jäger for those passionate discussions about our project and for those laughs. My sincere thanks also goes to Andrzej Buras who provided me an opportunity to disentangle this amazing field of Flavour physics, and to Christoph Bobeth for that time shared in Munich this summer.

Thanks to those new people in Munich who have started sharing their lives with me. Particularly those who have been supporting me in this last stressful period. Thanks for reminding me that Munich will be a very lovely destination.

But, the biggest thanks of all goes to my patient supervisor, Martin Gorbahn, who gave me the opportunity to understand Flavour physics. He has been a constant source of knowledge and inspiration to me. Thank you for being always there. I cannot even count how many times you have been beside to me, particularly in those moments when I was a bit lost inside my own loop. For all of these things I will be forever grateful to you. It has been a pleasure to have shared this wonderful experience with you.

Contents

Chapter 1

Introduction

An apparent quality of humans is their desire to describe the laws of nature by means of formulating theories that could give a fundamental explanation for phenomena which are not well-understood at first sight. This interplay between theory and experiments has allowed us to classify some of the main properties of our Universe, which are epitomized in the famous Standard Model of particle physics (SM) [1–3]. Although it describes, with a very good accuracy, most of the phenomena occurring around us, there are still a number of effects that cannot be explained within this framework. For instance, there is no proper candidate to describe the dynamics of Dark matter and Dark energy, which comprise the largest contribution to the energy of our Universe. Moreover, the nature of neutrino masses has not been clarified yet. In addition, the SM is unable to account for the observed matter-antimatter asymmetry in the Universe, which, in thermal baryogenesis scenarios, requires CP-violation (Sakharov's condition) [4]. Furthermore, the mass spectra hierarchy of quarks and leptons and the hierarchy of their flavour changing interactions are still a mystery to us, and their understanding is one of the most coveted goals in particle physics. These drawbacks of the SM lead to the common thinking that this model is incomplete and that at some higher energy scale it must be embedded into a more fundamental theory, which describes at least part of the unanswered questions.

Several Experiments are currently in operation or will start taking data soon, such as ATLAS, CMS, LHCb, Belle II, NA62, with the aim to search for new physics that could address the shortcomings of the SM. The particle physics activities comprise of two search strategies that probe the "high energy" and the "high intensity" frontiers. The first category involves the search for new particles directly using high energy proton proton collisions at ATLAS and CMS. In the high intensity frontier, many particles such as kaons, pions or B-mesons are produced and their properties are measured with high precision. Even though there has not been a signal of a new particle yet, several intriguing anomalies have been reported in the flavour sector which could imply the presence of new physics. Theoreticians have tried to explain some of these deviations (P_5', R_K, R_K^*, ε'/ε), through several models and, at the moment, the inclusion of a

heavy neutral gauge boson Z', supersymmetric particles or leptoquarks are the leading candidates among those proposed. Even though these tensions are very exciting, as they could imply that we are closer to the discovery of new particles, a more exhaustive analysis is required. There is hope to discover a more fundamental theory with the help of data collected in the high-energy experiments and the theoretical study of rare phenomena. This requires a very precise theoretical and experimental analysis, but it can give an insight into the dynamics beyond energy scales accessible in the "high energy" searches of the LHC. Flavour physics is a very promising area in the searches at the "high intensity" frontier since it provides a particularly good probe of high energy scales and directly addresses some of the open questions.

In this thesis we will focus on a particular precision observable, ε'/ε, which measures direct CP violation in Kaon decays. Recent progress in Lattice QCD [5–7] and subsequent analysis [8] of this ratio resulted in a 2.9σ discrepancy between the Standard Model predictions and experimental data. This inconsistency could have several sources, one of which could be the missing contribution of new particles in the theory predictions. However a reliable SM prediction is essential to disentangle possible new physics (NP) effects from the SM background. Yet the analyses of ε'/ε rely only on Next-to-Leading Order (NLO) accuracy in Renormalization group improved perturbation theory. Possible higher order corrections could significantly alter the theory prediction. This is particularly true for ε'/ε where the NLO corrections have been found to be large. To close this gap we aim to calculate the relevant matching corrections at Next-to-Next-to-Leading Order (NNLO) for this physical quantity and present a more accurate theoretical prediction within the SM. In addition, we will also study the impact of these higher order corrections to the CP conserving hadronic kaon decays. In this thesis we present a complete NNLO analysis of several observables for pure QCD contributions.

This document is organized as follows. Chapter 2 contains the main ideas of Gauge theories and quantum field theory within the path integral formalism. Chapter 3 explains the renormalization of QCD and QED. This part also describes the computation of Feynman integrals within dimensional regularization, and the method used to deal with infra-red divergences. The foundations of effective field theories are contained in Chapter 4. This part is very important since the basis of our calculations are explained in detail. Important concepts like renormalization of effective operators, the decoupling of heavy modes, the resummation of large logarithms, the change of operator basis, or scheme dependence are discussed in detail here. In addition, new results for the change of operator basis of the electroweak operators at NLO are presented. Moreover the anomalous dimension matrix (ADM) for a general number of flavours is also given for the first time in this thesis. The subsequent chapter, Chapter 5, contains our new NNLO results for the decoupling of the charm quark. A new formalism for renormalization group improved perturbation theory is also presented, where the

individual contributions are factorised into scheme and scale invariant quantities. Finally, in Chapter 6 we apply our new results to the phenomenological analysis of the important observable ε'/ε and give a more precise theoretical prediction. Moreover, we discuss the need of a more fundamental derivation for this observable in terms of the charged states, and the inclusion of isospin breaking effects, in particular the important electromagnetic contribution.

Chapter 2

Gauge Theories

One of the most beautiful, fascinating and valuable aspects of physics are the symmetry properties of nature. They facilitate the classification of our current understanding of fundamental interactions but also might provide the building blocks to unravel the secrets of the Universe. They are one of the fundamental keys for the search of the theory of everything, in which all the unsolved mysteries would hopefully be elegantly described. In this Chapter, we will present an important type of quantum field theory, the so-called *Gauge theory*. The SM, which currently gives a very good description of most particle physics data, is constructed according to the principle of local gauge invariance in conjunction with the Higgs mechanism [9–12]. Moreover we will introduce the concept of the quantum effective action, and describe the quantization of Gauge theories within the path integral formalism. While this chapter collects the quantum field theory concepts that are relevant for the later parts of this thesis, we do not aim to provide a complete and rigorous treatment of this subject. More details can be found in [13–15].

2.1 Abelian gauge theories (QED)

Quantum Electrodynamics (QED) is an abelian gauge theory. The simplest version of QED comprises a fermion of charge eQ_ψ and a photon field A_μ. Let us first consider the free fermion theory for the field $\psi(x)$ that is described by the Dirac Lagrangian

$$\mathcal{L}_\psi = \bar{\psi}(x)(i\partial\!\!\!/ - m)\psi(x)\,, \tag{2.1}$$

which is invariant under a global abelian transformation

$$\psi(x) \to \psi'(x) = e^{-ieQ_\psi\theta}\psi(x)\,, \tag{2.2}$$

where $e^{-ieQ_\psi\theta}$ are elements of a $U(1)$ symmetry group. Note that θ is x-independent and has to take the same value at all space-time points. Consequently, the phase of the

field $\psi(x)$ is not measurable, and can be chosen arbitrarily. When local gauge transformations are considered, the situation changes completely. Indeed, the requirement that the theory must be invariant under the phase rotation

$$\psi(x) \to \psi^{'}(x) = e^{-ieQ_{\psi}\theta(x)}\psi(x), \tag{2.3}$$

where the parameter $\theta(x)$ is an arbitrary function of space-time coordinates, leads to the introduction of the covariant derivative defined as

$$\not{D} = \not{\partial} + ieQ_{\psi}\not{A}(x). \tag{2.4}$$

The second term in the equation above compensates for the extra factor induced by the transformations at neighbouring space-time points, which is proportional to $\partial_{\mu}\theta(x)$. In fact $A^{\mu}(x)$ is a new vector field, called a gauge field, which transforms as

$$A^{'}_{\mu}(x) = A_{\mu}(x) + \partial_{\mu}\theta(x). \tag{2.5}$$

Therefore invariance under local abelian transformations leads to an interacting field theory described by the following Lagrangian,

$$\mathcal{L} = \mathcal{L}_{\psi} + \mathcal{L}_{A}. \tag{2.6}$$

Here the fermionic part is given by

$$\mathcal{L}_{\psi} = \bar{\psi}(x)(i\not{D} - m)\psi(x), \tag{2.7}$$

where the partial derivative has been replaced by the covariant term, and the gauge piece contains the dynamics of the gauge field $A_{\mu}(x)$,

$$\mathcal{L}_{A} = -\frac{1}{4}F_{\mu\nu}(x)F^{\mu\nu}(x), \tag{2.8}$$

where

$$F_{\mu\nu}(x) = \partial_{\mu}A_{\nu}(x) - \partial_{\nu}A_{\mu}(x), \tag{2.9}$$

is known as the field-strength tensor, and is obtained by requiring gauge-invariance.

Summing the above two terms we can write the classical Lagrangian for Quantum Electrodynamics as $\mathcal{L}_{\mathrm{QED}} = \mathcal{L}_{\psi} + \mathcal{L}_{A}$. Before we discuss the issues of quantisation (gauge fixing) we will extend the above formalism to a wider class of symmetry transformations.

2.2 Non-Abelian gauge theories (QCD)

The analysis for non-abelian gauge theories is more involved than the previous case. The main reason for this is that the generators of the symmetry group do not necessarily commute with each other. The associated symmetry group of Quantum Chromo Dynamics (QCD) [16, 17] is $SU(3)$ and the quark fields ψ_q transform as triplets under this local non-abelian gauge theory. Denoting the component of each quark by the index i we can write the action of the symmetry transformation as

$$\psi_{q,i}(x) \to \psi'_{q,i}(x) = U_{ij}(x)\psi_{q,j}(x), \quad \hat{U}(x) = e^{-iT^a\theta^a(x)}. \tag{2.10}$$

The requirement of gauge invariance leads to the introduction of a new covariant derivative

$$\not{D}_{ij} = \not{\partial}\delta_{ij} - ig_s T^a_{ij}\not{G}^a(x). \tag{2.11}$$

Here $G^a_\mu(x)$ is the gauge field that interacts with the matter fields. Thus, when local gauge invariance is imposed the theory is described by the following Lagrangian

$$\mathcal{L}_{\psi_q} = \bar{\psi}_{q,i}(x)(i\not{D}_{ij} - M\delta_{ij})\psi_{q,j}(x). \tag{2.12}$$

The kinetic term for the gauge field, obtained by imposing gauge invariance, is now given by

$$\mathcal{L}_G = -\frac{1}{4}G^a_{\mu\nu}(x)G^{a\mu\nu}(x), \tag{2.13}$$

where the tensor field strength is now defined as

$$G^a_{\mu\nu}(x) = \partial_\mu G^a_\nu(x) - \partial_\nu G^a_\mu(x) + g_s f^{abc}G^b_\mu(x)G^c_\nu(x). \tag{2.14}$$

One of the differences with respect to the previous case discussed is the existence of self-interactions for the gauge fields. The resulting classical QCD Lagrangian has the most general form, it is renormalizable and preserves invariance under Poincaré transformations, and local gauge transformations and it is given by $\mathcal{L}_{\rm QCD} = \mathcal{L}_{\psi_q} + \mathcal{L}_G$.

2.3 Quantum Effective Action

The Green's functions contain the full information of the particle interactions of a given quantum field theory and hence play an important role in practical calculations. These functions are defined in position space as the quantum mechanical vacuum expectation values (vev) of time-ordered products of field operators

$$G_{\alpha_1...\alpha_n}(x_1,...,x_n) = \langle 0|\mathrm{T}\Phi_{\alpha_1}(x_1)...\Phi_{\alpha_n}(x_n)|0\rangle, \tag{2.15}$$

and are directly connected, via the reduction formula of Lehmann, Symanzik and Zimmermann [18] (LSZ), to the prediction of physical observables. Their representation within the framework of the path integral formalism is very convenient for a perturbative description of a given quantum field theory. Indeed, as we will see later on, within this framework the process of quantization of a classical theory is depicted in an elegant and transparent manner.

Our aim here is to state the connection between the path integral formalism and the operator formulation of quantum mechanics. For this purpose, we will consider an interacting theory described by the action $S\{\Phi\} = S_0\{\Phi\} + S_{\mathrm{int}}\{\Phi\}$, and in the presence of an external source, $J(x)$, whose partition functional is given by

$$Z\{J\} = \int \mathcal{D}[\Phi] e^{iS\{\Phi\}} \exp\left(i\int d^4x J(x)\Phi(x)\right). \tag{2.16}$$

Here the integral is evaluated over all possible field values at all space-time points and the product $J(x)\Phi(x)$ is understood as a sum over all possible α indices: $\sum_i J_{\alpha_i}(x)\Phi_{\alpha_i}(x)$. Moreover, the action is related to the Lagrangian via $S\{\Phi\} = \int d^4x \mathcal{L}(\Phi)$. When the source field, which acts as a background field to the Φ dynamics, is sufficiently weak, we can perturbatively expand the functional $Z\{J\}$ in powers of $J(x)$. The second exponential of the expression above takes the following form up to second order,

$$\begin{aligned} \exp\left(i\int d^4x J(x)\Phi(x)\right) &= 1 + i\int d^4x J(x)\Phi(x) \\ &+ \frac{i^2}{2}\int d^4x d^4y J(x)\Phi(x)J(y)\Phi(y) + ... \end{aligned} \tag{2.17}$$

Thus in perturbation theory, one can generally express the previous functional (2.16) as the series expansion

$$T\{J\} \equiv \frac{Z\{J\}}{Z\{0\}} = \sum_{n=0}^{\infty}\frac{i^n}{n!}\int d^4x_1...d^4x_n G_{\alpha_1...\alpha_n}(x_1,...,x_n)J_{\alpha_1}(x_1)...J_{\alpha_n}(x_n). \tag{2.18}$$

The coefficients of the previous equation are the important Green's functions, which contain all physical information of the theory, and their representation within the path

integral formalism is given by

$$G_{\alpha_1...\alpha_n}(x_1,...,x_n) = \frac{\int \mathcal{D}[\Phi] e^{iS\{\Phi\}} \Phi_{\alpha_1}(x_1)...\Phi_{\alpha_n}(x_n)}{\int \mathcal{D}[\Phi] e^{iS\{\Phi\}}}. \tag{2.19}$$

Note that they can be reconstructed by functional differentiation with respect to the external source,

$$G_{\alpha_1...\alpha_n}(x_1,...,x_n) = (-i)^n \frac{\delta^n}{\delta J_{\alpha_1}(x_1)...\delta J_{\alpha_n}(x_n)} T\{J\} \big|_{J_\alpha(x)=0}. \tag{2.20}$$

A diagrammatic representation in terms of Feynman diagrams allows us to classify the different contributions. In this description, the functional $T\{J\}$ includes all types of diagrams: disconnected as well as connected graphs, without the insertion of the vacuum diagrams (graphs which are not attached to the external source), since they are cancelled out in the ratio $Z\{J\}/Z\{0\}$. The amplitudes represented by disconnected diagrams are products of the amplitudes described by connected graphs. Therefore the former can be trivially determined by the latter, which are defined via the functional derivative of $T_c\{J\} = \log(T\{J\})$. Moreover the connected diagrams contain portions of others calculated at lower orders in perturbation theory. Those graphs that fall into different pieces by cutting an internal line are known by the name of *one-particle reducible*, and the *one-particle irreducible* (1PI) graphs refer to the ones that do not separate into others by such a cut. The connected diagrams can be then easily constructed by replacing the vertices of tree-level diagrams with 1PI diagrams. Therefore, the 1PI diagrams contain the full quantum structure of our theory and it is possible to include all quantum effects by analysing only the *quantum effective action*, $\Gamma\{\Phi\}$, which is defined as the Legendre transform of the generating functional of connected graphs, in the presence of an external field,

$$i\Gamma\{\Phi\} = T_c\{J\} - i\int d^4x J(x)\Phi(x), \tag{2.21}$$

$$\frac{\delta\Gamma\{\Phi\}}{\delta\Phi(x)} = -J(x). \tag{2.22}$$

Note that in the absence of an external current, the effective action is extremal on the physical field expectation value. Thus it plays exactly the same role for the fully interacting quantum theory as the action does for the classical field configurations.

Another class of diagrams, the *one-light-particle irreducible* (1LPI) diagrams, and the associated effective action $\Gamma_{1\text{LPI}}$, are very important for the study of a given theory at low energy scales, as they contain all the relevant information to describe physical phenomena for sufficiently small energies, masses and momenta. The 1LPI diagrams are defined as graphs that cannot be separated by cutting a single *light* particle line. From the Legendre transformation of the generating functional built up of these connected Feynman graphs with light particle external lines, one constructs the respective light

particle effective action. This plays the main role in the evaluation of quantum effects. Chapter 4 covers this in more detail.

Finally, we state the relation of the Green's functions and the transition amplitudes between asymptotic states given by the LSZ reduction formula as

$$\langle -p_{s+1}, ..., -p_n|S|p_1, ..., p_s\rangle = R^{n/2}\tilde{G}_{\text{trunc}}(p_1, ..., p_n)\Big|_{p_i^2=M_i^2} , \tag{2.23}$$

where the factor $R^{n/2}$ stands for the wave-function renormalization constants, and the truncated Green's functions, in the momentum-space configuration, are defined as,

$$\tilde{G}_{\text{trunc}}(p_1, ..., p_n) = G^{-1}(p_1, -p_1)...G^{-1}(p_n, -p_n)\tilde{G}_c(p_1, ..., p_n). \tag{2.24}$$

Their relation to the space-time configuration Green's functions is given by the Fourier transform.

2.4 Quantization of Gauge Theories

In the path integral formalism, we have seen that the Green's functions can be expressed as an integral over all field configurations, see equation (2.19). The action S is invariant under a gauge transformation. Therefore the only possible gauge dependence appears in the field product. The integral over a gauge-variant object, such as the product of gauge non-singlet operators at different space-time points, vanishes due to the gauge independence of the integral. The fermion propagator is defined via an operator product of gauge non-singlet fields and would vanish, which would forbid a perturbative formulation of the theory.

Faddeev and Popov [19] solved this problem by expressing the integral over all gauge fields as the product of two integrals: one over fields which satisfy some given gauge conditions ($F^a[G, x] = f^a(x)$), and another over all gauge transformations. In this way the gauge-variant Green's functions do not vanish any more. For QCD we would have,

$$\langle 0|\,\mathrm{T}XY\,|0\rangle = \mathcal{N}\int [dG][d\bar{\psi}][d\psi]XY\exp(iS)\Delta[G]\prod_{x,a}\delta(F^a(x) - f^a(x)), \tag{2.25}$$

where we have denoted the product of different fields by X and Y, and the normalization term is given by,

$$\mathcal{N}^{-1} = \int [dG][d\bar{\psi}][d\psi]\exp(iS)\Delta[G]\prod_{x,a}\delta(F^a(x) - f^a(x)). \tag{2.26}$$

The factor $\Delta[G]$ is the corresponding Jacobian which arises due to the gauge transformations and the imposed gauge condition,

$$\Delta[G] = \int [d\eta^a][d\bar{\eta}^a]\exp(i\mathcal{L}_{\text{ghost}}). \tag{2.27}$$

The integral above is performed over the auxiliary Grassmann-fields η^a and $\bar{\eta}^a$ called Faddeev-Popov ghost fields, and the ghost Lagrangian is defined in terms of the infinitesimal transformation of the gauge condition,

$$\mathcal{L}_{\text{ghost}} = \bar{\eta}^a \delta F_a[G, x]. \tag{2.28}$$

For the covariant gauge: $F^a[G, x] = \partial^\mu G^a_\mu(x)$, it takes the form,

$$\mathcal{L}_{\text{ghost}} = \partial^\mu \bar{\eta}^a (\partial_\mu \eta^a + g f^{abc} \eta^b G^c_\mu), \tag{2.29}$$

$$S = \int d^4x (\mathcal{L}_{\text{inv}} + \mathcal{L}_{\text{gf}} + \mathcal{L}_{\text{ghost}}). \tag{2.30}$$

The inclusion of the gauge-fixing and the Faddeev-Popov ghost terms lead to an effective action that does not preserve the gauge symmetry. In fact the computed Green's functions depend on the choice of the gauge fixing and only physical quantities are gauge-independent order by order in perturbation theory. However, even if the desired gauge symmetry is not longer manifest, the action S is invariant under new non-linear Becchi-Rouet-Stora-Tyutin (BRST) transformations [20].

This global symmetry is constructed by expressing the gauge parameter as a product of the Faddeev-Popov field and a Grassmann parameter: $\delta\theta^a(x) = \eta^a(x)\delta\lambda$. The corresponding field transformations are given by,

$$\begin{aligned}
\delta_{\text{BRS}}\psi &= -ig(\eta^a \delta\lambda) T^a \psi = igT^a \eta^a \psi \delta\lambda \\
\delta_{\text{BRS}}\bar{\psi} &= ig\bar{\psi} T^a (\eta^a \delta\lambda) \\
\delta_{\text{BRS}} A^a_\mu &= \left(\partial_\mu \eta^a + g f^{abc} \eta^b A^c_\mu\right) \delta\lambda \\
\delta_{\text{BRS}}\eta^a &= -\frac{1}{2} g f^{abc} \eta^b \eta^c \delta\lambda \\
\delta_{\text{BRS}}\bar{\eta}^a &= \frac{1}{\xi} \partial^\mu A^a_\mu \delta\lambda.
\end{aligned} \tag{2.31}$$

For this new global symmetry the Green's functions satisfy complicated Slavnov-Taylor identities [21, 22]. In a general form they can be expressed as,

$$\delta_{\text{BRST}} \langle 0| \,\text{T} XY \,|0\rangle = \langle 0| \,\text{T}(\delta_{\text{BRST}} X) Y \,|0\rangle + \langle 0| \,\text{T} X (\delta_{\text{BRST}} Y) \,|0\rangle = 0. \tag{2.32}$$

2.4.1 Background Field Method

A very useful technique used in the description of quantized gauge theories is the well-known background field method (BFM) [23]. Within this approach, gauge invariance is not lost explicitly which results in technical and conceptual simplifications. The basic idea is to split the gauge fields which appear in the classical action into a background field denoted by the subscript "cl", and a quantum fluctuation parametrized by the index "Q",

$$\Phi^{\mu}(x) = \Phi^{\mu}_{\rm cl}(x) + \Phi^{\mu}_{\rm Q}(x), \tag{2.33}$$

the latter being the variable of integration in the functional integral. Moreover a choice of gauge, that only breaks the gauge invariance of the quantum field, is performed. Hence it is desirable to work only with background field Green's functions since these gauge fields preserve the symmetry.

In what follows, the formalism introduced in Section 2.3 is adapted to this approach. From the relation (2.33), the generating functional can be written as

$$\tilde{Z}\left\{J, \Phi_{\rm cl}\right\} = \int \mathcal{D}[\Phi_{\rm Q}] e^{iS\left\{\Phi_{\rm cl}+\Phi_{\rm Q}\right\}} \exp\left(i \int d^4x J(x)\Phi_{\rm Q}(x)\right). \tag{2.34}$$

Here we use a tilde to distinguish the background field quantities from the conventional ones. The relation between the functions computed in these two different frameworks is obtained by performing a shift in the integration variable of the functional integral,

$$\tilde{Z}\left\{J, \Phi_{\rm cl}\right\} = Z\left\{J\right\} \exp\left(-i \int d^4x J(x)\Phi_{\rm cl}(x)\right). \tag{2.35}$$

From the expression (2.34), one can define the new $\tilde{T}\{J, \Phi_{\rm cl}\}$ functional where the vacuum diagrams are subtracted by means of the ratio $\tilde{Z}\left\{J, \Phi_{\rm cl}\right\} / \tilde{Z}\left\{0, \Phi_{\rm cl}\right\}$. Furthermore, the disconnected diagrams can be removed by taking the logarithm of $\tilde{T}\{J, \Phi_{\rm cl}\}$, meaning the connected pieces are given by

$$\tilde{T_c}\left\{J, \Phi_{\rm cl}\right\} = \log\left(\tilde{T}\left\{J, \Phi_{\rm cl}\right\}\right), \tag{2.36}$$

which is related to the conventional quantity through

$$\tilde{T_c}\left\{J, \Phi_{\rm cl}\right\} = T_c\left\{J\right\} - i\left(\int d^4x J(x).\Phi_{\rm cl}(x)\right). \tag{2.37}$$

Finally, the background field effective action is obtained after a Legendre transformation

$$i\tilde{\Gamma}\left\{\Phi_{\rm cl}, \Phi_{\rm Q}\right\} = \tilde{T_c}\left\{J, \Phi_{\rm cl}\right\} - i \int d^4x J(x)\Phi_{\rm Q}(x). \tag{2.38}$$

The 1PI Green's functions, in the presence of the background field $\Phi_{\rm cl}(x)$, are obtained by computing the derivatives with respect to $\Phi_{\rm Q}(x)$, and its relation to the effective

action computed within the conventional method is given by

$$i\tilde{\Gamma}\left\{\Phi_{\rm cl},\Phi_{\rm Q}\right\} = i\Gamma\left\{\Phi_{\rm cl}+\Phi_{\rm Q}\right\}. \tag{2.39}$$

By setting the quantum field to zero in the background effective action: $\tilde{\Gamma}\left\{\Phi_{\rm cl},0\right\}$ the dependence on $\Phi_{\rm Q}$ disappears and therefore it generates no graphs with external lines. Indeed, $\tilde{\Gamma}\left\{\Phi_{\rm cl},0\right\}$ is the sum of all 1PI vacuum graphs in the presence of the $\Phi_{\rm cl}$, which obey the naive Ward identities of gauge invariance.

Chapter 3

Renormalization

Divergent results emerge in the computation of perturbative corrections of quantum field theories. Since the measurements of physical observables are represented by (finite) numbers, the divergences can only appear at an intermediate stage of the calculations. Obviously a procedure is required that will render the final theory prediction finite. This is done by regularizing the intermediate expressions and renormalizing the final result and we will summarise these ideas in this chapter. The first two sections are devoted to the regularization method employed and the renormalization scheme chosen in our calculations. In the remaining sections we will present the counter-terms required to renormalize QCD.

3.1 Dimensional Regularization

In order to deal with the singularities that appear in higher order corrections to Green's functions, the theory has to be regularized. The goal of this process is to keep track of divergences through a regulator. There are several approaches which allow us to isolate singularities. However we only stress here the important points of the *dimensional regularization* scheme [24, 25], which we employ in our calculations. The main idea of this scheme is to evaluate the integrals in an arbitrary number of space-time dimensions $d = 4 - 2\varepsilon$. Consequently, the results are expressed in terms of the regulator ε. In this manner the singular terms can be easily manipulated and in the limit $\varepsilon \to 0$ the apparent divergences are recovered. The advantage of using this technique is that it preserves gauge and Lorentz invariance. However, several issues related to the treatment of γ_5 in d-dimensions appear: while the Dirac algebra can be easily extended to d-dimensions, there is no natural continuation of γ_5. This issue can be observed when traces, like $Tr(\gamma_\alpha\gamma_\mu\gamma_\nu\gamma_\rho\gamma_\sigma\gamma^\alpha\gamma_5)$, are evaluated in d-dimensions by using the anti-commutation relation for γ_5 and the cyclicity of the trace. For instance, if one proceeds with the calculation it is easily seen that these objects are not uniquely defined, but that the ambiguity disappears when the limit $d = 4$ is taken or when the whole trace vanishes. For a consistent analysis of one-particle-irreducible diagrams within dimensional reg-

ularization a unique result must be obtained and the limit to four dimensions has to be restored. Several schemes were proposed to deal with the γ_5 problem. In what follows, we discuss the basic ideas of two of them: the *Naive Dimensional Regularization scheme* (NDR) [26] and the *'t Hooft-Veltman scheme* (HV) [24].

Due to the inconsistency mentioned previously, one could think about not extending the anti-commutation relation $\{\gamma^\mu, \gamma_5\} = 0$ in d-dimensions or not to use dimensional regularization for fermion loops. The first idea was followed by 't Hooft and Veltman. In their work, γ_5 is considered as a purely four dimensional object: $\gamma_5 = i\gamma^0\gamma^1\gamma^2\gamma^3$. This definition for γ_5 leads to anti-commutation relations for the 4-dimensional subset of γ-matrices and new commutation relations with the remaining $(d-4)$-dimensional ones. The biggest disadvantage of working in this framework is the fact that to restore chiral Ward identities we need to introduce non-invariant counter-terms for almost any diagram containing γ_5. In the case, where there is no real anomalous contributions and for an even number of γ_5 appearing in the traces, one can use the conventional definition of an anti-commuting γ_5. This is followed by the NDR-scheme. The limitation of this framework is that it is not possible to compute traces with an odd number of γ_5 unambiguously.

3.2 Evaluation of the Feynman Integrals

The Feynman diagrams that occur in our calculation will involve certain d-dimensional integrals. At one-loop, the integrals will have the following general expression

$$\mathcal{I}^{(1)}[k_i, m_i, \hat{f}] = \int \frac{d^d q\ \hat{f}(q, k_i)}{\prod_i [(q+k_i)^2 - m_i^2]}\,, \tag{3.1}$$

where q is the loop integration momenta, k_i represents different combinations of external momenta, $\hat{f}$ represents a tensor that is a function of q and k_i, and m_i refers to the masses of the respective particles. Notice that to simplify the notation the term $+i\varepsilon$ has been omitted in the definition of the propagators. At two loops, we can express our integrals as

$$\begin{aligned}&\mathcal{I}^{(2)}_{n_i n_j n_l}[k_i, k_j, k_l, m_i, m_j, m_l, \hat{f}] = \\ &\quad \int \frac{d^d q_1 d^d q_2\ \hat{f}(q_1, q_2, k_i, k_j, k_l)}{\prod_{ijl}[(q_1+k_i)^2 - m_i^2]^{n_i}[(q_2+k_j)^2 - m_j^2]^{n_j}[(q_1-q_2+k_l)^2 - m_l^2]^{n_l}}\,,\end{aligned} \tag{3.2}$$

where q are the one and two loop integration momenta and the external momenta, masses and tensors are denoted by k, m and $\hat{f}$. The exact evaluation of the previous expressions, for arbitrary values of external momenta and masses, is quite involved if it is even possible to find a closed analytical expression. Fortunately, we are only interested in the low energy behaviour of the integrals and several calculational procedures can hence be applied to simplify their evaluation. In particular, we can expand the integrand

in external momenta prior to integration over the virtual momenta. For instance, the simple case of one propagator with dependence in external and virtual momentum would expand as follows,

$$\frac{1}{(q+k)^2-m^2} = \frac{1}{(q^2-m^2)} - \frac{k^2+2(k.q)}{(q^2-m^2)^2}. \tag{3.3}$$

After expanding in external momenta, tensor reduction and partial fraction decomposition, the above integrals will reduce to a sum of the following integrals at one loop

$$I_n^{(1)}(m) = \int \frac{d^dq}{(q^2-m^2)^n}, \tag{3.4}$$

while the general two-loop result reads

$$I^{(2)}_{n_1n_2n_3}(m_1,m_2,m_3) = \int \frac{d^dq_1 d^dq_2}{\prod_{i=1}^2 \left(q_i^2-m_i^2\right)^{n_i} \prod_{i<j}^2 \left((q_i-q_j)^2-m_{i+j}^2\right)^{n_{i+j}}}, \tag{3.5}$$

which we have written in a form that can be extended also to three loops. The previous expressions can be represented by vacuum diagrams representing scalar particles.

Moreover the number of Feynman diagrams, required for the study of the desired observables, increases at higher orders in perturbation theory. This feature complicates their evaluation by hand, which makes it necessary to compute them automatically. We use *FeynArts* [27] to generate the diagrams, and a *Mathematica* routine, based on a code developed by M. Gorbahn, for their computation. In the following sections we will describe the algorithms used.

3.2.1 Taylor Expansion

We will be interested in determining the effective action for light particles. Here an expansion in external momenta of the propagator terms of the integrands can be performed [28] to simplify the calculation of the integrals (3.1) and (3.2). While this expansion leads to the appearance of infra-red divergences, these infrared divergences will cancel in the matching procedure that determines the effective action. We will discuss these cancellations in more detail in the chapter on effective field theories and continue with the description of our algorithm.

After Taylor expansion and partial fraction decomposition, having factored out the terms linear in external momenta, we arrive at vacuum tensor integrals. At one-loop we have

$$\mathcal{I}_n^{(1)}[m_i,\alpha] = \int d^dq \frac{q^{\mu_1}\dots q^{\mu_\alpha}}{(q^2-m^2)^n}, \tag{3.6}$$

while the two-loop expression reads:

$$\mathcal{I}^{(2)}_{n_1 n_2 n_3}[m_1, m_2, m_3, \alpha_1, \alpha_2] = \int \frac{d^d q_1 d^d q_2 \left(q_1^{\mu_1} \dots q_1^{\mu_{\alpha_1}}\right)\left(q_2^{\nu_1} \dots q_2^{\nu_{\alpha_2}}\right)}{\prod_{i=1}^{2}\left(q_i^2 - m_i^2\right)^{n_i} \prod_{i<j}^{2}\left((q_i - q_j)^2 - m_{i+j}^2\right)^{n_{i+j}}}. \tag{3.7}$$

3.2.2 Tensor Decomposition

The tensor vacuum integrals can be further simplified to scalar vacuum integrals by a method called tensor decomposition. This method relies on the Lorentz invariance of the regularised quantum field theory. The tensor integrals must be proportional to a sum of products of the metric tensor $g^{\mu\nu}$ and a scalar vacuum integral that only depends on the masses and the regularization parameters.

To clarify the basic idea of this method, we consider here the two-loop integral $\mathcal{I}^{(2)}_{1\,1\,1}[m_1, m_2, m_3, 2, 2]$, where we set $n_1 = n_2 = n_3 = 1$ for simplicity. Later it will become clear that the tensor decomposition works for an arbitrary choice of parameters. For $\mathcal{I}^{(2)}_{1\,1\,1}$, we write the integral as a sum

$$\int \frac{d^d q_1 d^d q_2 \cdot q_1^\mu q_1^\nu q_2^\rho q_2^\sigma}{(q_1^2 - m_1^2)(q_2^2 - m_2^2)((q_1 - q_2)^2 - m_3^2)} = F_1 g^{\mu\nu} g^{\rho\sigma} + F_2 (g^{\mu\rho} g^{\nu\sigma} + g^{\mu\sigma} g^{\nu\rho}) \tag{3.8}$$

where F_1 and F_2 are functions of the masses and the regularization parameters. Note that the right hand side of the above expression respects the symmetry $\mu \leftrightarrow \nu$ and $\rho \leftrightarrow \sigma$ that follows from the $q_1^\mu \leftrightarrow q_1^\nu$ and $q_2^\rho \leftrightarrow q_2^\sigma$ symmetry of the integrand.

The coefficients F_1 and F_2 can then be determined by contracting the tensor integral with: $g_{\mu\nu} g_{\rho\sigma}$ and $g_{\mu\rho} g_{\nu\sigma}$. These contractions lead to the following system,

$$\begin{pmatrix} d^2 & 2d \\ d & d(d+1) \end{pmatrix} \begin{pmatrix} F_1 \\ F_2 \end{pmatrix} = \begin{pmatrix} X_1 \\ X_2 \end{pmatrix}, \tag{3.9}$$

where the factors X_1 and X_2 correspond to the integrals

$$\begin{aligned} X_1 &= \int \frac{d^d q_1 d^d q_2 \cdot q_1^2 q_2^2}{(q_1^2 - m_1^2)(q_2^2 - m_2^2)((q_1 - q_2)^2 - m_3^2)}, \\ X_2 &= \int \frac{d^d q_1 d^d q_2 \cdot (q_1 \cdot q_2)^2}{(q_1^2 - m_1^2)(q_2^2 - m_2^2)((q_1 - q_2)^2 - m_3^2)}, \end{aligned} \tag{3.10}$$

which can be easily reduced to the familiar scalar vacuum integrals by means of the following relations:

$$\begin{aligned} q_1^2 &= (q_1^2 - m_1^2) + m_1^2, \\ q_2^2 &= (q_2^2 - m_2^2) + m_2^2, \\ (q_1 \cdot q_2) &= \frac{1}{2}\left\{(q_1^2 - m_1^2) + (q_2^2 - m_2^2) - \left[(q_1 - q_2)^2 - m_3^2\right] + m_1^2 + m_2^2 - m_3^2\right\}. \end{aligned} \tag{3.11}$$

Inspecting the above procedure, it is clear that it is independent of the particular power of each propagator and we can extend the formalism to arbitrary values of n_1, n_2 and n_3.

3.2.3 IBP relations

The two-loop scalar integrals of equation (3.5) can be further simplified to so-called master integrals by means of integration by parts (IBP) techniques [29]. The IBP technique relies on the vanishing of the surface term of dimensionally regularized non-trivial multiloop integrals,

$$0 = \int \frac{d^d q}{(2\pi)^d} \frac{\partial}{\partial q^\mu} f(q, ...). \tag{3.12}$$

One uses these relations to express integrals in terms of integrals with simpler structures. The resulting IBP identities, which arise after applying this property, relate integrals with different powers of propagators, and can for example be implemented on a computer through iteration. Continuous application of the identities expresses the integrals in terms of master integrals that can be evaluated analytically to an appropriate power of ε. This technique is advantageous since it allows us to write the final expression in terms of independent functions, which simplifies numerical evaluation and the inspection of the cancellation of the divergences becomes clear. We will briefly explain the technique using the rather trivial example of the one-loop integrals defined in equation (3.4). While the general result for a one-loop tadpole integral is known from textbooks [14],

$$I_n^{(1)} = (-m^2)^{\frac{d}{2}-n} \pi^{\frac{d}{2}} \frac{\Gamma(n - \frac{d}{2})}{\Gamma(n)}, \tag{3.13}$$

it is instructive to study the IBP relations for this simple example first:

$$\begin{aligned} 0 &= \int \frac{d^d q}{(2\pi)^d} \frac{\partial}{\partial q_\mu} \left[\frac{q_\mu}{(q^2 - m^2)^n} \right] = \int \frac{d^d q}{(2\pi)^d} \left[\frac{d}{(q^2 - m^2)^n} - n \frac{2q^2}{(q^2 - m^2)^{n+1}} \right] \\ &= \int \frac{d^d q}{(2\pi)^d} \left\{ \frac{d}{(q^2 - m^2)^n} - 2n \left[\frac{m^2}{(q^2 - m^2)^{n+1}} + \frac{1}{(q^2 - m^2)^n} \right] \right\}, \end{aligned} \tag{3.14}$$

where in the last line we have replaced q^2 by $(q^2 - m^2) + m^2$. Notice that this allows us to find a recursive relation for the integrals,

$$2nm^2 I_{n+1}^{(1)}(m) = (d - 2n) I_n^{(1)}(m). \tag{3.15}$$

Hence, the one-loop Feynman integrals with higher powers of denominators can be evaluated in terms of the master integral $I_n^{(1)}(m)$.

The evaluation of the two-loop integral is more involved. Here we will follow Ref. [28] and first note that $I_{n_1 n_2 n_3}^{(2)}$ is totally symmetric under permutations of its indices. When one of its indices in non-positive, one can reduce the integral to a product of one-loop integrals. When all of the indices are positive, one finds the following recursion relation

with the use of integration by parts, which holds for $n_i \geq 1$,

$$\begin{aligned} I^{(2)}_{(n_1+1)n_2n_3} &= \frac{1}{n_1 m_1^2 \Delta(m_1^2, m_2^2, m_3^2)} \\ &\times \Big\{ \big[n_2(m_1^2 - m_3^2)(m_1^2 - m_2^2 + m_3^2) + n_3(m_1^2 - m_2^2)(m_1^2 + m_2^2 - m_3^2) \\ &+ d m_1^2(-m_1^2 + m_2^3 + m_3^2) - n_1 \Delta(m_1^2, m_2^2, m_3^2) \big] I^{(2)}_{n_1n_2n_3} \\ &+ n_2 m_2^2(m_1^2 - m_2^2 + m_3^2) \left[I^{(2)}_{n_1(n_2+1)(n_3-1)} - I^{(2)}_{(n_1-1)(n_2+1)n_3} \right] \\ &+ n_3 m_3^2(m_1^2 + m_2^2 - m_3^2) \left[I^{(2)}_{n_1(n_2-1)(n_3+1)} - I^{(2)}_{(n_1-1)n_2(n_3+1)} \right] \Big\}, \end{aligned} \tag{3.16}$$

where,

$$\Delta(m_1^2, m_2^2, m_3^2) = 2(m_1^2 m_2^2 + m_1^2 m_3^2 + m_2^2 m_3^2) - (m_1^4 + m_2^4 + m_3^4). \tag{3.17}$$

The expressions for $I^{(2)}_{n_1(n_2+1)n_3}$ and $I^{(2)}_{n_1n_2(n_3+1)}$ can be obtained using the symmetry of the integrals under the interchange $(n_i, m_i) \leftrightarrow (n_j, m_j)$. Using these relations the power of the propagators is reduced with each application of the IBP relation. In case where one of the indices vanishes, the integral factorises into a product of two one-loop integrals. For the special case $n_1 = n_2 = n_3 = 1$ we cannot simplify the integral further and it will be called a master integral.

3.2.4 Master Integrals

The previous steps reduced the problem to the computation of a basic class of integrals, which cannot be reduced further. This section will cover the computation of massive vacuum two-loop integrals for the particular case of two different masses:

$$I^{(2)}_{n_1n_2n_3}(m, m, M) = \int \frac{d^d q_1 d^d q_2}{\left(q_1^2 - m^2\right)^{n_1} \left(q_2^2 - m^2\right)^{n_2} \left((q_1 - q_2)^2 - M^2\right)^{n_3}}. \tag{3.18}$$

The Feynman parametrization could be used to solve the integral (3.18). But this is not the only way to get an analytical solution for $I^{(2)}_{n_1n_2n_3}(m, m, M)$. The Mellin-Barnes representation is very often used for the computation of massive Feynman integrals, since a massive propagator can be expressed as a contour integral of products of gamma functions in the complex plane,

$$\frac{1}{(q^2 - m^2)^n} = \frac{1}{\Gamma(n)} \frac{1}{2\pi i} \int_{-i\infty}^{i\infty} ds \frac{(-m^2)^s}{(q^2)^{n+s}} \Gamma(-s)\Gamma(n+s). \tag{3.19}$$

The contour lines are determined in such a way that the poles of $\Gamma(-s)$ are located to the right and those of $\Gamma(n+s)$ to the left. The transformation (3.19) can be recursively applied to denominators with more than two terms. Notice that this relation applied to the third denominator of equation (3.18) leads to a vacuum integral with one massless line which can be analytically evaluated in terms of gamma functions (for a more

exhaustive explanation see [28]). For the interesting case when $n_1 = n_2 = n_3$ the integral (3.18) has the solution,

$$\begin{aligned} I^{(2)}_{111}(m,m,M) &= \pi^{4-2\varepsilon}(m^2)^{1-2\varepsilon}A(\varepsilon) \\ &\times \left(-\frac{1}{\varepsilon^2}(1+2z) + \frac{4z}{\varepsilon}\ln(4z) - 2z\ln^2(4z) + 2(1-z)\Phi(z)\right), \end{aligned} \tag{3.20}$$

where the dimensionless variable $z \equiv M^2/4m^2$ has been introduced for convenience. In addition, the function $A(\varepsilon)$ is defined as

$$\begin{aligned} A(\varepsilon) &\equiv \frac{\Gamma^2(1+\varepsilon)}{(1-\varepsilon)(1-2\varepsilon)} \\ &= 1 + \varepsilon(3-2\gamma_E) + \varepsilon^2(7 - 6\gamma_E + 2\gamma_E^2 + \frac{\pi^2}{6}) + \mathcal{O}(\varepsilon^3), \end{aligned} \tag{3.21}$$

γ_E being the Euler-Mascheroni constant, and the $\Phi(z)$ function is given in terms of hypergeometric functions,

$$\Phi(z) = 4z\left([2-\ln(4z)]{}_2F_1(1,1;\frac{3}{2};z) - \partial_a\ {}_2F_1(1,1;\frac{3}{2};z) - \partial_c\ {}_2F_1(1,1;\frac{3}{2};z)\right). \tag{3.22}$$

The notation used for the derivatives of the hypergeometric functions stands for

$$\begin{aligned} \partial_a\ {}_2F_1(a,b;c;z) &\equiv \frac{\partial}{\partial_c}\ {}_2F_1(a,b;c;z) \\ &\quad - \sum_{j=0}^{\infty}\frac{z^j}{j!}\frac{(a)_j(b)_j}{(c)_j}\left(\psi(a+j) - \psi(a)\right), \\ \partial_c\ {}_2F_1(a,b;c;z) &\equiv \frac{\partial}{\partial_a}\ {}_2F_1(a,b;c;z) \\ &\quad \sum_{j=0}^{\infty}\frac{z^j}{j!}\frac{(a)_j(b)_j}{(c)_j}\left(\psi(c+j) - \psi(c)\right), \end{aligned} \tag{3.23}$$

where $\psi(a) \equiv (d/da)\ln(\Gamma(a))$. For the case $0 \le z < 1$ one obtains

$${}_2F_1(1,1;\frac{3}{2};z) = \frac{\arcsin\sqrt{z}}{\sqrt{z(1-z)}} \tag{3.24}$$

$$\begin{aligned} &\partial_a\ {}_2F_1(1,1;\frac{3}{2};z) - \partial_c\ {}_2F_1(1,1;\frac{3}{2};z) - 2\ {}_2F_1(1,1;\frac{3}{2};z) \\ &= -\frac{1}{\sqrt{z(1-z)}}[\ln(4z)\arcsin\sqrt{z} + \mathrm{Cl}_2(2\arcsin\sqrt{z})]. \end{aligned} \tag{3.25}$$

The symbol $\mathrm{Cl}_2(z)$ denotes Clausen's integral function,

$$\mathrm{Cl}_2(z) = -\int_0^z dz\ln|2\sin(z/2)|. \tag{3.26}$$

The results of eq. (3.24) and eq. (3.25) can be derived by using a parametric integral representation of the hypergeometric function ${}_2F_1$, and its parametric derivatives. For more details, we refer the reader to reference [28]. Finally, It is worth pointing out that the function $\Phi(z)$ will play an important role in the cancellation of the infra-red divergences, as will be explained in detail in Chapter 4.

3.3 $\overline{\text{MS}}$-scheme

Once the divergences have been isolated in our regularization procedure we can redefine the physical parameters of our theory, such as the coupling constants and particle masses, to absorb the divergences. For a renormalizable theory the Green's functions that are expressed in terms of these new parameters will be finite. When choosing a renormalization scheme we have an additional freedom to subtract finite terms in combination with the divergences as long as the symmetry of the theory is preserved. Hence there are many renormalization prescriptions. Two of the most popular schemes are the on-shell scheme and the *modified minimal subtraction* ($\overline{\text{MS}}$) *scheme* [30]. While the first scheme is a so-called physical scheme that is explicitly decoupling, the latter scheme is useful for practical calculations, in particular in the context of the strong interaction. We will state the important ideas of the $\overline{\text{MS}}$ scheme that we employ later in our calculations. Its definition is intimately connected to dimensional regularization in the sense that only the poles of ε and some universal finite terms are removed. In addition higher-order calculations can be simplified by performing an expansion in external momenta and masses before integration over loop momenta, since all the UV counter-terms are polynomial both in momenta and in masses. Moreover this renormalization scheme has the particular advantage of yielding mass-independent renormalization group functions which makes the renormalization group improvement of perturbation theory easy and clear. However, as we will explain in the next chapter, the decoupling of heavy particles is not transparent in this framework.

3.4 Infra-red Rearrangement

The fact that divergent results are polynomial in the masses and momenta of the theory suggests some sort of an expansion can be made to extract the renormalization constants of a given theory. Yet masses and external momenta regularize the infra-red divergences of the Feynman integrals. While the ultra-violet (UV) divergences of an integral are independent of the assumptions made for the external states, these divergences could be modified through the dimensional regularization of the infrared singularities. Hence one cannot simply Taylor expand in the masses and momenta to simplify the calculation. This would induce new spurious infra-red divergences which would appear as $1/\varepsilon^i$ poles that are indistinguishable from the ultra-violet divergences in the framework of dimensional regularization. Hence, the identification and subtraction of the UV

divergences is nontrivial. In this work we use the technique of IR rearrangement [31,32] to determine the necessary counter-terms.

IR rearrangement is based on the idea of introducing an artificial mass parameter m_r to regularize the spurious infra-red divergences. The exact decomposition of a scalar propagator is given by

$$\frac{1}{(k+q)^2-M^2} = \frac{1}{q^2-m_r^2} + \frac{M^2-k^2-2(k.q)-m_r^2}{(q^2-m_r^2)}\frac{1}{(k+q)^2-M^2}. \tag{3.27}$$

In the equation above k is a linear combination of external momenta, q is a linear combination of loop momenta, and M symbolizes the mass of the particle. Notice that the last term of equation (3.27) has the same form as the original propagator. Therefore it can be decomposed in the same way and we find:

$$\begin{aligned}\frac{1}{(k+q)^2-M^2} = &\frac{1}{q^2-m_r^2} + \frac{M^2-k^2-2(k\cdot q)}{(q^2-m_r^2)^2} + \frac{[M^2-k^2-2(k\cdot q)]^2}{(q^2-m_r^2)^3} \\ &- \frac{m_r^2}{(q^2-m_r^2)^2} + \frac{m_r^4-2m_r^2[M^2-k^2-2(k\cdot q)]}{(q^2-m_r^2)^3} \\ &+ \frac{[M^2-k^2-2(k\cdot q)-m_r^2]^3}{(q^2-m_r^2)^3[(k+q)^2-M^2]}.\end{aligned} \tag{3.28}$$

Notice that the second term in the expression (3.27) reduces the UV degree of divergence. Consequently, there would be a point where these recursive substitutions of (3.27) would provide a finite result and one could drop the last term, apart from one subtlety: the last term contains the regulator mass. Removing this term requires the addition of counter-terms that are proportional to the regulator mass and compensate its removal [32]. Using this method we can extract the UV divergence using a modified expansion that allows us to control all the spurious infra-red divergences and simplify the Feynman diagram calculation.

3.5 QCD

This section describes the renormalization of a non-abelian gauge theory based on a gauge group G. The most general Lorentz invariant Lagrangian expressed in terms of bare fields and parameters is given by

$$\begin{aligned}\mathcal{L}_0^{\mathrm{QCD}} = &\bar{\psi}_{0i}\left(i\partial\!\!\!/ - M_0\right)\psi_{0i} + g_0\bar{\psi}_{0i}T^a_{ij}\not{G}^a_0\psi_{0j} \\ &- \frac{1}{4}\left(\partial_\mu G^a_{0\nu} - \partial_\nu G^a_{0\mu}\right)^2 - \frac{1}{2\xi_{0,G}}\left(\partial^\mu G^a_{0\mu}\right)^2 \\ &- g_0 f^{abc}\left(\partial^\mu G_0^{a\nu}\right)G^b_{0\mu}G^c_{0\nu} - \frac{g_0^2}{4}f^{abc}f^{ade}G^b_{0\mu}G^c_{0\nu}G_0^{d\mu}G_0^{e\nu} \\ &- \bar{\eta}^a_0\partial^2\eta^a_0 - g_0 f^{abc}\left(\partial^\mu\bar{\eta}^a_0\right)\eta^b_0 G^c_{0\mu}.\end{aligned} \tag{3.29}$$

Here $G^a_{0\mu}$ are the gauge fields and ψ_{0i} are multiplets of fermions. The ghost fields are represented by $\bar{\eta}^a_0$ and η^a_0, and $\xi_{0,G}$ stands for the unrenormalized gauge parameter. The generators for the fermion representations, T^a_{ij}, and the structure constants, f^{abc}, are defined by the following relations

$$\begin{aligned} [T^a, T^b] &= i f^{abc} T^c, \\ \mathrm{Tr}(T^a T^b) &= T_F \delta^{ab}, \\ T^a_{ik} T^a_{kj} &= C_F \delta_{ij}, \\ f^{abc} f^{acd} &= C_A \delta^{bd}, \end{aligned} \tag{3.30}$$

where T_F is a constant that depends on the fundamental representation, and the factors C_F and C_A are the quadratic Casimir operators. In particular, for the fundamental representation of $SU(N_c)$ the group invariants T_F, C_F and C_A take the values:

$$T_F = \frac{1}{2}, \quad C_F = \frac{N_c^2 - 1}{2N_c}, \quad C_A = N_c. \tag{3.31}$$

As explained in the previous sections a redefinition of fields and parameters has to be made to compute physical observables. Therefore the bare fields and the bare parameters are expressed in terms of renormalized quantities by means of the following equations

$$G_0^{a,\mu} = Z_G^{1/2} G^{a,\mu}, \quad \psi_0 = Z_\psi^{1/2} \psi, \quad \bar{\eta}_0 = Z_{\bar{\eta}}^{1/2} \bar{\eta}, \quad \eta_0 = Z_\eta^{1/2} \eta, \tag{3.32}$$

$$g_0 = Z_g \mu^\varepsilon g, \quad \xi_{0,G} = Z_G \xi_G, \quad M_0 = Z_M M. \tag{3.33}$$

The parameter μ is introduced since the bare coupling constant is not dimensionless in the scheme of dimensional regularization. From the Lagrangian it is easy to observe that g_0 has dimensions of $(\text{mass})^\varepsilon$. Hence the above redefinition of the bare coupling allows us to work with a dimensionless renormalized coupling constant. The arbitrary parameter μ plays an important role in the study of the asymptotic behaviour of the theory.

The proportionality factors Z_a that relate bare and renormalized parameters and fields are known as renormalization constants. In perturbation theory they can be expanded in terms of the coupling constant,

$$Z_a = 1 + \sum_{k=1}^{\infty} \left(\frac{g}{4\pi}\right)^{2k} Z_a^{(k)}, \tag{3.34}$$

where the expansion in terms of ε poles has been written down explicitly,

$$Z_a^{(k)} = \sum_{l=1}^{k} \frac{1}{\varepsilon^l} Z_a^{(k,l)}. \tag{3.35}$$

Note that only poles of ε appear at one-loop. For two loops also singular terms in ε^2 have to be included. Moreover it is worth pointing out the arbitrariness in the definition of the renormalization constants, which is fixed by the choice of a renormalization scheme. As mentioned previously, for the $\overline{\text{MS}}$-scheme only the pole parts and some universal factors are subtracted.

These Z_a factors have been computed by requiring that physical quantities are finite. Dimensional regularization and the $\overline{\text{MS}}$-scheme have been employed. In addition we have expanded in external momenta. In general this expansion introduces infrared divergences. To avoid these spurious singularities we have introduced an artificial mass for the gauge field within the framework of infrared rearrangement, as previously explained.

The results up to two-loops, which will be used in our calculations and which agree with the results published in reference [33], are given here:

- **One-Loop**:

$$\begin{aligned}
Z_G^{(1,1)} &= \left(\frac{13}{6} - \frac{1}{2}\xi_G\right) C_A - \frac{2}{3} n_f, \\
Z_\eta^{(1,1)} &= \left(\frac{3}{4} - \frac{1}{4}\xi_G\right) C_A, \\
Z_\psi^{(1,1)} &= -\xi_G C_F, \\
Z_g^{(1,1)} &= -\frac{11}{6} C_A + \frac{1}{3} n_f, \\
Z_M^{(1,1)} &= -3 C_F, \\
Z_{m_r}^{(1,1)} &= \left(-\frac{29}{24} - \frac{1}{8}\xi_G\right) C_A - \frac{2}{3} n_f
\end{aligned} \tag{3.36}$$

- **Two-loops**:

$$\begin{aligned}
Z_G^{(2,1)} &= \left(\frac{59}{16} - \frac{11}{16}\xi_G - \frac{1}{8}\xi_G^2\right) C_A^2 - C_F n_f - \frac{5}{4} C_A n_f, \\
Z_\eta^{(2,1)} &= \left(\frac{95}{96} + \frac{1}{32}\xi_G\right) C_A^2 - \frac{5}{24} C_A n_f, \\
Z_\psi^{(2,1)} &= \frac{3}{4} C_F^2 - \left(\frac{25}{8} + \xi_G + \frac{1}{8}\xi_G^2\right) C_F C_A + \frac{1}{2} C_F n_f, \\
Z_g^{(2,1)} &= -\frac{17}{6} C_A^2 + \frac{1}{2} C_F n_f + \frac{5}{6} C_A n_f, \\
Z_M^{(2,1)} &= -\frac{3}{4} C_F - \frac{97}{12} C_F C_A + \frac{5}{6} C_F n_f, \\
Z_{m_r}^{(2,1)} &= \left(-\frac{383}{192} - \frac{7}{64}\xi_G - \frac{3}{32}\xi_G^2\right) + \left(\frac{1}{2} + \frac{1}{4}\xi_G\right) C_F n_f + \left(\frac{5}{12} - \frac{5}{16}\xi_G\right) C_A n_f
\end{aligned} \tag{3.37}$$

$$
\begin{aligned}
Z_G^{(2,2)} &= \left(-\frac{13}{8} - \frac{17}{24}\xi_G + \frac{3}{16}\xi_G^2\right) C_A^2 + \left(\frac{1}{2} + \frac{1}{3}\xi_G\right) C_A n_f, \\
Z_\eta^{(2,2)} &= \left(-\frac{35}{32} + \frac{3}{32}\xi_G^2\right) C_A^2 + \frac{1}{4} C_A n_f, \\
Z_\psi^{(2,2)} &= \frac{1}{2}\xi_G^2 C_F^2 + \left(\frac{3}{4}\xi_G + \frac{1}{4}\xi^2\right) C_F C_A, \\
Z_g^{(2,2)} &= \frac{121}{24} C_A^2 - \frac{11}{2} C_F C_A - C_F n_f, \\
Z_M^{(2,2)} &= \frac{9}{2} C_F^2 + \frac{11}{2} C_F C_A - C_F n_f, \\
Z_{m_r}^{(2,2)} &= \left(\frac{1211}{384} + \frac{59}{192}\xi_G + \frac{5}{128}\xi_G^2\right) C_A^2 - \frac{1}{2}\xi_G C_F n_f + \left(\frac{7}{12} - \frac{1}{24}\xi_G\right) C_A n_f - \frac{2}{3} n_f^2
\end{aligned}
\tag{3.38}
$$

The terms $Z_{m_r}^{(k,l)}$ are the corresponding counter-terms for the regulator mass, which are introduced to regularize the infra-red divergences.

3.6 Renormalization Group

The process of renormalization allows us to subtract all the divergences which appear in Green's functions order-by-order in perturbation theory. This subtraction procedure is characterized by arbitrariness: in setting up the condition to extract the divergences, and of fixing the renormalization scale μ. Physical observables, such as the S-matrix elements, are independent of the scheme used to renormalize the corresponding theories [26]. The symmetry associated to this invariance is described by the renormalization group (RG) [34]. The bare fields and the bare coupling are renormalization-group invariants and the response of Green's functions and parameters to the variation of the renormalization scale μ is described by the renormalization group equations (RGE), which are employed to verify the validity of perturbation theory.

For a general theory with several couplings and masses the RGE takes the following form,

$$
\begin{aligned}
\left(\mu\frac{\partial}{\partial\mu} + \beta^j\frac{\partial}{\partial g_j} - \gamma_{m,\beta} m_\beta \frac{\partial}{\partial m_\beta} - n_B\gamma_B - n_f\gamma_f + \gamma_\xi\frac{\partial}{\partial\xi}\right) \\
\times\Gamma_R^{n_B,n_f}\left(p_k; g_i, m_\alpha, \xi; \mu\right) = 0,
\end{aligned}
\tag{3.39}
$$

where n_B and n_f refer to the number of bosonic and fermionic fields, respectively; and the renormalization functions, which play a crucial role in deriving fundamental properties of a given theory, are defined as:

$$
\beta^j(g, m, \xi; \mu) = \lim_{\varepsilon\to 0} \mu\frac{\partial}{\partial\mu} g_j\left(g_0\mu^\varepsilon, m_0, \xi_0; \mu\right) \tag{3.40}
$$

$$\gamma_{m,\beta}(g,m,\xi;\mu) = -\lim_{\varepsilon\to 0}\frac{1}{m_\beta}\mu\frac{\partial}{\partial\mu}m_\beta\left(g_0\mu^\varepsilon, m_0, \xi_0;\mu\right) \tag{3.41}$$

$$\gamma_B(g,m,\xi;\mu) = -\lim_{\varepsilon\to 0}\frac{1}{2R_B}\mu\frac{\partial}{\partial\mu}R_B\left(g_0\mu^\varepsilon, m_0, \xi_0;\mu\right) \tag{3.42}$$

$$\gamma_f(g,m,\xi;\mu) = -\lim_{\varepsilon\to 0}\frac{1}{2R_f}\mu\frac{\partial}{\partial\mu}R_f\left(g_0\mu^\varepsilon, m_0, \xi_0;\mu\right) \tag{3.43}$$

$$\gamma_\xi(g,m,\xi;\mu) = \lim_{\varepsilon\to 0}\mu\frac{\partial}{\partial\mu}\xi\left(g_0\mu^\varepsilon, m_0, \xi_0;\mu\right) \tag{3.44}$$

The expression (3.39) is the generalized Callan-Symanzik equation appropriate for correlation functions. It simply states that the couplings and wave-function renormalization factors change as we change the scale in such a way that correlation functions remain unchanged. It is worth pointing out here that if the theory is $\overline{\text{MS}}$-renormalized the above renormalization-group coefficients do not depend on the mass. Moreover the β and the γ_m functions are gauge-independent and simply related to coefficients of counter-terms which renormalize ultraviolet divergences.

Chapter 4

Effective Field Theories

Effective field theory (EFT) plays an important role in the description of phenomena which are spread out over different energy or length scales. Its realization simplifies calculations or even allows model-independent statements. This chapter describes the basis of this powerful tool and covers the techniques used within this framework. The content is organized as follows: Section 4.1 is an overview of what EFT is. In the succeeding section, Section 4.2, the renormalization of an effective theory is described. Section 4.3 explains the process of decoupling of heavy modes within the $\overline{\text{MS}}$-scheme. Some calculations for the dimension four terms are presented in Section 4.4, where we explicitly show the cancellation of infra-red divergences. The matching equations for higher-dimensional terms are summarized in Section 4.5. There we explain the matching between a complete theory and an effective field theory, and how the decoupling of heavy particles occurs between two effective field theories. The last part of the chapter is devoted to the cancellations of scheme dependence and the solution of the renormalization group invariant equation for the Wilson coefficients.

4.1 Introduction to Effective Field Theories

Interesting physical phenomena appear everywhere. Fortunately, there is no need to understand all this fantastic richness of events at the same time. In fact, for very different energy scales, one can isolate all those desired observables from all the rest and focus on their study. By doing this, one gets an approximate description of the relevant physics. The effects of those terms which have been neglected can be included as perturbations. Thus the Lagrangian of an effective field theory is expanded into a finite number of terms of dimension four or less, and a tower of higher dimensional operators: $Q_{i,0}$,

$$\mathcal{L}_0^{\text{eff}} = [\mathcal{L}_0]_{d\leq 4} + \sum_i \frac{C_{i,0}}{\Lambda^{\dim[Q_i]-4}} Q_{i,0}. \tag{4.1}$$

Here the factor Λ parametrizes a UV energy scale and the subscript 0 refers to bare quantities. The coefficient functions $C_{i,0}$ can be understood as effective couplings which encode the information of high energy physics. These important terms are known by the name of Wilson coefficients and can be calculated in perturbation theory. The process of determining these low energy parameters is called *matching*. The basic requirement is that the effective Lagrangian, which is displayed in equation (4.1), reproduces the physics of the more fundamental theory. When the previous series is truncated, the short distance physics changes, hence the values of the low energy parameters are modified to account for these effects. Moreover, the sum in equation (4.1) is infinite and includes all possible Lorentz singlet gauge invariant operators which preserve the quantum numbers of the corresponding theory. The equations of motion can be used to reduce the number of terms [35]. Those operators that are reducible to full derivatives give vanishing contributions to the physical matrix elements and can be discarded when the on-shell matching is performed. For the off-shell case the equation of motion operators play an important role in the renormalization of an effective field theory as we will see in the coming chapters.

4.2 Renormalization of Composite Operators

In the previous chapter we discussed the importance of renormalization and how this procedure takes place for a complete theory. Here we aim to describe this required feature within the framework of EFT, where the information of high energy physics is encoded in the tower of operators. To renormalize the effective Green's functions, one needs to understand the renormalization of the bare operators. Let us consider a general structure for an unrenormalized four-fermion operator,

$$Q_{i,0} = (\bar{\psi}_0 \Gamma_\mu \psi_0)(\bar{\psi}_0 \tilde{\Gamma}^\mu \psi_0), \tag{4.2}$$

where Γ_μ and $\tilde{\Gamma}^\mu$ denote the Dirac matrices. For simplicity the colour and flavour indices are not displayed. The above expression implies that any renormalized operator involves the renormalization of the fields from which it is constructed. However, it is well known that this is not enough to get a finite result. The renormalization of bare operators might require counter-terms proportional to other operators of the same dimension and Lorentz structure, $Q_{j,0}$. This is known under the name of *operator mixing* [36]. With all of this information at hand, one is ready to write down a relation between the bare and renormalized operators which is given by the expression below,

$$Q_{i,0} = Z_\psi^2 Z_{ij} Q_j. \tag{4.3}$$

The matrix Z_{ij} describes the mixing between operators. A NNLO analysis typically requires the evaluation of the one-, two- and three-loop Feynman diagrams with insertions of the physical operators and the evanescent operators listed in section 4.6.4. This element can be perturbatively expanded in a power series of the coupling constants,

$$Z_{ij} = \delta_{ij} + \sum_{\substack{n,m=0 \\ n+m\geq 1}} [\tilde{\alpha}_s(\mu_0)]^n \, [\tilde{\alpha}_e(\mu_0)]^m \, Z_{ij}^{(n,m)}, \tag{4.4}$$

where the tilde notation denotes: $\tilde{\alpha}_k = \alpha_k/(4\pi)$, with $k = s, e$. Within the $\overline{\text{MS}}$-scheme the mixing matrix is given by pure poles

$$Z_{ij}^{(n,0)} = \sum_{l=0}^{n} \frac{1}{\varepsilon^l} Z_{ij}^{(n,l)}, \quad Z_{ij}^{(0,m)} = \sum_{l=0}^{m} \frac{1}{\varepsilon^l} Z_{ij}^{(m,l)}, \quad Z_{ij}^{(es)} = \sum_{l=0}^{2} \frac{1}{\varepsilon^l} Z_{ij}^{(es,l)}. \tag{4.5}$$

It is worth mentioning here that this is not the case when the index i corresponds to an evanescent operator, but j does not. This kind of operator, that appears within dimensional regularization and vanishes in the limit to four dimensions, requires a finite piece to fully accomplish this [37]. In section 4.6.4 we will introduce the evanescent operators in more detail.

4.3 Decoupling Relations

The realization of the Appelquist-Carazzone decoupling theorem [38,39] within a gauge theory renormalized by the minimal subtraction (MS) scheme has been studied in the past [40–43]. As is well known, this theorem is not directly implemented when MS-schemes are employed. The main reason is that the β and γ_m functions governing the behaviour of the running coupling constant, $\alpha(\mu)$, and the light-fermion masses, $m_i(\mu)$, are independent of any mass. Consequently, the disconnection of heavy particles does not hold true in its naïve sense. To circumvent this problem a rescaling of the coupling constant, the gauge parameter, the masses for the light fermions, and the fields for the light particles has to be performed in the effective field side to include the effects of heavy particles that appear in the loops.

To obtain the corresponding decoupling equations for the MS-scheme to arbitrary order in the loop expansion we use as an intermediate step the so-called momentum subtraction (MO) scheme where the validity of the decoupling theorem holds to each order in perturbation theory. The fundamental idea here is that any MO-renormalized Green's function, $\hat{\Gamma}_R$, is related to its MS-renormalized version, Γ_R, by a product of a finite wave function renormalization, $z_\Gamma(\alpha, m_i, M, \xi, \mu) \equiv z_\Gamma$,

$$\hat{\Gamma}_R(p_k; \hat{\alpha}, \hat{m}_i, \hat{M}, \hat{\xi}, \mu) = z_\Gamma \; \Gamma_R(p_k; \alpha, m_i, M, \xi, \mu). \tag{4.6}$$

Note that the quantities of the momentum subtraction scheme have been denoted by hats. Any parameter without this notation is considered as a MS-variable.

For an energy scale $\mu \ll \hat{M}$, we have, to any given order in the loop expansion, decoupling of the heavy fermions from $\hat{\Gamma}_R$ and also from the renormalization group functions governing the scale behaviour of $\hat{\alpha}$, $\hat{m}_i$, $\hat{\xi}$. In this range the MO-renormalized Green's function of the complete theory is, up to terms of order $1/\hat{M}$, identical to the corresponding quantities obtained from the MO-renormalized effective Green's function,

$$\hat{\Gamma}_R(p_k;\hat{\alpha},\hat{m}_i,\hat{M},\hat{\xi},\mu) = \hat{\Gamma}'_R(p_k;\hat{\alpha}',\hat{m}'_i,\hat{\xi}',\mu) + \mathcal{O}\left(\frac{1}{\hat{M}}\right), \tag{4.7}$$

where Γ'_R depends on the effective quantities which have been denoted by primes. Similar to equation (4.6) we have,

$$\hat{\Gamma}'_R(p_k;\hat{\alpha}',\hat{m}'_i,\hat{\xi}',\mu) = z'_\Gamma\ \Gamma'_R(p_k;\alpha',m'_i,\xi',\mu). \tag{4.8}$$

Combining all the previous results we obtain the decoupling equation for the MS-scheme,

$$\Gamma'_R(p_k;\alpha',m'_i,\xi',\mu) = \frac{z_\Gamma}{z'_\Gamma}\ \Gamma_R(p_k;\alpha,m_i,M,\xi,\mu) + \mathcal{O}\left(\frac{1}{\hat{M}}\right), \tag{4.9}$$

with

$$\frac{z'_\Gamma}{z_\Gamma} \equiv \zeta_\Gamma. \tag{4.10}$$

This ζ_Γ term encodes the contributions from the heavy particles and plays an important role in the definition of the effective parameters. Indeed, at higher orders in perturbation theory, this factor controls the discontinuities of the coupling and the fermion mass that appear at the threshold scale. From equation (4.9) it is easy to see that these corrections can be determined through a matching between the fundamental theory with all heavy modes and its effective realization built up only with light fields. The respective calculation requires the equality of the Green's functions in the two theories at the matching scale $\mu_i = \mathcal{O}(M_i)$, where M_i is the mass of the heavy particle.

4.4 Threshold corrections for the $d = 4$ terms

In what follows we will explain the basis behind this technique by means of the computation of the rescaling for the gauge field, the strong coupling and the light fermion fields and masses. For this purpose we consider a non-abelian gauge theory with gauge group G and n_f fermions, of which n_h are heavy distinct multiplets of fermions, ψ_h, with non-vanishing mass M, and n_l light fermion fields, ψ_l, with a lighter mass m. All the fields are in the fundamental representation of G. The Lagrangian which describes this theory is given in section 3.5. The results presented in the subsequent subsections were previously computed in [41,42], although here we use an independent technique to

regularise the infra-red divergences in the matching. The confirmation of the literature results serves as a test of our calculational setup. The threshold corrections obtained will be used for our computation of Next-to-Next-to-leading order corrections for the hadronic $\Delta S = 1$ effective Hamiltonian discussed in Chapter 5.

4.4.1 The gluon field

In this part we aim to compute the decoupling of a heavy particle and its effect on the redefinition of the effective gluon field up to second order in perturbation theory. This rescaling is given by

$$G'^{a}_{\mu} = \sqrt{\frac{Z_G}{Z'_G}\zeta^0_G} G^a_\mu = \sqrt{\zeta_G} G^a_\mu, \tag{4.11}$$

where the unknown ζ_G refers to the threshold corrections due to heavy particles. To obtain this quantity we require the calculation of the two-point Green's functions in both theories,

$$1 + \sum_{i=1}^{2} \Pi^{(i)(2G)}(p^2) = \zeta_G \left(1 + \sum_{i=1}^{2} \Pi'^{(i)(2G')}(p^2) \right). \tag{4.12}$$

In the equation above $\Pi^{(2G)}(p^2)$ and $\Pi^{(2G')}(p^2)$ stand for the gluon vacuum polarizations in the full and in the effective field theory respectively. Diagrams with virtual heavy particles have been omitted in the effective field side. Equation (4.12) leads to

$$\zeta_G = \left(1 + \sum_{i=1}^{2} \Pi_h^{(i)(2G)}(p^2) \right), \tag{4.13}$$

where $\Pi_h^{(2G)}(p^2)$ is the heavy contribution to the gluon vacuum polarization. The situation is as follows: only one graph contributes at one-loop, and, at two-loop, six diagrams have to be considered. After having computed these gluon self-energy diagrams up to order $\mathcal{O}(\tilde{\alpha}_s^2)$ and for $N_c = 3$, we finally obtain

$$\zeta_G = 1 + \tilde{\alpha}_s(\mu)\frac{2}{3}\ln\left(\frac{\mu^2}{m_h^2}\right) + \tilde{\alpha}_s^2(\mu)\left[\frac{91}{72} + \frac{29}{6}\ln\left(\frac{\mu^2}{m_h^2}\right) + \frac{3}{2}\ln^2\left(\frac{\mu^2}{m_h^2}\right)\right]. \tag{4.14}$$

Notice that the first contribution appears at one-loop level. Moreover, it is important to stress the case of the gauge parameter ξ_G, which also receives threshold corrections at one-loop. Hence, the effective parameter is related to the one in the full theory by means of

$$\xi'_G = \zeta_{\xi_G}\xi_G, \tag{4.15}$$

where the threshold correction parameter is obtained through the heavy contribution of the gluon self-energy,

$$\zeta_{\xi_G} = \left(1 + \sum_{i=1}^{2} \Pi_h^{(i)(2G)}(p^2)\right). \tag{4.16}$$

That $\zeta_{\xi_G} = \zeta_G$ can be easily understood from the gauge-fixing term in equation (3.29).

4.4.2 The strong coupling

Effects of heavy fields also require the redefinition of the effective coupling constant,

$$g_s' = \left(\frac{Z_g}{Z_g'}\zeta_g^0\right) g_s = \zeta_g g_s. \tag{4.17}$$

The end goal here is to compute ζ_g. Hence we consider the three-gluon vertex function $\Gamma^{(3G)}(p^2)$, and require consistency between both theories,

$$\left[g_s + \sum_{i=1}^{2} \Gamma^{(i)(3G)}(p^2)\right] \partial^\mu G^{a\nu} G_\mu^b G_\nu^c = \left[g_s' + \sum_{i=1}^{2} \Gamma'^{(i)(3G')}(p^2)\right] \partial^\mu G'^{a\nu} G'^{b}_\mu G'^{c}_\nu. \tag{4.18}$$

The term $\Gamma'^{(i)(3G)}(p^2)$ does not contain heavy contributions, that is, only diagrams with light fields have to be considered. Expressing the effective coupling and fields in terms of the full theory variables ones arrives at

$$\zeta_g = \frac{1 + \sum_{i=1}^{2} \Gamma_h^{(i)(3G)}(p^2)}{\zeta_G^{3/2}}. \tag{4.19}$$

According to the above equation two terms enter the calculation of ζ_g: the hard part of the gluon propagator and the three gluon vertex corrections. For convenience we use the relation $\alpha_s(\mu) = g_s^2/4\pi$ to rewrite equation (4.17) as

$$\tilde{\alpha}_s'(\mu) = \zeta_g^2 \tilde{\alpha}_s(\mu), \tag{4.20}$$

with $\tilde{\alpha}_s(\mu) = \alpha_s(\mu)/4\pi$, and present the results for ζ_g^2,

$$\begin{aligned} \zeta_{g^2} = 1 &+ \tilde{\alpha}_s(\mu)\left[-\frac{2}{3}\ln\left(\frac{\mu^2}{m_h^2}\right) + \frac{\varepsilon}{3}\left(\zeta_2 + \ln^2\left(\frac{\mu^2}{m_h^2}\right)\right)\right] \\ &+ \tilde{\alpha}_s^2(\mu)\left[\frac{13}{12}\frac{1}{N_c} + \frac{25}{36}N_c - \left(\frac{1}{N_c} + \frac{7}{3}N_c\right)\ln\left(\frac{\mu^2}{m_h^2}\right) + \frac{4}{9}\ln^2\left(\frac{\mu^2}{m_h^2}\right)\right]. \end{aligned} \tag{4.21}$$

Here we have denoted ζ_g^2 by ζ_{g^2}, and the term ζ_2 is the well-known Riemann zeta function. Moreover, we compute up to order $\mathcal{O}(\varepsilon)$ terms at one-loop since they are needed for later purpose. Equation (4.21) is valid for the general gauge group $SU(N_c)$. Note that $\zeta_{g^2}^{(1)} = -\zeta_G^{(1)}$, which will be used in the evaluation of threshold corrections

for the QCD penguin and the fermion self energy.

4.4.3 The quark field and mass

In our non-abelian gauge theory we consider the scenario of light and heavy fermion fields. Then not all the fermion fields are integrated out as a dynamical degree of freedom and the light fields have to be redefined as follows:

$$\psi'_q = \sqrt{\frac{Z_{\psi_q}}{Z'_{\psi_q}}\zeta^0_{\psi_q}}\psi_q = \sqrt{\zeta_{\psi_q}}\psi_q. \tag{4.22}$$

The evaluation of the fermion self-energy diagrams is necessary to determine the renormalized decoupling constant ζ_{ψ_q},

$$1 + \sum_{i=1}^{2} \Sigma_V^{(i)(2\psi)}(p^2) = \zeta_{\psi_q}\left(1 + \sum_{i=1}^{2} \Sigma_V^{\prime(i)(2\psi')}(p^2)\right). \tag{4.23}$$

In analogy to the two cases presented above, only the diagrams involving the heavy fermions contribute. We write

$$\zeta_{\psi_q} = \left(1 + \sum_{i=1}^{2} \Sigma_{V,h}^{(i)(2\psi)}(p^2)\right), \tag{4.24}$$

where $\Sigma_{V,h}^{(2\psi)}(p^2)$ are the vector components of the heavy fermion self-energy. Note that the first contribution will appear at two loops and only one diagram has to be evaluated. The explicit result reads

$$\zeta_{\psi_q} = 1 + \tilde{\alpha}_s^2(\mu) C_F \left[\frac{5}{12} - \ln\left(\frac{\mu^2}{m_h^2}\right)\right]. \tag{4.25}$$

We will give more details on this calculation after having discussed how the decoupling of the ψ_h fields modify the effective mass parameter.

If the light fermions are massive their effective masses are affected by the threshold corrections of heavy fields as well,

$$m'_\psi(\mu) = \frac{Z_m}{Z'_m}\zeta^0_{m_\psi} m_\psi(\mu) = \zeta_{m_\psi} m_\psi(\mu). \tag{4.26}$$

From the Lagrangian we have $\mathcal{L}_m^{\text{eff}} = m'_0 \bar{\psi}'_0 \psi'_0$. Therefore, to calculate ζ_{ψ_m}, we have to divide by the decoupling factor ζ_{ψ_q} and find

$$\zeta_{m_\psi} = \frac{\left(1 - \sum_{i=1}^{2} \Sigma_{S,h}^{(i)(2\psi)}(p^2)\right)}{\left(1 + \sum_{i=1}^{2} \Sigma_{V,h}^{(i)(2\psi)}(p^2)\right)}. \tag{4.27}$$

Remember that there are no one-loop diagrams contributing to $\Sigma_{V,h}^{(2\psi)}(p^2)$ and $\Sigma_{S,h}^{(2\psi)}(p^2)$. At the next order in perturbation theory there is just one diagram and its evaluation results in

$$\zeta_{m_\psi} = 1 + \tilde{\alpha}_s^2(\mu) C_F \left[\frac{89}{36} - \frac{5}{3} \ln\left(\frac{\mu^2}{m_h^2}\right) + \ln^2\left(\frac{\mu^2}{m_h^2}\right) \right]. \tag{4.28}$$

Gauge dependence and Infra-red logarithms

In what follows we aim to show the beauty of the cancellation of the gauge dependence and the infra-red (IR) logarithms that takes place in the computation of ζ_{ψ_q} and ζ_{m_ψ}. For this goal we will show some intermediate results such as the one-loop amplitudes. The reason for doing this is that at two-loops extra contributions proportional to this one-loop term will appear once the threshold corrections of the coupling and the gauge parameter are incorporated. For this will be useful to understand the threshold corrections for the effective operators, in particular the case when we will set the light quark mass to zero.

In the complete theory the fermion self-energy,

$$\Sigma^{(2\psi)}(p^2) = \not{p}\Sigma_V^{(2\psi)}(p^2) + m_q \Sigma_S^{(2\psi)}(p^2), \tag{4.29}$$

has the following expansion in the strong coupling,

$$\Sigma^{(2\psi)}(p^2) = \Sigma^{(0)(2\psi)}(p^2) + \tilde{\alpha}_s(\mu)\Sigma^{(1)(2\psi)}(p^2) + \tilde{\alpha}_s^2(\mu)\Sigma^{(2)(2\psi)}(p^2). \tag{4.30}$$

At two-loops, only the diagram containing the heavy fermion as a virtual particle has to be computed, $\Sigma_h^{(2)(2\psi)}(p^2)$. To renormalize this amplitude we also include the corresponding one-loop diagram with inserted counter-term, and the local overall counter-term. The first one is needed to extract the divergences of the sub-diagram, and the second one is required to renormalize the full result. We have used dimensional regularization and the $\overline{\text{MS}}$-scheme, getting the following results up to two loops,

- **Tree-Level**:

$$\Sigma_V^{(0)(2\psi)} = 1, \tag{4.31}$$

$$\Sigma_S^{(0)(2\psi)} = 1. \tag{4.32}$$

- **One-Loop**:

$$\Sigma_V^{(1)(2\psi)} = C_F \xi_G \left[\frac{1}{2} + \ln\left(\frac{\mu^2}{m^2}\right) \right] \delta_{ij}, \tag{4.33}$$

$$\Sigma_S^{(1)(2\psi)} = C_F \left[1 + \xi_G + (3 + \xi_G) \ln\left(\frac{\mu^2}{m^2}\right) \right] \delta_{ij} + \mathcal{O}(\varepsilon). \tag{4.34}$$

- **Two-Loops**:

$$\begin{aligned}\Sigma_V^{(2)(2\psi)} = C_F \Bigg[& \frac{1}{2\varepsilon} n_l - \frac{5}{4} n_h + 6 f_1(n_h, M, m, \mu) \\ & - (1 + 6\frac{M^2}{m^2}) f_2(n_h, m, \mu) + f_{V,3}(n_h, M, m) \Bigg] \delta_{ij},\end{aligned} \tag{4.35}$$

$$\begin{aligned}\Sigma_S^{(2)(2\psi)} = C_F \Bigg[& \frac{1}{\varepsilon^2}(3C_F\xi_G - n_l) + \frac{4}{3\varepsilon} n_l + \frac{2}{3} n_h + f_{S,3}(n_h, M, m) \\ & - \left(\frac{22}{3} + 8\frac{M^2}{m^2} + \frac{2}{n_h}\frac{m^2}{M^2} f_1(M, m, \mu) \right) f_2(n_h, m, \mu) \\ & + \left(8 + 4\frac{m^2}{M^2} + \frac{1}{n_h}\frac{m^4}{M^4} f_1(M, m, \mu) \right) f_1(M, m, \mu) \Bigg] \delta_{ij}.\end{aligned} \tag{4.36}$$

To simplify the results at two-loops, we have defined the following functions,

$$\begin{aligned} f_1(n_h, M, m, \mu) &= \frac{M^2}{m^2} n_h \left[\ln\left(\frac{\mu^2}{M^2}\right) - 2 \right], \\ f_2(n_h, m, \mu) &= n_h \ln\left(\frac{\mu^2}{m^2}\right), \\ f_{V,3}(M, m) &= 6\frac{M^4}{m^4} n_h \Phi\left(\frac{m^2}{4M^2}\right), \\ f_{S,3}(n_h, M, m) &= \left[8\frac{M^4}{m^4} + 2\frac{M^2}{m^2} - 1 \right] n_h \Phi\left(\frac{m^2}{4M^2}\right), \end{aligned} \tag{4.37}$$

where the function $\Phi\left(m^2/4M^2\right)$ arises due to the calculation of the two-loop massive integrals, see Section 3.2.4.

On the effective field side there are no diagrams which contain the heavy fields, and only the local overall counter-term must be included, $\Sigma_{ct}^{\prime(2)(2\psi)}(p^2)$. In our calculations we have kept the mass of the light particles and we have expressed everything in terms of the effective coupling $\tilde{\alpha}_s'(\mu)$ and the gauge parameter ξ_G of the full theory. The expansion can be regarded as

$$\begin{aligned}\Sigma^{\prime(2\psi)}(p^2) = & \Sigma^{\prime(0)(2\psi)}(p^2) + \tilde{\alpha}_s(\mu)\Sigma^{\prime(1)(2\psi)}(p^2) \\ & + \tilde{\alpha}_s^2(\mu) \left[\Sigma^{\prime(2)(2\psi)}(p^2) + \zeta_{g^2}^{(1)} \Sigma^{\prime(1)(2\psi)}(p^2) + \zeta_{\xi_G}^{(1)} \Sigma_\xi^{\prime(1)(2\psi)}(p^2) \right].\end{aligned} \tag{4.38}$$

Here the subscript ξ in the last term denotes only the ξ dependent part of the one-loop fermion self-energy function. To simplify the notation of our discussion we will denote the $\mathcal{O}(\tilde{\alpha}_s)$ term by $\tilde{\Sigma}^{\prime(2)(2\psi)}(p^2)$. The latter has to be understood as the sum of all the components appearing in the last line of equation (4.38). Finally, up to two loops we get:

- **Tree-Level**:

$$\Sigma_V'^{(0)(2\psi)} = 1, \tag{4.39}$$

$$\Sigma_S'^{(0)(2\psi)} = 1. \tag{4.40}$$

- **One-Loop**:

$$\Sigma_V'^{(1)(2\psi)} = C_F \xi_G \left[\frac{1}{2} + \ln\left(\frac{\mu^2}{m^2}\right)\right] \delta_{ij}, \tag{4.41}$$

$$\Sigma_S'^{(1)(2\psi)} = C_F \left[1 + \xi_G + (3+\xi_G)\ln\left(\frac{\mu^2}{m^2}\right)\right] \delta_{ij} + \mathcal{O}(\varepsilon). \tag{4.42}$$

- **Two-Loops**:

$$\tilde{\Sigma}_V'^{(2)(2\psi)} = C_F \left[\frac{n_l}{2\varepsilon} + \xi_G \left[\zeta_{\xi_G}^{(1)} + \zeta_{g^2}^{(1)}\right] \left(\frac{1}{2} + \frac{1}{n_h} f_2(n_h, m, \mu)\right)\right] \delta_{ij}, \tag{4.43}$$

$$\begin{aligned}\tilde{\Sigma}_S'^{(2)(2\psi)} = C_F \Bigg[&\frac{1}{\varepsilon^2}(3C_F\xi_G - n_l) + \frac{4}{3\varepsilon} n_l + \zeta_{g^2}^{(1)} \left(1 + \frac{3}{n_h} f_2(n_h, m, \mu)\right) \\ &+ \xi_G \left[\zeta_{\xi_G}^{(1)} + \zeta_{g^2}^{(1)}\right] \left(1 + \frac{1}{n_h} f_2(n_h, m, \mu)\right)\Bigg] \delta_{ij}.\end{aligned} \tag{4.44}$$

Notice that the sum $\zeta_{\xi_G}^{(1)} + \zeta_{g^2}^{(1)}$ vanishes since $\zeta_{\xi_G}^{(1)} = -\zeta_{g^2}^{(1)}$. In addition, performing the matching at two loops we observed that the remaining infra-red divergences cancel out when the function $\Phi(m^2/4M^2)$ is expanded around $x = m/M$:

$$\Phi\left(\frac{m^2}{4M^2}\right) \approx \frac{5m^4}{18M^4} - \frac{m^4}{6M^4}\ln\left(\frac{m^2}{M^2}\right) + \frac{2m^2}{M^2} - \frac{m^2}{M^2}\ln\left(\frac{m^2}{M^2}\right). \tag{4.45}$$

Finally, we end with a finite result, see eq. (4.25) and eq. (4.28), as it should be. That this result agrees with the results in the literature where the light mass was neglected from the start [44] serves as a further check of our calculational setup and also makes the cancellation in intermediate steps of the calculation more apparent.

4.5 Threshold corrections for higher order dimensional operators

So far we only discussed the matching of renormalizable theories such as QCD. Yet effective theories also receive matching corrections and these matching correction can play an important contribution to precision observables. In the following section we will specify the concepts described in Section 4.3 to theories that incorporate higher dimensional operators. In the following sub-sections, we give the general expressions for the low-energy parameters obtained through the matching process. Two different cases are discussed: the first relates a complete theory and an effective theory, and in the second the decoupling of heavy particles is performed between two effective field theories.

4.5.1 Matching of Full Theories onto Effective Theories

In equation (4.9) only terms up to order $1/M$ have been considered. This formalism can be extended to incorporate the effects of the irrelevant operators, ($d > 4$). For analogy with our projects, we will make the assumption that there will not be any contribution at $d = 5$, and that the first non-zero contribution appears at $d = 6$. To incorporate these new effects we extend the previous expression up to order $1/M^3$, and we match the Green's functions of the complete and the effective field theory. The latter are obtained by using the effective Lagrangian presented in equation (4.1).

The Green's functions of the full theory can be perturbatively expanded in the following general form,

$$\Gamma_R(p_k; \tilde{\alpha}_i, m_i, M, \xi, \mu_0) = \langle \vec{Q} \rangle^{(0)T} \sum_{\substack{n,m=0 \\ n+m \geq 1}} [\tilde{\alpha}_s(\mu_0)]^n \, [\tilde{\alpha}_e(\mu_0)]^m \, \vec{T}^{(n,m)}(\mu_0), \tag{4.46}$$

where the terms $\langle \vec{Q} \rangle^{(0)}$ represent the tree-level matrix elements, which can be written as sums of products of spinors, polarisation vectors, Dirac gamma matrices and Lorentz structures formed out of incoming and outgoing momenta. The factors $\vec{T}^{(n,m)}$ appearing in the expression above are extracted by computing all the possible Feynman diagrams with their respective radiative corrections. To renormalize the amplitude we have to insert all the required counter-terms. Beyond one-loop, the $(l-1)$-diagrams with inserted counter-terms are also needed to subtract the UV divergences of the sub-graphs.

In the same way, one expands perturbatively the renormalized effective amplitude to the same order in perturbation theory,

$$\Gamma'_R(p_k;\tilde{\alpha}'_i,m'_i,\xi',\mu_0)=\langle\vec{Q}\rangle^{(0)T}\sum_{\substack{n,m=0\\ n+m\geq 1}}\left[\tilde{\alpha}'_s(\mu_0)\right]^n\left[\tilde{\alpha}'_e(\mu_0)\right]^m\left[\hat{r}^{(n,m)}\right]^T\vec{C}(\mu_0). \quad (4.47)$$

The matrices $\hat{r}^{(n,m)}$ include the mixing and the wave function renormalization of the fields in the operators. The parameters of the low energy theory are also expanded in a power series of the couplings,

$$\vec{C}(\mu_0)=\sum_{\substack{n,m=0\\ n+m\geq 1}}\left[\tilde{\alpha}'_s(\mu_0)\right]^n\left[\tilde{\alpha}'_e(\mu_0)\right]^m\vec{C}^{(n,m)}(\mu_0). \quad (4.48)$$

Requiring that both theories describes the same physics one can extract the initial conditions for the Wilson coefficients, order-by-order in perturbation theory. Up to two loops they are parametrized by the following expression,

$$\begin{aligned}
\vec{C}^{(0)}(\mu_0) &= \vec{T}^{(0)},\\
\vec{C}_s^{(1)}(\mu_0) &= \vec{T}_s^{(1)}-\hat{r}_s^{(1)T}\vec{T}^{(0)},\\
\vec{C}_e^{(1)}(\mu_0) &= \vec{T}_e^{(1)}-\hat{r}_e^{(1)T}\vec{T}^{(0)},\\
\vec{C}_s^{(2)}(\mu_0) &= \vec{T}_s^{(2)}-\hat{r}_s^{(1)T}\left[\vec{T}_s^{(1)}-\hat{r}_s^{(1)T}\vec{T}_s^{(0)}\right]-\hat{r}_s^{(2)T}\vec{T}_s^{(0)},\\
\vec{C}_e^{(2)}(\mu_0) &= \vec{T}_e^{(2)}-\hat{r}_e^{(1)T}\left[\vec{T}_e^{(1)}-\hat{r}_e^{(1)T}\vec{T}_e^{(0)}\right]-\hat{r}_e^{(2)T}\vec{T}_e^{(0)},\\
\vec{C}_{se}^{(2)}(\mu_0) &= \vec{T}_{se}^{(2)}-\hat{r}_s^{(1)T}\vec{T}_e^{(1)}-\hat{r}_e^{(1)T}\vec{T}_s^{(1)}+\left[\hat{r}_s^{(1)T}\hat{r}_e^{(1)T}+\hat{r}_e^{(1)T}\hat{r}_s^{(1)T}-\hat{r}_{se}^{(2)T}\right]\vec{T}^{(0)}.
\end{aligned} \quad (4.49)$$

For convenience we have simplified the notation here. Note that se stands for the order $(1,1)$, the subscript s describes the $(n,0)$ corrections, and e refers to the $(0,m)$ terms. In addition, the μ_0 dependence of the $\vec{T}$ elements has been omitted.

4.5.2 Matching of Effective Theories onto Effective Theories

When the physical phenomena of interest occur at sufficiently small energy scales, it is possible to modify the theory again and construct a new effective field theory that does not contain the heaviest particles of the previous one. In this situation we would match two effective field theories, and their respective Wilson coefficients would be related via

$$\vec{C}'(\mu_i)=\hat{M}(m_i,\mu_i)\vec{C}(\mu_i). \quad (4.50)$$

Here the prime notation stands for the lower energy theory, and $\hat{M}(m_i,\mu_i)$ is the finite matching matrix obtained at the threshold scale μ_i. These corrections are determined by matching renormalized effective Green's functions, equation (4.47), with operator

insertions in both theories at the threshold scale $\mu_i = \mathcal{O}(m_i)$. For higher orders, the discontinuities for the fields, masses and couplings have to be included. In our calculations all quantities will be expressed in terms of the coupling constant $\tilde{\alpha}'(\mu_i)$ and all the fields in terms of the ones in the fundamental theory.

The process of renormalization is not very obvious. In fact, for higher order corrections one should be careful. For instance, to get rid of the UV divergences of the one-particle-irreducible sub-diagrams the inclusion of EOM-operators are required, as we perform an off-shell matching procedure. This will be explained in more detail in Section 5.3.1.

Introducing the following discontinuities for the Wilson coefficients and the matrix elements

$$\delta C_\alpha^{(l)}(\mu_i) = C_\alpha^{(l)}(\mu_i) - C_\alpha^{\prime(l)}(\mu_i), \quad \delta \hat{r}_\alpha^{(l)}(\mu_i) = \hat{r}_\alpha^{(l)}(\mu_i) - \hat{r}_\alpha^{\prime(l)}(\mu_i), \tag{4.51}$$

with l referring to the order of expansion and α to the type of corrections, one finds the following relations up to two-loops,

$$\begin{aligned}
&\delta\vec{C}^{(0)}(\mu) = 0, \\
&\delta\vec{C}_\alpha^{(1)}(\mu) = -\vec{C}^{(0)}(\mu)\delta\hat{r}_\alpha^{(1)}(\mu), \\
&\delta\vec{C}_\alpha^{(2)}(\mu) = -\vec{C}_\alpha^{(1)}(\mu)\left(\delta\hat{r}_\alpha^{(1)}(\mu) - \zeta_{g^2}^{(1)}\right) \\
&\qquad\qquad - \vec{C}^{(0)}(\mu)\left(\delta\hat{r}_\alpha^{(2)}(\mu) - \delta\hat{r}_\alpha^{(1)}(\mu)\hat{r}_\alpha^{\prime(1)}(\mu) - \zeta_{g^2}^{(1)}\hat{r}_\alpha^{(1)}(\mu)\right).
\end{aligned} \tag{4.52}$$

In Section 5.3.1, we will give a more exhaustive explanation for the cancellation of the threshold corrections and the relation of the matrices $\hat{r}$ and $\hat{r}'$ with the wave function renormalization terms and the mixing matrices.

4.6 Operators in the Modern Basis

In the Chapter of Renormalization, Chapter 3, we have already discussed the technical difficulties which arise when γ_5 is extended to d-dimensions. Several schemes, that deal with this problem, were discussed there. Even though they allow us to compute diagrams with traces of γ_5, these approaches require complicated algebraic manipulations and additional finite renormalisation that restore the Ward identities. In addition, γ_5 cannot be defined in odd space-time dimensions. Calculation of multi-loop Feynman diagrams within the dimensional regularization framework would enormously simplify in the absence of traces with γ_5. In that case one can define the d-dimensional γ_5 as

$$\gamma_5 = i^{\frac{(d-1)(d-2)}{2}}\gamma^0 ... \gamma^{d-1}. \tag{4.53}$$

The above definition satisfies the anti-commutation relation in even dimensions with the remaining gamma matrices, and its square is equal to unity.

Here we present an operator basis which is free of the γ_5 problem and which is defined by the requirement that the effective Lagrangian reproduces the Standard Model $\Delta F = 1$ transitions at first order in the Fermi constant, but to all orders in strong and electromagnetic interactions. This means that higher-order dimensional operators, $d > 6$, have been neglected here. This simple scheme was introduced for the first time by the authors of references [45] and later extended to include higher order QCD [46] and QED [47, 48] corrections. The scheme is very useful when higher-order corrections are computed, since no traces involving γ_5 have to be evaluated which simplifies the definition of dimensional regularization. Moreover, it is worth mentioning that this choice of basis is not unique. In fact, other linear combinations of physical operators could have been chosen; or even a redefinition of them could have been done by adding some non-physical operators.

The operators of equation (4.1) are classified in three groups: The first group contains all the operators that are invariant under gauge transformations and that do not vanish when the equations of motion are applied, they are known by the name of *physical operators* and *evanescent operators*. The latter type has to be considered when the calculations are performed within the framework of dimensional regularization; the second class stands for the gauge invariant operators which vanish by the use of the equations of motion: *EOM-operators*. These operators play an important role when one does the matching off-shell, that is, they are required counter-terms for the cancellation of the remaining divergences; finally, the third set contains the gauge-variant operators: *BRST-operators* [15, 49, 50]. Under renormalization *physical operators* and *evanescent operators* mix with *EOM-operators* and *BRST-operators*. The third group of operators (*BRST-operators*) mix among themselves and into operators of the second class (*EOM-operators*), and the latter only mix among operators of the same group. When the study is performed within the background-field gauge, there is no mixing with the gauge variant operators. Chapter 12 of reference [15] covers this in more details.

4.6.1 Physical Operators

The first type of operators to discuss are the physical operators. This set can be further classified as: *current-current*, *penguin*, and *chromomagnetic* operators.

Current-Current Operators

A set of four current-current operators will appear at an energy scale above the charm mass. When the analysis is performed below that threshold only $\mathcal{O}_i^u$ operators have to

be considered.

$$\begin{aligned}
\mathcal{O}_1^u &= (\bar{s}_L \gamma_\mu T^a u_L)\,(\bar{u}_L \gamma^\mu T^a d_L)\,, \\
\mathcal{O}_1^c &= (\bar{s}_L \gamma_\mu T^a c_L)\,(\bar{c}_L \gamma^\mu T^a d_L)\,, \\
\mathcal{O}_2^u &= (\bar{s}_L \gamma_\mu u_L)\,(\bar{u}_L \gamma^\mu d_L)\,, \\
\mathcal{O}_2^c &= (\bar{s}_L \gamma_\mu c_L)\,(\bar{c}_L \gamma^\mu d_L)\,.
\end{aligned} \tag{4.54}$$

The operator $\mathcal{O}_2^q$, with $q = u, c$, describes the tree-level process displayed in fig. 4.1 at low energy scales below the mass of the W-boson. Here we apply the definition initially developed for B-physics [45] to the case of K-physics.

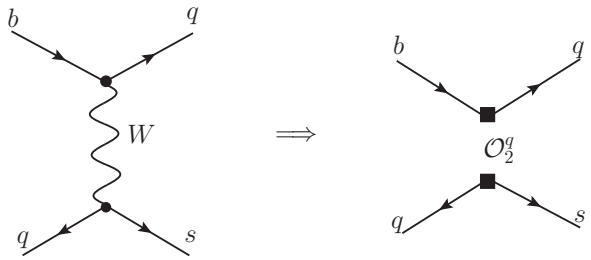

Figure 4.1: 1PI diagrams describing the decays $b \to su\bar{u}$ and $b \to sc\bar{c}$ in the full and the effective field theory

If QCD-corrections are taken into account, see fig. 4.2, counter-terms proportional to the mixing of $\mathcal{O}_1^q$ and $\mathcal{O}_2^q$, with $q = u, c$, and the non-physical evanescent operator $E_1^{(1)}$ must be included to renormalize the amplitude.

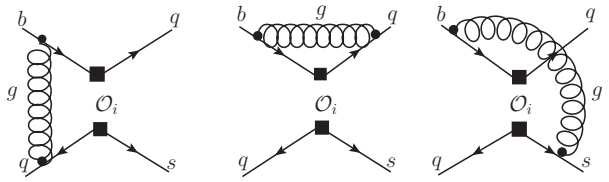

Figure 4.2: NLO QCD-corrections to the current-current diagrams

QCD Penguin Operators

$$\begin{aligned}
\mathcal{O}_3 &= (\bar{s}_L\gamma_\mu d_L)\sum_q (\bar{q}\gamma^\mu q)\,,\\
\mathcal{O}_4 &= (\bar{s}_L\gamma_\mu T^a d_L)\sum_q (\bar{q}\gamma^\mu T^a q)\,,\\
\mathcal{O}_5 &= (\bar{s}_L\gamma_\mu\gamma_\nu\gamma_\rho d_L)\sum_q (\bar{q}\gamma^\mu\gamma^\nu\gamma^\rho q)\,,\\
\mathcal{O}_6 &= (\bar{s}_L\gamma_\mu\gamma_\nu\gamma_\rho T^a d_L)\sum_q (\bar{q}\gamma^\mu\gamma^\nu\gamma^\rho T^a q)\,.
\end{aligned} \tag{4.55}$$

This sort of operators are generated via operator mixing from the insertion of $\mathcal{O}_2^q$ into the diagrams sketched in fig. 5.1. To renormalize them a counter-term proportional to $(\bar{s}_L T^a\gamma^\mu d_L)D^\nu G^a_{\mu\nu}$ must be included. This can be written in terms of a linear combination of the physical operator $\mathcal{O}_4$ and the EOM-vanishing non-physical operator $\mathcal{O}_{12}$ defined below. The insertion of the QCD-penguin operator $\mathcal{O}_4$ into the fig. 4.2 requires counter-terms proportional to $\mathcal{O}_5$ and $\mathcal{O}_6$. If the operator inserted in these same diagrams is $\mathcal{O}_6$ a counter-term proportional to $\mathcal{O}_3$ is necessary. Here we again follow the definition of Ref. [45] where products of three gamma matrices, such as $(\bar{s}_L\gamma_\mu\gamma_\nu\gamma_\rho d_L)\,(\bar{q}\gamma^\mu\gamma^\nu\gamma^\rho q)$ in (4.55) are not further simplified to terms proportional to $(\bar{s}_L\gamma_\mu d_L)\,(\bar{q}\gamma^\mu q)$ and $(\bar{s}_L\gamma_\mu d_L)\,(\bar{q}\gamma^\mu\gamma_5 q)$. Hence the only appearance of γ_5 is in the flavour violating $(\bar{s}_L\gamma_\mu d_L)$ current. QCD corrections, which are flavour conserving, cannot induce a trace over γ_5 in this basis if we consider only single insertions of the flavour violating current.

Electromagnetic Penguin Operators

When QED interactions are also present, another kind of penguin operators have to be considered [47, 48]. They will have a similar form to the QCD penguin operators, but the dependence on the electric charge has to be included,

$$\begin{aligned}
\mathcal{O}_3^Q &= (\bar{s}_L\gamma_\mu d_L)\sum_q e_q\,(\bar{q}\gamma^\mu q)\,,\\
\mathcal{O}_4^Q &= (\bar{s}_L\gamma_\mu T^a d_L)\sum_q e_q\,(\bar{q}\gamma^\mu T^a q)\,,\\
\mathcal{O}_5^Q &= (\bar{s}_L\gamma_\mu\gamma_\nu\gamma_\rho d_L)\sum_q e_q\,(\bar{q}\gamma^\mu\gamma^\nu\gamma^\rho q)\,,\\
\mathcal{O}_6^Q &= (\bar{s}_L\gamma_\mu\gamma_\nu\gamma_\rho T^a d_L)\sum_q e_q\,(\bar{q}\gamma^\mu\gamma^\nu\gamma^\rho T^a q)\,.
\end{aligned} \tag{4.56}$$

These operators will describe processes with emission of photons. Thus, we will have the analogous diagrams as the one displayed in fig. 5.1 but where the gluon is replaced by a photonic line.

The group formed by the current-current, QCD-penguin, and QED-penguin operators is closed under QCD and QED renormalization, up to nonphysical counter-terms, if we consider only four quark operators formed out of light quarks and neglect their masses.

Chromomagnetic Operators

For a non-zero strange-quark mass two additional operators are introduced through QCD and QED effects, the (chromo-)magnetic moment operators [51],

$$\begin{aligned} \mathcal{O}_{7\gamma} &= \frac{e^2}{g_s^2} m_s \left(\bar{s}_L \sigma^{\mu\nu} d_R\right) F_{\mu\nu}, \\ \mathcal{O}_{8g} &= \frac{1}{g_s^2} m_s \left(\bar{s}_L \sigma^{\mu\nu} T^a d_R\right) G^a_{\mu\nu}. \end{aligned} \tag{4.57}$$

These dimension five operators do not require any counter-terms proportional to dimension-six operators. One can show that no more physical operators are needed for the analysis of the $\Delta F = 1$ weak decays, by only writing all the possible $\Delta F = 1$ operators allowed by gauge symmetry and reducing them by equations of motion. The arguments are worked out explicitly for the traditional operator basis [52] and can be trivially adopted to the operator basis of this work. The contributions of these operators to hadronic K decays is suppressed by the smallness of the strange-quark mass and can often be neglected.

Electroweak Box Operators

When electroweak corrections are considered, two additional operators are generated [53] through box type diagrams. The original definition involved an axial current in a flavour singlet current. We can circumvent by defining the operators as

$$\begin{aligned} \mathcal{O}_{b1} &= -\frac{1}{3} \left(\bar{s}_L \gamma_\mu d_L\right) \left(\bar{b} \gamma^\mu b\right) + \frac{1}{12} \left(\bar{s}_L \gamma_\mu \gamma_\nu \gamma_\lambda d_L\right) \left(\bar{b} \gamma^\mu \gamma^\nu \gamma^\lambda b\right), \\ \mathcal{O}_{b2} &= \left(\bar{s}_L \gamma_\mu b_L\right) \left(\bar{b}_L \gamma^\mu d_L\right) . \end{aligned} \tag{4.58}$$

The Operators $\mathcal{O}_{b1}$ and $\mathcal{O}_{b2}$ contribute only via QCD running to Kaon physics observables at lower energy. Hence, they are often neglected in phenomenological analyses.

In principle a Higgs penguin could also generate scalar operators in the Standard Model. But the smallness of the light Yukawa couplings and the according suppression of the Wilson coefficients renders the contribution of these scalar operators totally negligible within the Standard Model.

Semi-leptonic Operators

When the physical process of interest contains leptons in the final state, another set of operators must be included for the analysis,

$$\begin{aligned}\mathcal{O}_9 &= \frac{e^2}{g_s^2}\left(\bar{s}_L\gamma_\mu d_L\right)\sum_l\left(\bar{l}\gamma^\mu l\right),\\ \mathcal{O}_{10} &= \frac{e^2}{g_s^2}\left(\bar{s}_L\gamma_\mu d_L\right)\sum_l\left(\bar{l}\gamma^\mu\gamma_5 l\right).\end{aligned} \tag{4.59}$$

This completes the definition of the relevant physical operators.

4.6.2 Equation of Motion Operators

As previously mentioned, we also have to consider operators that vanish by the equations of motion when renormalized off-shell Green's functions are computed, since the latter are only expanded perturbatively in the deep Euclidean region. This implies that one has to fix the gauge to perform the calculation and consequently the renormalization of the truncated gauge-fixed Green's functions requires the mixing of gauge-variant and equation-of-motion operators. Even though these operators do not contribute to physical matrix elements, they play an important role when one compute off-shell matching calculation. The Becchi-Rouet-Stora-Tyutin transformations restricts the number of allowed operators. This set of operators can be classified as gauge-invariant and gauge-variant.

Gauge invariant EOM-vanishing Operators

$$\begin{aligned}\mathcal{O}_{11} &= \frac{e^2}{g_s^2}\left(\bar{s}_L\gamma_\mu d_L\right)\partial_\nu F^{\mu\nu} + \frac{e^2}{g_s^2}\left(\bar{s}_L\gamma_\mu d_L\right)\sum_f Q_f\left(\bar{f}\gamma^\mu f\right)\\ \mathcal{O}_{12} &= \frac{1}{g_s}\left(\bar{s}_L\gamma^\mu T^a d_L\right)D^\nu G^a_{\mu\nu} + \mathcal{O}_4\\ \mathcal{O}_{13} &= \frac{1}{g_s^2}m_d\bar{s}_L\vec{\not{D}}\vec{\not{D}}d_R\\ \mathcal{O}_{14} &= \frac{i}{g_s^2}\bar{s}_L\vec{\not{D}}\vec{\not{D}}\vec{\not{D}}d_R\\ \mathcal{O}_{15} &= \frac{ie}{g_s^2}\left(\bar{s}_L\overleftarrow{\not{D}}\sigma^{\mu\nu}d_L F_{\mu\nu} - F_{\mu\nu}\bar{s}_L\sigma^{\mu\nu}\vec{\not{D}}d_L\right) + \mathcal{O}_7\\ \mathcal{O}_{16} &= \frac{i}{g_s^2}\left(\bar{s}_L\overleftarrow{\not{D}}\sigma^{\mu\nu}T^a d_L G^a_{\mu\nu} - G^a_{\mu\nu}\bar{s}_L T^a\sigma^{\mu\nu}\vec{\not{D}}d_L\right) + \mathcal{O}_8\end{aligned} \tag{4.60}$$

Gauge-variant EOM-vanishing Operators

$$
\begin{aligned}
\mathcal{O}_{17} &= \frac{i}{g_s} m_d \bar{s}_L \left(\overleftarrow{\not{D}} \not{G} - \not{G} \vec{\not{D}} \right) d_R \\
\mathcal{O}_{18} &= i \bar{s}_L \left(\overleftarrow{\not{D}} \not{G} \not{G} - \not{G} \not{G} \vec{\not{D}} \right) d_L + m_d \bar{s}_L \not{G} \not{G} d_R \\
\mathcal{O}_{19} &= \frac{1}{g} \left[\bar{s}_L \left(\overleftarrow{\not{D}} \overleftarrow{\not{D}} \not{G} + \not{G} \vec{\not{D}} \vec{\not{D}} \right) d_L + i m_d \bar{s}_L \not{G} \vec{\not{D}} d_R \right] \\
\mathcal{O}_{20} &= i \left[\bar{s}_L \left(\overleftarrow{\not{D}} G^a_\mu G^{a\mu} - G^a_\mu G^{a\mu} \vec{\not{D}} \right) d_L - i m_d \bar{s}_L G^a_\mu G^{a\mu} d_R \right] \\
\mathcal{O}_{21} &= \frac{1}{g_s} \left[\bar{s}_L \left(\overleftarrow{\not{D}} \overleftarrow{D}_\mu G^\mu + G_\mu D^\mu \vec{\not{D}} \right) d_L + i m_d \bar{s}_L G_\mu D^\mu d_R \right] \\
\mathcal{O}_{22} &= \frac{1}{g_s} \left[\bar{s}_L \left(\overleftarrow{\not{D}} T^a + T^a \vec{\not{D}} \right) d_L + i m_d \bar{s}_L T^a d_R \right] \partial^\mu G^a_\mu \\
\mathcal{O}_{23} &= \frac{1}{g_s} \left[\bar{s}_L \overleftarrow{\not{D}} \not{G} \vec{\not{D}} d_L + i m_d \bar{s}_L \overleftarrow{\not{D}} \not{G} d_R \right] \\
\mathcal{O}_{24} &= d^{abc} \left[\bar{s}_L \left(\overleftarrow{\not{D}} T^a - T^a \vec{\not{D}} \right) d_L - i m_d \bar{s}_L T^a d_R \right] G^b_\mu G^{c\mu}
\end{aligned}
\tag{4.61}
$$

4.6.3 BRST-Operators

In the previous section we have listed the EOM-operators. In principle, for a quantized gauge theory, there would be contributions from the gauge-fixing and the ghost terms of the Lagrangian, which appear only in a combination that is BRST-variation of other operators. Hence they correspond to BRST-exact operator.

$$
\begin{aligned}
B_1 &= s \left[\frac{1}{g_s} \left(\partial_\mu \bar{\eta}^a \right) \left(\bar{s}_L \gamma^\mu T^a d_L \right) \right] \\
&= -\frac{1}{g_s} \left[\frac{1}{\xi} \partial_\mu \partial^\nu G^a_\nu + g_s f^{abc} \left(\partial_\mu \bar{\eta}^b \right) \eta^c \right] \left(\bar{s}_L \gamma^\mu T^a d_L \right)
\end{aligned}
\tag{4.62}
$$

4.6.4 Evanescent Operators

The evanescent operators are the final class of operators that we discuss. They are an artefact of dimensional regularization and their relevance in the context of effective field theories was pointed out by the authors of references [37,54,55]. The first defining property of an evanescent operator is that it vanishes in the limit of four space-time dimensions. This property on its own does not ensure that evanescent operators do not contribute to physical observables. The UV ε pole of an evanescent operator could cancel with the ε that is generated by taking the limit $d \to 4$ when projecting onto a physical operator. This would result in a finite matrix element, if no additional finite renormalisation is present. This finite term results from a pure UV pole and is mass independent [15]. The finite term can then be subtracted in a unique manner, which is then an implicit part of the definition of the $\overline{\text{MS}}$-scheme, and the matrix element of the evanescent operator is going to vanish when projected onto a physical state. It turns out that this very finite renormalisation forbids renormalisation group mixing into the physical operators.

In our case the following four operators,

$$\begin{aligned}
E_1^{(1)} &= (\bar{s}_L\gamma_\mu\gamma_\nu\gamma_\sigma T^a c_L)\,(\bar{c}_L\gamma^\mu\gamma^\nu\gamma^\sigma T^a d_L) - 16\mathcal{O}_1,\\
E_2^{(1)} &= (\bar{s}_L\gamma_\mu\gamma_\nu\gamma_\sigma c_L)\,(\bar{c}_L\gamma^\mu\gamma^\nu\gamma^\sigma d_L) - 16\mathcal{O}_2,\\
E_3^{(1)} &= (\bar{s}_L\gamma_\mu\gamma_\nu\gamma_\sigma\gamma_\rho\gamma_\lambda d_L)\sum_q\left(\bar{q}\gamma^\mu\gamma^\nu\gamma^\sigma\gamma^\rho\gamma^\lambda q\right) + 64\mathcal{O}_3 - 20\mathcal{O}_5,\\
E_4^{(1)} &= (\bar{s}_L\gamma_\mu\gamma_\nu\gamma_\sigma\gamma_\rho\gamma_\lambda T^a d_L)\sum_q\left(\bar{q}\gamma^\mu\gamma^\nu\gamma^\sigma\gamma^\rho\gamma^\lambda T^a q\right) + 64\mathcal{O}_4 - 20\mathcal{O}_6,
\end{aligned} \tag{4.63}$$

are required as counter-terms for the renormalization of the one-loop current-current diagrams with insertions of $\mathcal{O}_1, ..., \mathcal{O}_6$ at NLO. In the presence of electromagnetic interactions this set has to be enlarged by two more operators,

$$\begin{aligned}
E_3^{Q(1)} &= (\bar{s}_L\gamma_\mu\gamma_\nu\gamma_\sigma\gamma_\rho\gamma_\lambda d_L)\sum_q Q_q\left(\bar{q}\gamma^\mu\gamma^\nu\gamma^\sigma\gamma^\rho\gamma^\lambda q\right) + 64\mathcal{O}_3 - 20\mathcal{O}_5,\\
E_4^{Q(1)} &= (\bar{s}_L\gamma_\mu\gamma_\nu\gamma_\sigma\gamma_\rho\gamma_\lambda T^a d_L)\sum_q Q_q\left(\bar{q}\gamma^\mu\gamma^\nu\gamma^\sigma\gamma^\rho\gamma^\lambda T^a q\right) + 64\mathcal{O}_4 - 20\mathcal{O}_6.
\end{aligned} \tag{4.64}$$

When the previous operators are inserted in the effective vertices of the diagrams shown in figure fig. 5.2, other evanescent operators with five Dirac matrices appear,

$$
\begin{aligned}
E_1^{(2)} &= (\bar{s}_L\gamma_\mu\gamma_\nu\gamma_\sigma\gamma_\rho\gamma_\lambda T^a c_L)\left(\bar{c}_L\gamma^\mu\gamma^\nu\gamma^\sigma\gamma^\rho\gamma^\lambda T^a d_L\right) - 256\mathcal{O}_1 - 20E_1^{(1)},\\
E_2^{(2)} &= (\bar{s}_L\gamma_\mu\gamma_\nu\gamma_\sigma\gamma_\rho\gamma_\lambda c_L)\left(\bar{c}_L\gamma^\mu\gamma^\nu\gamma^\sigma\gamma^\rho\gamma^\lambda d_L\right) - 256\mathcal{O}_2 - 20E_2^{(1)},\\
E_3^{(2)} &= (\bar{s}_L\gamma_\mu\gamma_\nu\gamma_\sigma\gamma_\rho\gamma_\lambda\gamma_\theta\gamma_\delta d_L)\sum_q\left(\bar{q}\gamma^\mu\gamma^\nu\gamma^\sigma\gamma^\rho\gamma^\lambda\gamma^\theta\gamma^\delta q\right) + 1280\mathcal{O}_3 - 336\mathcal{O}_5,\\
E_4^{(2)} &= (\bar{s}_L\gamma_\mu\gamma_\nu\gamma_\sigma\gamma_\rho\gamma_\lambda\gamma_\theta\gamma_\delta T^a d_L)\sum_q\left(\bar{q}\gamma^\mu\gamma^\nu\gamma^\sigma\gamma^\rho\gamma^\lambda\gamma^\theta\gamma^\delta T^a q\right) + 1280\mathcal{O}_4 - 336\mathcal{O}_6.
\end{aligned}
\tag{4.65}
$$

It is worth mentioning here that there is an arbitrariness in the definition of the above operators. Indeed, one could add ε times any physical operator to any evanescent operator. This would lead to a scheme dependence that we will discuss in more detail in the next section.

4.7 Renormalization Scheme Dependence and ADM

The renormalization of operators and all the parameters contained in the Lagrangian, as well as the arbitrariness in the definition of the finite parts introduce a scheme dependence in the calculations. Employing a scheme like $\overline{\text{MS}}$, this scheme dependence is fixed for a given operator basis. Yet in our definition of the $\overline{\text{MS}}$-scheme we subtract the finite projection of the evanescent operators onto the physical operators. Hence the fact that the choice of an operator basis is not uniquely defined leads to a one to one correspondence of scheme dependence and choice of operator basis. However, physical quantities neither depend on the choice of a renormalization scheme nor on the definition for the operators. Hence it is important to analyse how observables turn out to be independent of a different choice of renormalization scheme or operator basis. Here we aim to discuss the part of the renormalization scheme in detail and state the relations for some scheme dependent quantities like the matrix elements and the anomalous dimensions matrices. A change of basis will be considered in the succeeding section.

Imagine the same physical process is evaluated using different renormalization schemes. The theoretical predictions obtained from both of them must be the same, since as we stated before that physical observables do not depend on any choice performed during the calculations. The renormalized matrix elements of two different renormalization schemes are related by a finite matrix, $\Delta\hat{r}^{(n,m)}$,

$$
\langle\vec{Q}\rangle' = \sum_{\substack{n,m=0\\ n+m\geq 1}} \left[\tilde{\alpha}_s'(\mu_0)\right]^n \left[\tilde{\alpha}_e'(\mu_0)\right]^m \Delta\hat{r}^{(n,m)}\langle\vec{Q}\rangle, \tag{4.66}
$$

where we have used prime to denote one of the scheme employed. At one-loop, we would have the following relations,

$$\begin{aligned}\hat{r}_s'^{(1)} &= \hat{r}_s^{(1)} + \Delta\hat{r}_s^{(1)},\\ \hat{r}_e'^{(1)} &= \hat{r}_e^{(1)} + \Delta\hat{r}_e^{(1)},\end{aligned} \tag{4.67}$$

for QCD and QED corrections, respectively. Remember that the subscript denotes the type of interaction, and that we use this notation to simplify the expressions. At the next order in perturbation theory, the corresponding contributions are given by

$$\begin{aligned}\hat{r}_s'^{(2)} &= \hat{r}_s^{(2)} + \Delta\hat{r}_s^{(1)}\hat{r}_s^{(1)} + \Delta\hat{r}_s^{(2)},\\ \hat{r}_e'^{(2)} &= \hat{r}_e^{(2)} + \Delta\hat{r}_e^{(1)}\hat{r}_e^{(1)} + \Delta\hat{r}_e^{(2)},\\ \hat{r}_{se}'^{(2)} &= \hat{r}_{se}^{(2)} + \Delta\hat{r}_s^{(1)}\hat{r}_e^{(1)} + \Delta\hat{r}_e^{(1)}\hat{r}_s^{(1)} + \Delta\hat{r}_{se}^{(2)}.\end{aligned} \tag{4.68}$$

Finally, for the case of three loops when a combination of QCD×QED interactions are considered, we find:

$$\hat{r}_{s^2e}'^{(3)} = \hat{r}_{s^2e}^{(3)} + \Delta\hat{r}_s^{(1)}\hat{r}_{se}^{(2)} + \Delta\hat{r}_s^{(2)}\hat{r}_e^{(1)} + \Delta\hat{r}_s^{(2)}\Delta\hat{r}_e^{(1)} + \Delta\hat{r}_{s^2e}^{(3)}. \tag{4.69}$$

Here the subscript s^2e refers to the order $\mathcal{O}(\tilde{\alpha}_s^2\tilde{\alpha}_e)$. The expression (4.69) is only given by completeness.

The RGE for effective field theories governs the scale dependence of the Wilson coefficients,

$$\mu\frac{d}{d\mu}\vec{C}(\mu) = \hat{\gamma}^T\vec{C}(\mu). \tag{4.70}$$

Here $\hat{\gamma}(\mu)$ is the anomalous dimension matrix, which has the following perturbative expansion in terms of the QCD and QED couplings,

$$\hat{\gamma}(\mu) = \sum_{\substack{n,m=0\\ n+m\geq 1}} \hat{\gamma}^{(n,m)}\left[\tilde{\alpha}_s(\mu)\right]^n\left[\tilde{\alpha}_e(\mu)\right]^m, \tag{4.71}$$

and which is related to the mixing matrix according to the following relation:

$$\hat{\gamma}_{ij}(\mu) = \hat{Z}_{ik}\mu\frac{d}{d\mu}\hat{Z}^{-1}_{kj}. \tag{4.72}$$

In the $\overline{\text{MS}}$-scheme the mixing matrix depends on the renormalization scale μ only through the coupling constant. Hence we could parametrize the previous expression in terms of the $\tilde{\alpha}_s$ coupling by

$$\hat{\gamma}_{ij}(\mu) = 2\beta_s(\varepsilon,\tilde{\alpha}_s,\tilde{\alpha}_e)\ \hat{Z}_{ik}\mu\frac{d}{d\tilde{\alpha}_s}\hat{Z}^{-1}_{kj} + 2\beta_e(\varepsilon,\tilde{\alpha}_s,\tilde{\alpha}_e), \tag{4.73}$$

where the functions $\beta_s(\varepsilon, \tilde{\alpha}_s, \tilde{\alpha}_e)$ and $\beta_e(\varepsilon, \tilde{\alpha}_s, \tilde{\alpha}_e)$ contain an ε dependence,

$$\beta_s(\varepsilon, \tilde{\alpha}_s, \tilde{\alpha}_e) = \tilde{\alpha}_s \left(-\varepsilon + \beta_s(\tilde{\alpha}_s, \tilde{\alpha}_e)\right), \tag{4.74}$$

$$\beta_e(\varepsilon, \tilde{\alpha}_s, \tilde{\alpha}_e) = \tilde{\alpha}_s \left(-\varepsilon + \beta_e(\tilde{\alpha}_s, \tilde{\alpha}_e)\right). \tag{4.75}$$

From the perturbative expansion of the beta functions in terms of the coupling constants,

$$\beta_s(\tilde{\alpha}_s, \tilde{\alpha}_e) = \sum_{n,m=0} \beta^s_{mn} \tilde{\alpha}^m_s \tilde{\alpha}^n_e \quad \text{and} \quad \beta_e(\tilde{\alpha}_s, \tilde{\alpha}_e) = \sum_{n,m=0} \beta^e_{nm} \tilde{\alpha}^n_e \tilde{\alpha}^m_s \,, \tag{4.76}$$

and the mixing matrices (4.4), we arrive at the following relations for the anomalous dimension matrices,

$$\begin{aligned}
\hat{\gamma}^{(1,0)} &= 2\hat{Z}^{(1,1)}, \\
\hat{\gamma}^{(2,0)} &= 4\hat{Z}^{(2,1)} - 2\hat{Z}^{(1,1)}\hat{Z}^{(1,0)} - 2\hat{Z}^{(1,0)}\hat{Z}^{(1,1)} + 2\beta^s_{00}\hat{Z}^{(1,0)}, \\
\hat{\gamma}^{(3,0)} &= 6\hat{Z}^{(3,1)} - 4\hat{Z}^{(2,1)}\hat{Z}^{(1,0)} - 2\hat{Z}^{(1,1)}\hat{Z}^{(2,0)} - 4\hat{Z}^{(2,0)}\hat{Z}^{(1,1)} - 2\hat{Z}^{(1,0)}\hat{Z}^{(2,1)} \\
&+ 2\hat{Z}^{(1,1)}\hat{Z}^{(1,0)}\hat{Z}^{(1,0)} + 2\hat{Z}^{(1,0)}\hat{Z}^{(1,0)}\hat{Z}^{(1,1)} \\
&+ 2\beta^s_{10}\hat{Z}^{(1,0)} + 4\beta^s_{00}\hat{Z}^{(2,0)} - 2\beta^s_{00}\hat{Z}^{(1,0)}\hat{Z}^{(1,0)}, \\
\hat{\gamma}^{(0,1)} &= 2\hat{Z}^{(1,1)}, \\
\hat{\gamma}^{(1,1)} &= 4\hat{Z}^{(es,1)} - 2\hat{Z}^{(1,1)}\hat{Z}^{(e,0)} - 2\hat{Z}^{(1,0)}\hat{Z}^{(e,1)} \\
&- 2\hat{Z}^{(e,1)}\hat{Z}^{(1,0)} - 2\hat{Z}^{(e,0)}\hat{Z}^{(1,1)} + 2\beta_{00}\hat{Z}^{(e,0)} + 2\beta_{01}\hat{Z}^{(1,0)}.
\end{aligned} \tag{4.77}$$

Here the second index of the matrices $\hat{Z}$ referres to the power of the ε-pole. The relations in (4.77) agree with the results presented by the authors in reference [32].

The fact that physical quantities cannot depend on any scheme leads to the following change for the pure QCD-mixing matrix,

$$\hat{Z}' = \hat{Z}\left[\hat{1} - \tilde{\alpha}_s(\mu)\Delta\hat{r}^{(1)}_s - \tilde{\alpha}^2_s(\mu)\left(\Delta\hat{r}^{(2)}_s - [\Delta\hat{r}^{(1)}_s]^2\right)\right], \tag{4.78}$$

with l the order of the expansion for the coupling. This expression would look the same for pure QED-corrections by replacing: $\tilde{\alpha}_s$ for $\tilde{\alpha}_e$ and $\hat{r}^{(l)}_s$ by $\hat{r}^{(l)}_e$. From the relation between the ADM and the mixing matrix, and using eq. (4.78), one can easily obtain the expressions for the first ones. At NLO, we reproduce the results obtained by the authors of references [56, 57],

$$\begin{aligned}
\hat{\gamma}'^{(1)}_s &= \gamma^{(1)}_s + [\Delta\hat{r}^{(1)}_s, \gamma^{(0)}_s] + 2\beta^s_{00}\Delta\hat{r}^{(1)}_s, \\
\hat{\gamma}'^{(1)}_e &= \gamma^{(1)}_e + [\Delta\hat{r}^{(1)}_e, \gamma^{(0)}_e] - 2\beta^e_{00}\Delta\hat{r}^{(1)}_e, \\
\hat{\gamma}'^{(0)}_{es} &= \gamma^{(0)}_{es} + [\Delta\hat{r}^{(1)}_s, \gamma^{(0)}_e] + [\Delta\hat{r}^{(1)}_e, \gamma^{(0)}_s].
\end{aligned} \tag{4.79}$$

Moreover, we also agree with the result obtained for pure strong interactions at NNLO given in [46],

$$\begin{aligned}\hat{\gamma}_s'^{(2)} &= \gamma_s^{(2)} + [\Delta\hat{r}_s^{(1)}, \gamma_s^{(1)}] + [\Delta\hat{r}_s^{(2)}, \gamma_s^{(0)}] - [\Delta\hat{r}_s^{(1)}, \gamma_s^{(0)}]\Delta\hat{r}_s^{(1)} \\ &\quad + 2\beta_{10}^s\Delta\hat{r}_s^{(1)} - 2\beta_{00}^s[\Delta\hat{r}_s^{(1)}]^2 + 4\beta_{00}^s\Delta\hat{r}_s^{(2)}.\end{aligned} \tag{4.80}$$

We have also derived the NNLO expression for pure electromagnetic corrections,

$$\begin{aligned}\hat{\gamma}_e'^{(2)} &= \gamma_e^{(2)} + [\Delta\hat{r}_e^{(1)}, \gamma_e^{(1)}] + [\Delta\hat{r}_e^{(2)}, \gamma_e^{(0)}] - [\Delta\hat{r}_e^{(1)}, \gamma_e^{(0)}]\Delta\hat{r}_e^{(1)} \\ &\quad - 2\beta_{10}^e\Delta\hat{r}_e^{(1)} + 2\beta_{00}^e[\Delta\hat{r}_e^{(1)}]^2 - 4\beta_{00}^e\Delta\hat{r}_e^{(2)}.\end{aligned} \tag{4.81}$$

Notice that the relations (4.80) and (4.81) differ on the sign of the beta terms as it should be. Furthermore, we have obtained here the corresponding expression for $\hat{\gamma}_{es}'^{(1)}$ given by

$$\begin{aligned}\hat{\gamma}_{es}'^{(1)} &= \gamma_{es}^{(1)} + [\Delta\hat{r}_e^{(1)}, \gamma_s^{(1)}] - [\Delta\hat{r}_e^{(1)}, \gamma_s^{(0)}]\Delta\hat{r}_s^{(1)} - [\Delta\hat{r}_s^{(1)}, \gamma_{es}^{(0)}] \\ &\quad + [\Delta\hat{r}_{se}^{(2)}, \gamma_s^{(0)}] + [\Delta\hat{r}_s^{(2)}, \gamma_e^{(0)}] - [\Delta\hat{r}_s^{(1)}, \gamma_e^{(0)}]\Delta\hat{r}_s^{(1)} \\ &\quad - [\Delta\hat{r}_s^{(1)}, \gamma_s^{(0)}]\Delta\hat{r}_e^{(1)} + 2\beta_{01}^s\Delta\hat{r}_s^{(1)} + 2\beta_{00}^s\Delta\hat{r}_{se}^{(2)} - 2\beta_{00}^s\Delta\hat{r}_s^{(1)}\Delta\hat{r}_e^{(1)}.\end{aligned} \tag{4.82}$$

This relation would be needed when the running QCD×QED is performed at three loops. Even if we do not employ it in our calculations, we thought it could be useful to have it in case other people take the challenge to go to a higher order in the perturbation series expansion.

4.8 Change of the Operator Basis

The operator basis used for our calculations allowed us to simplify the evaluation of higher order diagrams since no traces with γ_5 appear. However, for the phenomenological study of several observables, like ε'/ε, another different set of operators is commonly used. Hence it is convenient to transform our results to this traditional basis. The present section aims to explain how the change between different definitions of the operators is performed. Basically, it is based on a series of subsequent redefinitions of the physical and evanescent operators. While the idea seems not to be very complicated, the presence of these non-physical operators, which arise when dimensional regularization is employed, convolute this transformation. In fact, for a NNLO analysis of the current-current and QCD-penguin operators, the renormalization of the evanescent structures in d-dimensions has to be fixed, which results in a choice of operator basis that fixes the renormalization scheme [45, 46]. These scheme changes associated with the choice of basis for the current-current and QCD-penguin operators were derived at NLO in [45] and extended to NNLO in QCD by the authors of reference [46]. Here we will widen this to the electroweak penguins at NLO after having discussed the general idea. Moreover we present here the one- and two-loop ADM matrices in the modern

basis for a general number of flavours for the first time.

Within d-dimensions two different operator bases are related by the following transformations,

$$\vec{Q}' = \hat{R}\left(\vec{\mathcal{O}} + \hat{W}\vec{E}\right), \quad \vec{E}' = \hat{M}\left((\varepsilon\hat{U} + \varepsilon^2\hat{V})\vec{\mathcal{O}} + \left[\hat{1} + (\varepsilon\hat{U} + \varepsilon^2\hat{V})\hat{W}\right]\vec{E}\right). \tag{4.83}$$

The matrix $\hat{W}$ appears when evanescent operators are added to the physical ones. $\hat{U}$ and $\hat{V}$ encode the addition of multiples of ε and ε^2 times physical operators to the non-physical ones. Finally, the matrices $\hat{R}$ and $\hat{M}$ parametrise a linear transformation among the physical and evanescent operators, respectively.

If we still assume that this transformation affects the $\hat{Z}$ and the ADM matrices in a similar manner as the four dimensional case, where there is no mixing between physical and evanescent operators,

$$\hat{Z}' = \hat{R}\hat{Z}\hat{R}^{-1}, \quad \text{and} \quad \hat{\gamma}' = \hat{R}\hat{\gamma}\hat{R}^{-1}, \tag{4.84}$$

but replacing the linear transformation, $\hat{R}$, by the new one, which takes into account the effects of these non-physical operators needed at d-dimensions,

$$\hat{X} = \begin{pmatrix} \hat{R} & 0 \\ 0 & \hat{M} \end{pmatrix} \begin{pmatrix} 1 & 0 \\ \varepsilon\hat{U} + \varepsilon^2\hat{V} & 1 \end{pmatrix} \begin{pmatrix} 1 & \hat{W} \\ 0 & 1 \end{pmatrix}, \tag{4.85}$$

one observes that a finite renormalization constant for the physical operators in the new basis is generated. The latter is determined by assuming that the Green's functions must be invariant under the basis transformation and renormalized according to the $\overline{\text{MS}}$-scheme. Up to two loops one gets

$$\hat{Z}'^{(1,0)}_{QQ} = \hat{R}\left[\hat{W}\hat{Z}^{(1,0)}_{EQ} - \left(\hat{Z}^{(1,1)}_{QE} + \hat{W}\hat{Z}^{(1,1)}_{EE} - \frac{1}{2}\gamma^{(0)}_s\hat{W}\right)\hat{U}\right]\hat{R}^{-1}, \tag{4.86}$$

$$\begin{aligned}\hat{Z}'^{(2,0)}_{QQ} = \hat{R}\Bigg[\hat{W}\hat{Z}^{(2,0)}_{EQ} - \Bigg(&\hat{Z}^{(2,1)}_{QE} + \hat{W}\hat{Z}^{(2,1)}_{EE} - \frac{1}{4}\gamma^{(1)}_s\hat{W} - \frac{1}{2}\hat{\gamma}^{(1)}_s\hat{W} \\ &- \frac{1}{2}\hat{Z}^{(1,1)}_{QE}Z^{(1,0)}_{EQ}\hat{W} - \frac{1}{2}\hat{W}\hat{Z}^{(1,0)}_{EE}\hat{W} - \frac{1}{4}\hat{W}\hat{Z}^{(1,0)}_{EQ}\hat{\gamma}^{(0)}_s\hat{W} + \frac{1}{2}\beta_0\hat{W}\hat{Z}^{(1,0)}_{EQ}\hat{W}\Bigg)\hat{U}\Bigg]\hat{R}^{-1}.\end{aligned} \tag{4.87}$$

Therefore, to restore the standard $\overline{\text{MS}}$-scheme definitions one also has to perform a change of scheme. Thus, within dimensional regularization a change of operator basis can be seen as a rotation and a change of scheme to recover the $\overline{\text{MS}}$-scheme definitions.

With the general idea in mind our next aim would be to show the new result for the electroweak penguin operators at NLO. For this purpose, we proceed with the discussion by introducing the set of operators in the traditional basis. The physical operators are given by:

Current-Current:

$$Q_1' = (\bar{s}_\alpha u_\beta)_{V-A}\,(\bar{u}_\beta d_\alpha)_{V-A} \qquad Q_2' = (\bar{s}u)_{V-A}\,(\bar{u}d)_{V-A} \tag{4.88}$$

QCD–Penguins:

$$Q_3' = (\bar{s}d)_{V-A}\sum_{q=u,d,s,c,b}(\bar{q}q)_{V-A} \qquad Q_4' = (\bar{s}_\alpha d_\beta)_{V-A}\sum_{q=u,d,s,c,b}(\bar{q}_\beta q_\alpha)_{V-A} \tag{4.89}$$

$$Q_5' = (\bar{s}d)_{V-A}\sum_{q=u,d,s,c,b}(\bar{q}q)_{V+A} \qquad Q_6' = (\bar{s}_\alpha d_\beta)_{V-A}\sum_{q=u,d,s,c,b}(\bar{q}_\beta q_\alpha)_{V+A} \tag{4.90}$$

Electroweak Penguins:

$$Q_7' = \frac{3}{2}\,(\bar{s}d)_{V-A}\sum_{q=u,d,s,c,b} e_q\,(\bar{q}q)_{V+A} \quad Q_8' = \frac{3}{2}\,(\bar{s}_\alpha d_\beta)_{V-A}\sum_{q=u,d,s,c,b} e_q\,(\bar{q}_\beta q_\alpha)_{V+A} \tag{4.91}$$

$$Q_9' = \frac{3}{2}\,(\bar{s}d)_{V-A}\sum_{q=u,d,s,c,b} e_q\,(\bar{q}q)_{V-A} \qquad Q_{10}' = \frac{3}{2}\,(\bar{s}_\alpha d_\beta)_{V-A}\sum_{q=u,d,s,c,b} e_q\,(\bar{q}_\beta q_\alpha)_{V-A} \tag{4.92}$$

where e_q denotes the electric quark charges and $(\bar{q}q)_{V\pm A} \equiv \bar{q}_\alpha\gamma_\mu(1\pm\gamma_5)q_\alpha$. In addition a different set of evanescent operators was used in the evaluation of the hadronic matrix elements [7] and the evaluation of the Wilson coefficients [56–61]. We present here only the relevant evanescent operators in the traditional basis,

$$\begin{aligned}
E_3'^{Q(1)} &= (\bar{s}_L^\alpha\gamma_{\mu_1\mu_2\mu_3}b_L^\alpha)\sum_q e_q(\bar{q}_L^\beta\gamma^{\mu_1\mu_2\mu_3}q_L^\beta) - (16-4\varepsilon)\,Q_3'\,,\\
E_4'^{Q(1)} &= (\bar{s}_L^\alpha\gamma_{\mu_1\mu_2\mu_3}b_L^\beta)\sum_q e_q(\bar{q}_L^\beta\gamma^{\mu_1\mu_2\mu_3}q_L^\alpha) - (16-4\varepsilon)\,Q_4'\,,\\
E_5'^{Q(1)} &= (\bar{s}_L^\alpha\gamma_{\mu_1\mu_2\mu_3}b_L^\alpha)\sum_q e_q(\bar{q}_R^\beta\gamma^{\mu_1\mu_2\mu_3}q_R^\beta) - (4+4\varepsilon)\,Q_5'\,,\\
E_6'^{Q(1)} &= (\bar{s}_L^\alpha\gamma_{\mu_1\mu_2\mu_3}b_L^\beta)\sum_q e_q(\bar{q}_R^\beta\gamma^{\mu_1\mu_2\mu_3}q_R^\alpha) - (4+4\varepsilon)\,Q_6'\,.
\end{aligned} \tag{4.93}$$

In order to arrive at a complete transformation of the operators we have to extend both the standard as well as the traditional basis. The electroweak penguin operators of the standard basis,

$$\begin{aligned}
\vec{\mathcal{O}}^{QT} &= (\mathcal{O}_7,\ldots,\mathcal{O}_{10})\,,\\
\vec{E}^{QT} &= (E_3^{Q(1)},\ldots,E_8^{Q(1)})\,,
\end{aligned} \tag{4.94}$$

involve the following additional operators

$$\begin{aligned}
E_5^{Q(1)} &= (\bar{s}_L\gamma_{\mu_1}d_L)\sum_q e_q(\bar{q}\gamma^{\mu_1}\gamma_5 q) - \frac{5}{3}\mathcal{O}_3^Q + \frac{1}{6}\mathcal{O}_5^Q\,,\\
E_6^{Q(1)} &= (\bar{s}_L\gamma_{\mu_1}T^a d_L)\sum_q e_q(\bar{q}\gamma^{\mu_1}\gamma_5 T^a q) - \frac{5}{3}\mathcal{O}_4^Q + \frac{1}{6}\mathcal{O}_6^Q\,,\\
E_7^{Q(1)} &= (\bar{s}_L\gamma_{\mu_1\mu_2\mu_3}d_L)\sum_q e_q(\bar{q}\gamma^{\mu_1\mu_2\mu_3}\gamma_5 q) - \frac{32}{3}\mathcal{O}_3^Q + \frac{5}{3}\mathcal{O}_5^Q,\\
E_8^{Q(1)} &= (\bar{s}_L\gamma_{\mu_1\mu_2\mu_3}T^a d_L)\sum_q e_q(\bar{q}\gamma^{\mu_1\mu_2\mu_3}\gamma_5 T^a q) - \frac{32}{3}\mathcal{O}_4^Q + \frac{5}{3}\mathcal{O}_6^Q,
\end{aligned} \tag{4.95}$$

which do not play a role of counter-terms in the modern basis, but they are needed since some physical or evanescent operators in the traditional basis have some linear combinations of these set of non-physical operators. On the other hand, the operators of the traditional basis,

$$\begin{aligned}
\vec{Q}'^T &= (Q'_7,\ldots,Q'_{10})\,,\\
\vec{E}'^T &= (E_3'^{Q(1)},\ldots,E_6'^{Q(1)},E_3^{Q(1)},E_4^{Q(1)})\,,
\end{aligned} \tag{4.96}$$

are complemented with the evanescent operators $E_3^{Q(1)}$ and $E_4^{Q(1)}$ defined in the modern basis. Following the steps explained at the beginning of the section, one finds that the rotations of the physical and evanescent operators read

$$R^Q = \begin{pmatrix} 2 & 0 & -\frac{1}{8} & 0\\ \frac{2}{3} & 4 & -\frac{1}{24} & -\frac{1}{4}\\ -\frac{1}{2} & 0 & \frac{1}{8} & 0\\ -\frac{1}{6} & -1 & \frac{1}{24} & \frac{1}{4}\end{pmatrix}, \quad M^Q = \begin{pmatrix} 0 & 0 & 12 & 0 & -\frac{3}{4} & 0\\ 0 & 0 & 4 & 24 & -\frac{1}{4} & -\frac{3}{2}\\ 0 & 0 & -3 & 0 & \frac{3}{4} & 0\\ 0 & 0 & -1 & -6 & \frac{1}{4} & \frac{3}{2}\\ 1 & 0 & 0 & 0 & 0 & 0\\ 0 & 1 & 0 & 0 & 0 & 0\end{pmatrix}, \tag{4.97}$$

while the explicit contribution of standard basis evanescent operators to the traditional basis physical operators and the standard basis operators to the traditional evanescent operators are

$$W^Q = \begin{pmatrix} 0 & 0 & 0 & 0 & 0 & 0\\ 0 & 0 & 0 & 0 & 0 & 0\\ 0 & 0 & -6 & 0 & 0 & 0\\ 0 & 0 & 0 & -6 & 0 & 0\end{pmatrix}, \quad \text{and} \quad U^Q = \begin{pmatrix} 0 & 0 & 0 & 0\\ 0 & 0 & 0 & 0\\ -\frac{10}{9} & 0 & \frac{1}{9} & 0\\ 0 & -\frac{10}{9} & 0 & \frac{1}{9}\\ -\frac{136}{9} & 0 & \frac{10}{9} & 0\\ 0 & -\frac{136}{9} & 0 & \frac{10}{9}\end{pmatrix}, \tag{4.98}$$

respectively.

Even though we show here only the relevant pieces corresponding to the QED-penguin operators. The calculation has been performed including all set of operators: ten physical operators and twenty-two evanescent operators. Our results obtained for the current-current and the QCD-penguin contributions agree with the once obtained in the references cited previously, and the ones for QED-penguins are published for the first time in this thesis, even if they are well-known by some of the experts of this field.

Having computed the matrices which parametrize the change of basis within d-dimensions we proceed to obtain the finite part by using equation (4.86). One important piece of this calculation is the mixing involving the insertion of the additional evanescent operators. The latter was computed in references [46] for the analogous QCD structures. The insertion of $E_5^{(1)} - E_8^{(1)}$ into the diagrams of fig. 4.3 introduces traces with γ_5 in the present calculation. The authors compute this contributions by introducing a trace evanescent operator. The full explanation of how this mixing was obtained can be found in their work cited previously [46]. From their results we could extract the $\hat{Z}$-factors corresponding to the insertion of QED $E_5^{Q(1)} - E_8^{Q(1)}$ operators without having to compute the diagrams. At one-loop only the four diagrams displayed in fig. 4.3 enter into the game for the mixing onto $\mathcal{O}_4$. The first, second and third diagrams are proportional to e_d, $e_d n_d + e_u n_u$ and e_q, respectively. Here e_d refers to the down-quark charge and e_u to the up-quark charge, $q = u$ or d, and the factors n_d and n_u stand for the number of down-type and up-type quarks. Furthermore the contribution of the fourth diagram is cancelled by the wave function renormalization. When the inserted operator does not contain a T^a factor there is no contribution from the second diagram, thus the mixing of the QED-$\mathcal{O}_i$ operator would be: $e_d\ Z_{\mathcal{O}_i\mathcal{O}_4}$. For the case when an inserted operator contains a color factor T^a, the second diagram has to be also considered, and the extraction of the mixing is a bit more complicated. Indeed, one has to consider the contribution of the EOM-operator $\mathcal{O}_{12}$.

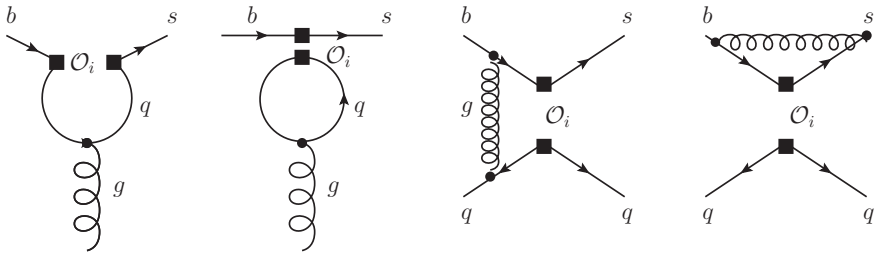

Figure 4.3: 1PI diagrams for the mixing of QCD and electroweak penguin operators

With all of this, one finally gets the following matrix for the set of ten physical operators,

$$Z'^{(1,0)}_{QQ} = \begin{pmatrix} -\frac{7}{3} & -1 & 0 & 0 & 0 & 0 & 0 & 0 & 0 & 0 \\ -2 & \frac{2}{3} & 0 & 0 & 0 & 0 & 0 & 0 & 0 & 0 \\ 0 & 0 & \frac{178}{27} & -\frac{34}{9} & -\frac{164}{27} & \frac{20}{9} & 0 & 0 & 0 & 0 \\ 0 & 0 & 1-\frac{q_p}{9} & \frac{q_p}{3}-\frac{25}{3} & -\frac{q_p}{9}-2 & \frac{q_p}{3}+6 & 0 & 0 & 0 & 0 \\ 0 & 0 & -\frac{160}{27} & \frac{16}{9} & \frac{146}{27} & -\frac{2}{9} & 0 & 0 & 0 & 0 \\ 0 & 0 & \frac{q_p}{9}-2 & -\frac{q_p}{3}+6 & \frac{q_p}{9}+3 & -\frac{q_p}{9}-\frac{1}{3} & 0 & 0 & 0 & 0 \\ 0 & 0 & -\frac{1}{27} & \frac{1}{9} & -\frac{1}{27} & \frac{1}{9} & \frac{16}{3} & 0 & -6 & 2 \\ 0 & 0 & -\frac{q_{2m}}{18} & \frac{q_{2m}}{6} & -\frac{q_{2m}}{18} & -\frac{q_{2m}}{6} & 3 & -\frac{11}{3} & -2 & 6 \\ 0 & 0 & \frac{1}{27} & -\frac{1}{9} & \frac{1}{27} & -\frac{1}{9} & -6 & 2 & \frac{20}{3} & -4 \\ 0 & 0 & \frac{q_{2m}}{18} & -\frac{q_{2m}}{6} & \frac{q_{2m}}{18} & -\frac{q_{2m}}{6} & -2 & 6 & 1 & -\frac{25}{3} \end{pmatrix} \tag{4.99}$$

The notation q_p stands for $d+u$, and the symbol q_{2m} refers for $d-2u$, being d the number of down-type quarks and u the one for the up-type quarks. The current-current and QCD-penguin contributions were first computed by [45] at NLO, and extended to NNLO for the QCD-penguins by authors of reference [46]. The results presented in equation (4.99), which also include the electroweak penguin operators, are new in the literature.

After having discussed the relations between two different operator bases, our next goal will be to explain how this transformation takes place for the anomalous dimension matrices and the Wilson coefficients obtained within the framework of dimensional regularization. The relations for the ADM matrices computed in the different operator bases are obtained in a straightforward way by means of equations (4.79) and (4.80). For pure QCD, we get up to three loops,

$$\begin{aligned} \hat{\gamma}'^{(0)}_s &= \hat{R}\hat{\gamma}^{(0)}_s\hat{R}^{-1}, \\ \hat{\gamma}'^{(1)}_s &= \hat{R}\hat{\gamma}^{(1)}_s\hat{R}^{-1} - \left[\hat{Z}'^{(1,0)}_{QQ}, \hat{\gamma}'^{(0)}_s\right] - 2\beta^s_{00}\hat{Z}'^{(1,0)}_{QQ}, \\ \hat{\gamma}'^{(2)}_s &= \hat{R}\hat{\gamma}^{(2)}_s\hat{R}^{-1} - \left[\hat{Z}'^{(2,0)}_{QQ}, \hat{\gamma}'^{(0)}_s\right] - \left[\hat{Z}'^{(1,0)}_{QQ}, \hat{\gamma}'^{(1)}_s\right] + \left[\hat{Z}'^{(1,0)}_{QQ}, \hat{\gamma}'^{(0)}_s\right]\hat{Z}'^{(1,0)}_{QQ} \\ &\quad - 4\beta^s_{00}\hat{Z}'^{(2,0)}_{QQ} - 2\beta^s_{10}\hat{Z}'^{(1,0)}_{QQ} + 2\beta^s_{00}\left(\hat{Z}'^{(1,0)}_{QQ}\right)^2. \end{aligned} \tag{4.100}$$

With this result and using equation (4.100) one can find the one- and two-loop ADM in the modern basis for a general number of down- and up-type quarks. To reduce the size of the two-loop matrix we present our result in blocks by defining the general

structure of the QCD anomalous dimension matrix as

$$\hat{\gamma}_s^{(l)} = \begin{pmatrix} [\hat{\gamma}_{\rm CC}^{(l)}]_{2\times 2} & [\hat{\gamma}_{\rm CP}^{(l)}]_{2\times 4} & [\hat{\gamma}_{\rm CQ}^{(l)}]_{2\times 4} \\ [\hat{\gamma}_{\rm PC}^{(l)}]_{4\times 2} & [\hat{\gamma}_{\rm PP}^{(l)}]_{4\times 4} & [\hat{\gamma}_{\rm PQ}^{(l)}]_{4\times 4} \\ [\hat{\gamma}_{\rm QC}^{(l)}]_{4\times 2} & [\hat{\gamma}_{\rm QP}^{(l)}]_{4\times 4} & [\hat{\gamma}_{\rm QQ}^{(l)}]_{4\times 4} \end{pmatrix}. \tag{4.101}$$

Here we understand the sub-indices as follows: C stands for current-current operators, P refers to the QCD-penguin operators, and Q will encode the electroweak penguin operators. At one loop we obtain,

$$\hat{\gamma}_{\rm CC}^{(0)} = \begin{pmatrix} -4 & \frac{8}{3} \\ 12 & 0 \end{pmatrix}, \qquad \hat{\gamma}_{\rm CP}^{(0)} = \begin{pmatrix} 0 & -\frac{2}{9} & 0 & 0 \\ 0 & \frac{4}{3} & 0 & 0 \end{pmatrix}, \qquad \hat{\gamma}_{\rm CQ}^{(0)} = 0_{2\times 4} \tag{4.102}$$

$$\hat{\gamma}_{\rm PC}^{(0)} = 0_{4\times 2}, \quad \hat{\gamma}_{\rm PP}^{(0)} = \begin{pmatrix} 0 & -\frac{52}{3} & 0 & 2 \\ -\frac{40}{9} & \frac{4}{3}q_p - \frac{160}{9} & \frac{4}{9} & \frac{5}{6} \\ 0 & -\frac{256}{3} & 0 & 20 \\ -\frac{256}{9} & \frac{40}{3}q_p - \frac{544}{9} & \frac{40}{9} & -\frac{2}{3} \end{pmatrix}, \quad \hat{\gamma}_{\rm PQ}^{(0)} = 0_{4\times 4} \tag{4.103}$$

$$\hat{\gamma}_{\rm QC}^{(0)} = 0_{4\times 2}, \ \hat{\gamma}_{\rm QP}^{(0)} = \begin{pmatrix} 0 & -\frac{8}{9} & 0 & 0 \\ 0 & -\frac{4}{9}q_{2p} + \frac{4}{27} & 0 & 0 \\ 0 & -\frac{128}{9} & 0 & 0 \\ 0 & -\frac{40}{9}q_p + \frac{64}{27} & 0 & 0 \end{pmatrix}, \ \hat{\gamma}_{\rm QQ}^{(0)} = \begin{pmatrix} 0 & -20 & 0 & 2 \\ -\frac{40}{9} & -\frac{52}{3} & \frac{4}{9} & \frac{5}{6} \\ 0 & -128 & 0 & 20 \\ -\frac{256}{9} & -\frac{160}{3} & \frac{40}{9} & -\frac{2}{3} \end{pmatrix}, \tag{4.104}$$

and a two loops the results read

$$\hat{\gamma}_{\rm PC}^{(1)} = 0_{4\times 2}, \qquad \hat{\gamma}_{\rm PQ}^{(1)} = 0_{4\times 4}, \qquad \hat{\gamma}_{\rm QC}^{(1)} = 0_{4\times 2} \tag{4.105}$$

$$\hat{\gamma}_{\rm CC}^{(1)} = \begin{pmatrix} \frac{16}{9}q_p - \frac{145}{3} & \frac{40}{27}q_p - 26 \\ \frac{20}{3}q_p - 45 & -\frac{28}{3} \end{pmatrix}, \ \hat{\gamma}_{\rm CP}^{(1)} = \begin{pmatrix} -\frac{1412}{243} & -\frac{1369}{243} & \frac{134}{243} & -\frac{35}{162} \\ -\frac{416}{81} & \frac{1280}{81} & \frac{56}{81} & \frac{35}{27} \end{pmatrix}, \ \hat{\gamma}_{\rm CP}^{(1)} = 0_{2\times 4}, \tag{4.106}$$

$$\hat{\gamma}^{(1)}_{\mathrm{QQ}} = \begin{pmatrix} -\frac{404}{9} & \frac{92}{9}q_p - 393 & \frac{32}{9} & -\frac{2}{9}q_p + \frac{119}{4} \\ \frac{184}{81}q_p - \frac{134}{3} & \frac{88}{27}q_p - \frac{2825}{9} & -\frac{4}{81}q_p - \frac{1}{18} & -\frac{5}{54}q_p + \frac{1531}{72} \\ \frac{1280}{9}q_p - \frac{25472}{9} & -\frac{832}{9}q_p - 1104 & -\frac{128}{9}q_p + \frac{2348}{9} & \frac{148}{9}q_p + 98 \\ -\frac{1664}{81}q_p + \frac{1504}{3} & -\frac{3680}{27}q_p + \frac{808}{9} & \frac{296}{81}q_p - \frac{908}{9} & \frac{422}{27}q_p - \frac{2219}{18} \end{pmatrix}, \tag{4.107}$$

$$\hat{\gamma}^{(1)}_{\mathrm{PP}} = \begin{pmatrix} -\frac{4468}{81} & -\frac{52}{9}q_p - \frac{29129}{81} & \frac{400}{81} & -\frac{2}{9}q_p + \frac{3493}{108} \\ \frac{368}{81}q_p - \frac{13678}{243} & \frac{1334}{81}q_p - \frac{79409}{243} & -\frac{8}{81}q_p + \frac{509}{486} & -\frac{5}{27}q_p + \frac{13499}{648} \\ -\frac{160}{9}q_p - \frac{244480}{81} & -\frac{2200}{9}q_p - \frac{29648}{81} & \frac{16}{9}q_p + \frac{23116}{81} & \frac{148}{9}q_p + \frac{3886}{27} \\ -\frac{1264}{81}q_p + \frac{77600}{243} & \frac{164}{81}q_p - \frac{28808}{243} & \frac{400}{81}q_p - \frac{20324}{243} & \frac{622}{27}q_p - \frac{21211}{162} \end{pmatrix}, \tag{4.108}$$

$$\hat{\gamma}^{(1)}_{\mathrm{QP}} = \begin{pmatrix} \frac{832}{243} & \frac{16}{3}q_{2m} - \frac{2704}{243} & -\frac{112}{243} & -\frac{70}{81} \\ -\frac{184}{243}q_{2m} + \frac{2824}{729} & -\frac{1070}{243}q_m + \frac{3134}{729} & \frac{4}{243}q_{2m} - \frac{268}{729} & \frac{5}{162}q_m + \frac{35}{243} \\ \frac{160}{3}q_m + \frac{15232}{243} & \frac{152}{3}q_{2m} - \frac{59776}{243} & -\frac{16}{3}q_m - \frac{1984}{243} & -\frac{1240}{81} \\ -\frac{400}{243}q_m + \frac{44224}{729} & -\frac{11204}{243}q_{2m} + \frac{50624}{729} & -\frac{104}{243}q_{2m} - \frac{4192}{729} & -\frac{200}{81}q_{2m} + \frac{620}{243} \end{pmatrix}. \tag{4.109}$$

Finally, the Wilson coefficients change according to

$$\vec{C}'(\mu) = \left[1 + \tilde{\alpha}_s(\mu)\hat{Z}'^{(1,0)}_{QQ} + \tilde{\alpha}_s^2\hat{Z}'^{(2,0)}_{QQ}\right]^T (R^{-1})^T \vec{C}(\mu). \tag{4.110}$$

4.9 Solution of the Renormalization Group Equations

The Wilson coefficients C_i have a logarithmic dependence on the mass of the heavy particles, which have been integrated out as dynamical degrees of freedom. This fact can be schematically parametrized as

$$\vec{C}(M, \tilde{\alpha}'(\mu), \mu) = \sum_{\substack{n=0 \\ m\leq n}} [\tilde{\alpha}'(\mu)]^n \vec{C}^{(n)}_m \ \log^m\left(\frac{\mu^2}{M^2}\right), \tag{4.111}$$

where M denotes the masses of heavy particles evaluated at fixed scale and the term $\vec{C}^{(n)}_m$ is a vector of pure numbers determined by the matching calculation after the numerical values of M have been used. From the previous equation it seems logical to choose $\mu \approx M$, since in this manner one would avoid large logarithmic terms, which could break the perturbative convergence. However, many flavour changing processes occur at energy scales $\mu \approx m$, where m stands for the mass of a light particle. Generally, both masses satisfy $m \ll M$, and consequently terms of the form $[\tilde{\alpha}'(\mu)]^n \log\left(\frac{m^2}{M^2}\right)$ lead to a breakdown of perturbation theory (in the $\overline{\mathrm{MS}}$-scheme), even if the coupling is very

small. Fortunately, the renormalization group in the EFT allows us to resum the logarithmically enhanced terms to all orders by solving the RG evolution equations for the coupling constants, see equation (3.40), and for the Wilson coefficients eq. (4.70). The general solution for the latter is given in terms of the evolution matrix

$$\vec{C}(\mu) = \hat{U}(\mu, \mu_0)\vec{C}(\mu_0). \tag{4.112}$$

This matrix is formally defined in terms of the ADM and the beta functions as

$$\hat{U}(\mu, \mu_0) = T_g \exp\left[\int_{4\pi\sqrt{\tilde{\alpha}(\mu_0)}}^{4\pi\sqrt{\tilde{\alpha}(\mu)}} d\tilde{\alpha}' \, \frac{2\pi}{\sqrt{\tilde{\alpha}'}} \frac{\hat{\gamma}(\tilde{\alpha}')}{\beta(\tilde{\alpha}')}\right]. \tag{4.113}$$

The symbol T_g denotes the time ordering of the coupling constants $\tilde{\alpha}(\mu)$ such that their values increase from right to left. From the corresponding perturbative expansions of the matrix $\hat{\gamma}$, equation (4.71), and the function β eq. (4.76), one gets the following breakdown for the evolution matrix [56, 62],

$$\hat{U}(\mu, \mu_0) = \hat{K}(\mu)\hat{U}^{(0)}(\mu, \mu_0)\hat{K}^{-1}(\mu_0). \tag{4.114}$$

The leading order term is defined as follows,

$$\hat{U}^{(0)}_{\alpha}(\mu, \mu_0) = \hat{V}\left[\left(\frac{\tilde{\alpha}_\alpha(\mu_0)}{\tilde{\alpha}_\alpha(\mu)}\right)^{\vec{a}}\right]_D \hat{V}^{-1}. \tag{4.115}$$

Here the index α refers to the type of corrections, that is, pure QCD would be denoted by $\alpha = s$, pure QED would be referred by $\alpha = e$. Moreover, the factors a_i are known by the name of magic numbers, and they correspond to the eigenvalues of the diagonal leading order ADM,

$$\left[\hat{V}^{-1}\hat{\gamma}^{(0)T}_{\alpha}\hat{V}\right]_{ij} = 2\beta^{\alpha}_{00}a_i\delta_{ij}. \tag{4.116}$$

The leading order QCD-evolution matrix is needed to sum terms proportional to $(\tilde{\alpha}_s \log)^l$, where $\log = \log(\mu/\mu_0)$ with $\mu \ll \mu_0$. On the other hand, the leading QED contribution to the evolution matrix sums all terms of the form $(\tilde{\alpha}_e \log)(\tilde{\alpha}_s \log)^l$.

For higher order corrections the previous matrices $K(\mu)$ and $K^{-1}(\mu_0)$ play an important role, and they can be factorized as

$$\hat{K}(\mu) = \left[\hat{1} + \tilde{\alpha}_e J^{(2)}_{se}\right]\left[\hat{1} + \tilde{\alpha}_s(\mu)J^{(1)}_s + \tilde{\alpha}^2_s(\mu)J^{(2)}_s\right]\left[\hat{1} + \frac{\tilde{\alpha}_e}{\tilde{\alpha}_s(\mu)}J^{(1)}_e\right], \tag{4.117}$$

$$\begin{aligned}\hat{K}^{-1}(\mu_0) = &\left[\hat{1} - \frac{\tilde{\alpha}_e}{\tilde{\alpha}_s(\mu)}J^{(1)}_e\right]\left[\hat{1} - \tilde{\alpha}_s(\mu_0)J^{(1)}_s - \tilde{\alpha}^2_s(\mu_0)\left(J^{(2)}_s - [\hat{J}^{(1)}_s]^2\right)\right] \\ &\times \left[\hat{1} - \tilde{\alpha}_e J^{(2)}_{se}\right],\end{aligned} \tag{4.118}$$

where the terms $\hat{J}_\alpha$ are defined by

$$\hat{J}_\alpha^{(n)} = \hat{V}\hat{S}_\alpha^{(n)}\hat{V}^{-1}. \tag{4.119}$$

For pure QCD corrections, $\alpha = s$, we obtain, up to NNLO [56, 62]

$$\left[\hat{S}_s^{(1)}\right]_{ij} = \frac{\beta_{10}^s}{\beta_{00}^s}a_i\delta_{ij} - \frac{\left[\hat{G}_s^{(1)}\right]_{ij}}{2\beta_{00}^s(1+a_i-a_j)}, \tag{4.120}$$

$$\begin{aligned}\left[\hat{S}_s^{(2)}\right]_{ij} = {} & \frac{\beta_{20}^s}{2\beta_{00}^s}a_i\delta_{ij} - \frac{\left[\hat{G}_s^{(2)}\right]_{ij}}{2\beta_{00}^s(1+a_i-a_j)} \\ & + \sum_k \frac{1+a_i-a_k}{2+a_i-a_j}\left(\left[\hat{S}_s^{(1)}\right]_{ik}\left[\hat{S}_s^{(1)}\right]_{kj} - \frac{\beta_{10}^s}{\beta_{00}^s}\left[\hat{S}_s^{(1)}\right]_{ij}\delta_{jk}\right),\end{aligned} \tag{4.121}$$

with

$$\hat{G}_\alpha^{(n)} = \hat{V}^{-1}\left[\hat{\gamma}_\alpha^{(n)}\right]^T\hat{V}. \tag{4.122}$$

The NLO and the NNLO QCD-evolution matrices sum terms proportional to $\tilde{\alpha}_s\,(\tilde{\alpha}_s\log)^l$ and $\tilde{\alpha}_s^2\,(\tilde{\alpha}_s\log)^l$, respectively. Notice that the $\hat{S}_s$ matrix can develop singularities for certain combinations of the eigenvalues a_i. Luckily, the evolution matrix always remains finite after a proper combination of relevant terms. We will discuss this in more detail further below.

When also electromagnetic interactions enter into the game, extra factors have to be included for a consistent QCD evolution,

$$\left[\hat{S}_e^{(1)}\right]_{ij} = \frac{\left[\hat{G}_e^{(1)}\right]_{ij}}{2\beta_{00}^s(1+a_j-a_i)}, \tag{4.123}$$

$$\left[\hat{S}_{se}^{(2)}\right]_{ij} = \frac{1}{2\beta_{00}^s(a_j-a_i)}\left[\hat{G}_{se}^{(2)} + \left[\hat{G}_e^{(1)},\hat{S}_s^{(1)}\right] - \frac{\beta_{11}^{se}}{\beta_{00}^s}\hat{G}_s^{(1)} - \frac{\beta_{10}^s}{\beta_{00}^s}\hat{G}_e^{(1)}\right]_{ij}. \tag{4.124}$$

The matrices $\hat{S}_e^{(1)}$ and $\hat{S}_{se}^{(2)}$ also can develop singularities for certain combinations of the eigenvalues a_i and a_j.

In what follows, we will explain in more detail the issue of the singularities for the case of pure QCD. In this case it is instructive first to consider a scheme change that transforms the higher order anomalous dimensions to zero. From equations (4.79) and (4.80), we would have

$$\begin{aligned}0 &= \gamma_s^{(1)} + [\Delta\hat{r}_s^{(1)},\gamma_s^{(0)}] + 2\beta_{00}^s\Delta\hat{r}_s^{(1)}, \\ 0 &= \gamma_s^{(2)} + [\Delta\hat{r}_s^{(1)},\gamma_s^{(1)}] + [\Delta\hat{r}_s^{(2)},\gamma_s^{(0)}] - [\Delta\hat{r}_s^{(1)},\gamma_s^{(0)}]\Delta\hat{r}_s^{(1)}, \\ &\quad + 2\beta_{10}^s\Delta\hat{r}_s^{(1)} - 2\beta_{00}^s[\Delta\hat{r}_s^{(1)}]^2 + 4\beta_{00}^s\Delta\hat{r}_s^{(2)}.\end{aligned} \tag{4.125}$$

The Wilson coefficients of this new scheme would satisfy the following RGE,

$$\mu\frac{d}{d\mu}\vec{C}' = \tilde{\alpha}_s\hat{\gamma}'^{(0)T}\vec{C}', \tag{4.126}$$

and the solution would be similar to the leading order solution. In practice the μ dependence is traded for an α_s dependence in the solution of the renormalisation group equation. To take this into account we transform to a slightly different scheme that fulfills the following renormalisation group equations:

$$\mu\frac{d}{d\mu}\vec{C}' = \tilde{\alpha}_s\frac{\beta_s}{\beta_{00}^s}\hat{\gamma}'^{(0)T}\vec{C}'. \tag{4.127}$$

Using this definition the resulting expressed in α_s would read

$$\frac{d}{d\alpha_s}\hat{C}' = -\frac{1}{\tilde{\alpha}_s}\frac{\hat{\gamma}_s^{(0)^T}}{2\beta_{00}^s}\hat{C}', \tag{4.128}$$

where the total derivative in the strong coupling constant implies that the μ dependencies of all other couplings such as α_e are expressed via their dependence on α_s. Note that the Wilson coefficients defined in Eq. (4.128) are related to the renormalisation group invariant Wilson coefficients that we will define below through a simple multiplication with the μ dependent part of the leading order evolution. These resulting Wilson coefficients will be only dependent on the renormalization scale μ through numerical artifacts, that we will call residual scale dependence.

We can parametrize the relation between the Wilson coefficients in both schemes by means of a matrix $\hat{S}$:

$$\vec{C}' = \hat{S}\vec{C}(\mu), \tag{4.129}$$

which has a perturbative expansion in $\tilde{\alpha}_s$. The $\vec{C}(\mu)$ Wilson coefficients are the ones satisfying the RGE in eq. (4.70). Our aim is to solve the previous RGE, equation (4.128), and to get some useful algebraic relations that allow us to understand the problem of the singularities. We proceed as follows: the differential operator $\mu\ d/d\mu$ is written in terms of the the $\tilde{\alpha}_s$ dependence

$$\mu\frac{d}{d\mu} = -2\alpha_s^2\frac{\beta_s}{4\pi}\left(\frac{\partial}{\partial\alpha_s} - \frac{\alpha_e^2}{\alpha_s^2}\frac{\beta_e}{\beta_s}\frac{\partial}{\partial\alpha_e}\right). \tag{4.130}$$

Here the implicit μ dependence in α_e is now understood as $\alpha_e(\mu) = \alpha_e\left(\alpha_s(\mu)\right)$. By using (4.129) we obtain the following differential equations for the matrix $\hat{S}$

$$\left(\frac{\partial\hat{S}}{\partial\tilde{\alpha}_s} - \frac{\tilde{\alpha}_e^2}{\tilde{\alpha}_s^2}\frac{\beta_e}{\beta_s}\frac{\partial\hat{S}}{\partial\tilde{\alpha}_e}\right) - \frac{1}{2\beta_s\tilde{\alpha}_s^2}\hat{S}\hat{\gamma}^T = -\frac{1}{\tilde{\alpha}_s}\frac{\hat{\gamma}_s^{(0)^T}}{2\beta_{00}^s}\hat{S}. \tag{4.131}$$

This formalism relies on the fact that we can modify the higher order anomalous dimensions in such a way that Eq. (4.128) holds. In practice this is not always possible. Even in the pure QCD case a situation could arise where two eigenvalues of the leading order anomalous dimension differ by a factor of $2\beta^s_{00}$. In such a scenario and working in the eigenbasis, one would find that the off-diagonal element of the two-loop anomalous dimension matrix $\gamma_s^{(1)}$ associated with these above eigenvectors would be scheme independent. Hence it cannot be removed by a scheme transformation and one needs to modify the corresponding solution. One possible solution would be to work with a leading order solution that incorporates this scheme independent term in the exponential of a modified leading order anomalous dimension matrix. Expanding this solution would lead to logarithmic solutions. The alternative procedure is to rely on the fact that logarithmic terms will be generated and modify the ansatz to include logarithmic terms in $\hat{S}$,

$$\hat{S}(\mu) = \left[1 + \frac{\alpha_e}{4\pi}\left(J_0^{(1,1)} + J_1^{(1,1)} \ln \alpha_s + J_2^{(1,1)} (\ln \alpha_s)^2\right)\right]\left[1 + \frac{\alpha_s}{4\pi}\left(J_0^{(1,0)} + J_1^{(1,0)} \ln \alpha_s\right)\right] \times \left[1 + \frac{\alpha_e}{\alpha_s}\left(J_0^{(0,1)} + J_1^{(0,1)} \ln \alpha_s\right) + \frac{\alpha_e^2}{\alpha_s^2}\left(J_0^{(0,2)} + J_1^{(0,2)} \ln \alpha_s\right)\right]. \tag{4.132}$$

The form of the above solution can be understood by noting that the corresponding ordinary differential equation is of Fuchsian type and that the leading order anomalous dimension matrix is diagonal. Hence the solution can be written as a product $\vec{C}(\mu) = \hat{S}(\mu)\vec{C}'(\mu)$ where $\vec{C}'$ is the solution to the leading order renormalization group equation (4.128) while $\hat{S}(\mu)$ has the above form.

The differential equation (4.131) implies a set of simple algebraic equations for the matrices $J_l^{(i,j)}$ which read

$$
\begin{aligned}
0 &= \frac{\left[J_1^{(1,0)}, \gamma_s^{(0)^T}\right]}{2\beta_{00}^s} - J_1^{(1,0)}, \\
0 &= \frac{\left[J_0^{(1,0)}, \gamma_s^{(0)^T}\right]}{2\beta_{00}^s} + \frac{\beta_{10}^s \gamma_s^{(0)^T}}{2(\beta_{00}^s)^2} - \frac{\gamma_s^{(1)^T}}{2\beta_{00}^s} - J_0^{(1,0)} - J_1^{(1,0)}, \\
0 &= \frac{\left[J_1^{(0,1)}, \gamma_s^{(0)^T}\right]}{2\beta_{00}^s} + J_1^{(0,1)}, \\
0 &= \frac{\left[J_0^{(0,1)}, \gamma_s^{(0)^T}\right]}{2\beta_{00}^s} - \frac{\gamma_e^{(0)^T}}{2\beta_{00}^s} + J_0^{(0,1)} - J_1^{(0,1)}, \\
0 &= \frac{\left[J_2^{(1,1)}, \gamma_s^{(0)^T}\right]}{2\beta_{00}^s}, \\
0 &= \frac{\left[J_1^{(1,0)}, \gamma_e^{(0)^T}\right]}{2\beta_{00}^s} + \frac{\left[J_1^{(1,1)}, \gamma_s^{(0)^T}\right]}{2\beta_{00}^s} - 2J_2^{(1,1)}, \\
0 &= \frac{\left[J_0^{(1,0)}, \gamma_e^{(0)^T}\right]}{2\beta_{00}^s} + \frac{\left[J_0^{(1,1)}, \gamma_s^{(0)^T}\right]}{2\beta_{00}^s} + \frac{\beta_{10}^s \gamma_e^{(0)^T}}{2(\beta_{00}^s)^2} - \frac{\gamma_{se}^{(1)^T}}{2\beta_{00}^s} - J_1^{(1,1)}, \\
0 &= \frac{\left[J_1^{(0,2)}, \gamma_s^{(0)^T}\right]}{2\beta_{00}^s} - \frac{\gamma_e^{(0)^T} J_1^{(0,1)}}{2\beta_{00}^s} + \frac{J_1^{(0,1)} \beta_{00}^e}{\beta_{00}^s} + 2J_1^{(0,2)}, \\
0 &= \frac{\left[J_0^{(0,2)}, \gamma_s^{(0)^T}\right]}{4\beta_{00}^s} - \frac{\gamma_e^{(0)^T} J_0^{(0,1)}}{4\beta_{00}^s} + \frac{J_0^{(0,1)} \beta_{00}^e}{2\beta_{00}^s} + J_0^{(0,2)} - \frac{J_1^{(0,2)}}{2}\,.
\end{aligned}
\tag{4.133}
$$

Here the expansion coefficients β_{nm}^s and β_{nm}^e of the beta functions are defined via equation (4.76). This set of algebraic equations can be used to find a solution for the elements of the matrices $J_l^{(i,j)}$.

It is worth pointing that this set of equations were presented for the first time in [63], although in their first version the algebraic expressions were not fully correct due to missing terms of $\mathcal{O}(\tilde{\alpha}_e/\tilde{\alpha}_s)$. This was our motivation to compute a correct solution for the evolution matrix in the case of combined QCD and QED corrections. Our results presented in (4.133) were published in [64] and agree with the corrected version presented by the authors of reference [63].

4.10 Scheme Dependence of the Wilson coefficients

After having solved the renormalization group equations for the Wilson coefficients, we are now in a position to continue our discussion concerning the scheme dependence. From equation (4.112) and the corresponding transformation for the Wilson coefficients, which is given at NNLO by

$$\vec{C}'_s(\mu) = \left[\hat{1} - \tilde{\alpha}_s(\mu)\Delta\hat{r}_s^{(1)T} - \tilde{\alpha}_s^2(\mu)\left(\Delta\hat{r}_s^{(2)T} - [\Delta\hat{r}_s^{(1)T}]^2\right)\right]\vec{C}_s(\mu), \tag{4.134}$$

one can obtain the relations of the $\hat{J}$ matrices computed in two different bases. We only did that for NLO and NNLO pure-QCD interactions,

$$\begin{aligned}\hat{J}'^{(1)}_s &= \hat{J}^{(1)}_s - \Delta\hat{r}_s^{(1)T},\\ \hat{J}'^{(2)}_s &= \hat{J}^{(2)}_s - \Delta\hat{r}_s^{(1)T}\hat{J}^{(1)}_s - (\Delta\hat{r}_s^{(2)T} - [\Delta\hat{r}_s^{(1)T}]^2).\end{aligned}$$

These relations allow us to understand the scheme cancellation occurring at the electroweak scale between the upper part of the evolution matrix and the matrix elements. More precisely, the pure QCD-running of the Wilson coefficients up to two-loops is given by

$$\begin{aligned}\vec{C}_s(\mu) = \hat{K}_s\hat{U}_s^{(0)}(\mu,\mu_0)\Big(&\vec{T}^{(0)} + \tilde{\alpha}_s(\mu_0)\left[\vec{T}_s^{(1)} - \hat{R}_s^{(1)}\vec{T}^{(0)}\right]\\ &+\tilde{\alpha}_s^2(\mu_0)\left[\vec{T}_s^{(2)} - \hat{R}_s^{(1)}\vec{T}_s^{(1)} - (\hat{R}_s^{(2)} - (\hat{R}_s^{(1)})^2)\vec{T}^{(0)}\right]\Big),\end{aligned} \tag{4.135}$$

where the quantities $\hat{R}_s^{(1)} = \hat{r}_s^{(1)T} + \hat{J}_s^{(1)}$ and $\hat{R}_s^{(2)} = \hat{r}_s^{(2)T} + \hat{J}_s^{(2)} + \hat{r}_s^{(1)T}\hat{J}_s^{(1)}$, do not depend on the scheme. More details of how the scheme cancellation occurs will be given in Section 5.5 where this fact is explained for our particular calculation.

4.11 Summary of the main ideas for EFT

To finish our discussion, let us repeat the steps needed to construct the effective theory. First, one has to identify the degrees of freedom at the scale of interest. Second, the most general effective Lagrangian built up with only the light modes has to be constructed. The latter has to preserve the symmetries of the full theory, and the effects of higher energy particles can be incorporated perturbatively by means of higher-dimensional operators. The contribution of these terms to physical observables is suppressed by $(E/M)^n$, where M is a characteristic high-energy scale and E the energy of the interesting physical process. Consequently, only a finite number of operators is needed for the study of a given physical phenomena. Indeed, for an accuracy x the number can be determined by $n \approx \log(x)/\log(E/M)$. Although the latter can even be reduced by applying the EOM. The short-distance contributions are obtained by requiring that the effective field theory reproduces the physics of the full theory. The matching procedure can be performed on-shell, where the non-physical operators do not play any role, or can be computed off-shell and afterwards the EOM are applied to get the proper result. For a consistent evaluation of a given phenomenon at low-energy scales the RGE re-sum the large logarithms, which could destroy the meaning of perturbation theory.

Chapter 5

Matching Calculations

Here we use the formalism explained in the preceding chapters to complete the NNLO QCD corrections for the hadronic $|\Delta S| = 1$ effective Lagrangian. In section 5.1 we present the effective Lagrangian which describes these flavour transitions. In section 5.2 we describe the status of the short-distance part and comment on the missing pieces. Section 5.3 deals with the operator matching and presents our new results. In the following section 5.4 we present our new formalism that factorises the evolution at low energy scales and introduce new quantities that are scheme and scale independent. This property is checked analytically and explained in Section 5.5. The formalism employed in our numerics is presented in Section 5.6. Finally, Section 5.7 contains the residual scale dependence of our NNLO QCD corrections and a discussion about the validity of perturbation theory at very low energy scales.

5.1 Effective Lagrangian

The effective Lagrangian relevant to $|\Delta S| = |\Delta D| = 1$ transitions has the following form,

$$\begin{aligned}\mathcal{L}_{\text{eff}} &= \mathcal{L}_{\text{QCD}\times\text{QED}}(u,d,s,c,b,e,\mu,\tau) \\ &+ \frac{4G_F}{\sqrt{2}}\sum_{i=1}^{2}[V_{ud}V_{us}^*C_i^u\mathcal{O}_i^u + V_{cd}V_{cs}^*C_i^c\mathcal{O}_i^c] \\ &+ \frac{4G_F}{\sqrt{2}}\sum_{i=3}^{10}[V_{ud}V_{us}^*C_i^u + V_{cd}V_{cs}^*C_i^c + V_{td}V_{ts}^*C_i^t]\mathcal{O}_i\end{aligned} \tag{5.1}$$

where the first term comprises of the kinetic terms of the light SM particles as well as their QCD and QED interactions. The other two lines contain the higher dimensional operators of dimension $d \leq 6$, which describe $|\Delta S| = 1$ flavour transitions and which are only built out of the light fields; they can be found in section 4.6. Finally terms V_{ij} are elements of the Cabibbo-Kobayashi-Maskawa (CKM) matrix that satisfy unitarity relations. We use these to express the term $V_{cd}V_{cs}^*$ as a funtion of up- and top-quark

elements by means of $V_{cd}V_{cs}^* = -V_{ud}V_{us}^* - V_{td}V_{ts}^*$. After the GIM mechanism is applied, the previous effective Lagrangian reads

$$\begin{aligned}\mathcal{L}_{\text{eff}} &= \mathcal{L}_{\text{QCD}\times\text{QED}}(u,d,s,c,b,e,\mu,\tau) \\ &+ \frac{4G_F}{\sqrt{2}} V_{ud}V_{us}^* \left[\sum_{i=1}^{2}(C_i^u\mathcal{O}_i^u - C_i^c\mathcal{O}_i^c) + \sum_{i=3}^{10}(C_i^u - C_i^c)\mathcal{O}_i\right] \\ &+ \frac{4G_F}{\sqrt{2}} V_{td}V_{ts}^* \left[\sum_{i=3}^{10}(C_i^t - C_i^c)\mathcal{O}_i - \sum_{i=1}^{2} C_i^c\mathcal{O}_i^c\right].\end{aligned} \tag{5.2}$$

From equation (5.2) we can specialize the effective Lagrangian for different energy scales. In what follows, we discuss the respective contributions in detail and we provide the corresponding expressions for the effective Lagrangian.

For the case: $\mu > m_c$, the Wilson coefficients C_i^c and C_i^u satisfy the relation $C_i^c = C_i^u$. Consequently, the term $V_{ud}V_{us}^* \sum_{i=3}^{10}(C_i^u - C_i^c)\mathcal{O}_i$ in eq. (5.2) vanishes, and the effective Lagrangian reduces to

$$\begin{aligned}\mathcal{L}_{\text{eff}} &= \mathcal{L}_{\text{QCD}\times\text{QED}}(u,d,s,c,b,e,\mu,\tau) \\ &+ \frac{4G_F}{\sqrt{2}} V_{ud}V_{us}^* \left\{\sum_{i=1}^{2} C_i^u\tilde{\mathcal{O}}_i^u - \tau\sum_{i=1}^{10} C_i\mathcal{O}_i\right\},\end{aligned} \tag{5.3}$$

where we have defined a new current-current operator $\tilde{\mathcal{O}}_i^u$ $(i = 1, 2)$ as $\tilde{\mathcal{O}}_i^u = \mathcal{O}_i^u - \mathcal{O}_i^c$, and we understand $\mathcal{O}_{1,2}$ in the second sum as the current-current operators $\mathcal{O}_1^c$ and $\mathcal{O}_2^c$. Moreover, the Wilson coefficients C_i stand for $C_i^t - C_i^c$, and we introduce the ratio

$$\tau = -V_{td}V_{ts}^*/V_{ud}V_{us}^*. \tag{5.4}$$

Since the current-current Wilson coefficient C_2 is already generated at tree-level. This operator mixes into the penguin operators through the first diagram in fig. 4.3. This mixing between current-current and penguin operators generates a non-zero value for the coefficients C_1 and C_2 above the charm-quark mass scale: C_1^u=C_1 and C_2^u=C_2.

When the charm quark is integrated out as a dynamical degree of freedom, $\mu < m_c$ and the operators $\mathcal{O}_i^c$, $(i = 1, 2)$, do not appear in the expression (5.2). In addition, the term $V_{ud}V_{us}^* \sum_{i=3}^{10}(C_i^u - C_i^c)\mathcal{O}_i$ does not vanish. Indeed, we get,

$$V_{ud}V_{us}^* \sum_{i=3}^{10}(C_i^u - C_i^c)\mathcal{O}_i \to V_{ud}V_{us}^* \sum_{i=3}^{10} C_i^u\mathcal{O}_i. \tag{5.5}$$

Hence the corresponding expression for the effective Lagrangian at an energy scale below the charm-quark mass reads

$$\begin{aligned}\mathcal{L}_{\text{eff}} &= \mathcal{L}_{\text{QCD}\times\text{QED}}(u,d,s,c,b,e,\mu,\tau) \\ &\quad + \frac{4G_F}{\sqrt{2}} V_{ud}V_{us}^* \left\{ \sum_{i=1}^{10} C_i^u \mathcal{O}_i^u - \tau \sum_{i=3}^{10} C_i \mathcal{O}_i \right\}. \end{aligned} \tag{5.6}$$

Note that the Wilson coefficients C_i only stand for $i = 3 \ldots 10$ ($C_1 = C_2 = 0$), and that not-vanishing values for C_3^u to C_6^u have been generated.

5.2 Status of the short distance contributions

At present, the initial conditions $C_3(\mu_W) \ldots C_{10}(\mu_W)$ and $y_b(\mu_W)$ are known to NNLO-QCD at $\mathcal{O}(\tilde{\alpha}_s^2)$ for $i = 3 \ldots 6, b$ [48], and at $\mathcal{O}(\tilde{\alpha}_s\tilde{\alpha}_e)$ for $i = 7 \ldots 10$ [65]. In addition the ADM has been computed at NNLO for current-current and QCD-penguin operators [46]. The bottom-quark threshold contributions were determined at $\mathcal{O}(\tilde{\alpha}_s^2)$ (NNLO) by [66]. These authors used a different basis for the computation of the the current-current sub-block. Furthermore, at the energy scale of interest $\mu < m_c$, the Wilson coefficients y_i' with $i = 1 \ldots 6$ have been determined, using the traditional basis, to $\mathcal{O}(\tilde{\alpha}_s)$ (NLO) by the authors of references [56–59, 61]. In addition, the short-distance contributions parametrized by y_i' with $i = 7 \ldots 10$ were computed at $\mathcal{O}(\tilde{\alpha}_e)$, also in the traditional basis [57, 61]. The leading-order contribution to these coefficients are formally or order $\tilde{\alpha}_e/\tilde{\alpha}_s$. Moreover, the Wilson coefficients C_1^u and C_2^u are known to $\mathcal{O}(\tilde{\alpha}_s^2)$ (NNLO) [66]. The latter have also been computed in a different operator basis used by us. The charm-quark threshold contributions are unknown at the NNLO.

Our main goal in the next sections is to obtain these threshold corrections due to the removal of the bottom and charm quarks at NNLO accuracy, and use them to analyse the values of the Wilson coefficients at low-energy scales around 1.3 GeV. These important quantities are obtained by matching the $n_f + 1$-flavour and the n_f-flavour off-shell effective Green's functions perturbatively in $\tilde{\alpha}_s(\mu)$. When performing the matching, one sets the renormalization scale μ close to the mass that is removed as a dynamical degree of freedom, in order to reduce the size of the logarithms that appear, otherwise the perturbative expansion converges poorly.

5.3 Completing the NNLO corrections for the hadronic $|\Delta S| = 1$ effective Hamiltonian

There are several contributions to determine the effective Lagrangian relevant for ε'/ε at NNLO. This section aims to explain this calculation in detail and presents new results for the current-current and QCD-penguin operators.

Electroweak scale

First, the initial conditions for the Wilson coefficients at the electroweak scale are required, $\vec{C}(\mu_W)$, which are obtained by matching the SM Green's functions to those in the five-flavour theory, where the heavy particles have been integrated out. This relevant two-loop NNLO calculation was performed for B-physics [47] without employing the GIM mechanism [67].

For our effective Hamiltonian we have $C_i(\mu_W) = C_i^t(\mu_W) - C_i^c(\mu_W)$, where t and c denote the top and charm quark contribution respectively. Collecting the relevant results, the corresponding expressions for C_1 to C_6 are given by

$$
\begin{aligned}
C_1(\mu_W) &= \frac{\alpha_s^{(5)}(\mu_W)}{4\pi}\,(15+6L_W) \\
&\quad + \left(\frac{\alpha_s^{(5)}(\mu_W)}{4\pi}\right)^2 \left(\frac{7987}{72} + \frac{17}{3}\pi^2 + \frac{475}{6}L_W + 17L_W^2 - T(x_t)\right)\,, \\
C_2(\mu_W) &= 1 + \left(\frac{\alpha_s^{(5)}(\mu_W)}{4\pi}\right)^2 \left(\frac{127}{18} + \frac{4}{3}\pi^2 + \frac{46}{3}L_W + 4L_W^2\right)\,, \\
C_3(\mu_W) &= \left(\frac{\alpha_s^{(5)}(\mu)}{4\pi}\right)^2 \left(G_1^t(x_t) - \frac{680}{243} - \frac{20}{81}\pi^2 - \frac{68}{81}L_W - \frac{20}{27}L_W^2\right)\,, \\
C_4(\mu_W) &= \frac{\alpha_s^{(5)}(\mu)}{4\pi}\left(E_0^t(x_t) - \frac{7}{9} + \frac{2}{3}L_W\right) \\
&\quad + \left(\frac{\alpha_s^{(5)}(\mu)}{4\pi}\right)^2 \left(E_1^t(x_t) + \frac{842}{243} + \frac{10}{81}\pi^2 + \frac{124}{27}L_W + \frac{10}{27}L_W^2\right)\,, \\
C_5(\mu_W) &= \left(\frac{\alpha_s^{(5)}(\mu)}{4\pi}\right)^2 \left(\frac{2}{15}E_0^t(x_t) - \frac{1}{10}G_1^t(x_t) + \frac{68}{243} + \frac{2}{81}\pi^2 + \frac{14}{81}L_W + \frac{2}{27}L_W^2\right)\,, \\
C_6(\mu_W) &= \left(\frac{\alpha_s^{(5)}(\mu)}{4\pi}\right)^2 \left(\frac{1}{4}E_0^t(x_t) - \frac{3}{16}G_1^t(x_t) + \frac{85}{162} + \frac{5}{108}\pi^2 + \frac{35}{108}L_W + \frac{5}{36}L_W^2\right)\,.
\end{aligned}
\tag{5.7}
$$

The explicit form of the loop functions $T(x_t)$, $G_1^t(x_t)$, $E_0^t(x_t)$ and $E_1^t(x_t)$ can be found in Section 2 of Ref. [47]. Moreover, in this theory with five active quark flavours we have $C_1^u = C_1$ and $C_2^u = C_2$ to all orders in perturbation theory and $C_i^u = 0$ for $i > 2$. The factor $L_W = \log(\mu^2/M_W^2)$ parametrises the explicit dependence on the matching scale μ, which should be taken $\sim M_W$ to avoid large logarithms. Subsequently, the Wilson coefficients are evolved down to the bottom-quark scale using the RGE

$$\vec{C}(\mu_b) = \hat{U}(\mu_b, \mu_W)\vec{C}(\mu_W), \tag{5.8}$$

where $\hat{U}(\mu_b, \mu_W)$ describes pure QCD evolution. This step is essential to avoid large logarithms when the bottom quark is also removed as a degree of freedom. This will be described in more detail below.

Bottom scale

Afterwards, we compute the threshold corrections at $\mu_b = \mathcal{O}(m_b)$, which are parametrized by the matrix $\hat{M}(\mu_b)$. For this we match Green's functions with operator insertions in the five- and four-flavour theories. At $\mathcal{O}(\tilde{\alpha}_s^2)$ the relevant penguin operators $\mathcal{O}_i$ $(i = 3, 4, 5, 6)$ in both the $n_f = 5$ and $n_f = 4$ theories differ by the inclusion/omission of the bottom quark in the sum over flavours. In addition, at this level in the perturbation expansion the discontinuity of the strong coupling constant has to be treated carefully for a proper matching calculation. In our calculation we use dimensional regularization and avoid the appearance of traces over γ_5 by employing the so-called "modern basis". We expand in the external momenta (as appropriate for a matching onto dimension-six operators) and set the masses of the light quarks to zero. After renormalization, the five-flavour result still contains infra-red divergences in the form of poles in $\varepsilon = (4 - d)/2$, which have to be reproduced in the four-flavour theory. As the Green's functions in the four-flavour theory contain only massless tadpole loop diagrams (after expansion in the external momenta), they are given entirely in terms of the ultraviolet counter-terms in the four-flavour theory, which are related to known anomalous dimensions. The cancellation of divergences constitutes an important check of our calculation. In the end, the matching results in finite threshold corrections for the Wilson coefficients that can be concisely expressed in matrix form as

$$\vec{C}^{(4)}(\mu_b) = M^{(b)}(m_b/\mu_b)\vec{C}^{(5)}(\mu_b), \tag{5.9}$$

where $M^{(b)}$ has block form

$$M^{(b)} = \begin{pmatrix} M_{CC}^{(b)} & 0_{2\times 4} \\ M_{PC}^{(b)} & M_{PP}^{(b)} \end{pmatrix} \tag{5.10}$$

and the Wilson-coefficients in the n_f-flavour theory define the vector

$$\vec{C}^{(n_f)} = (C_1^{(n_f)}, \ldots, C_6^{(n_f)}). \tag{5.11}$$

Expanding the threshold matrix in terms of the strong coupling up to two loops

$$M^{(b)} = M^{(b,0)} + \tilde{\alpha}_s^{(4)}(\mu_b) M^{(b,1)} + [\tilde{\alpha}_s^{(4)}(\mu_b)]^2 M^{(b,2)} + \mathcal{O}(\alpha_s^3), \tag{5.12}$$

one has

$$M^{(b,0)} = \mathbf{1}_{6\times 6}\,, \tag{5.13}$$

which results from tree level matching. At the next order, only the insertions of $\mathcal{O}_4$ and $\mathcal{O}_6$, in the first diagram of fig. 5.1, give a non-vanishing contribution. The resulting matching matrix reads

$$M^{(b,1)} = \begin{pmatrix} 0 & 0 & 0 & 0 & 0 & 0 \\ 0 & 0 & 0 & 0 & 0 & 0 \\ 0 & 0 & 0 & 0 & 0 & 0 \\ 0 & 0 & 0 & \frac{2}{3}L_b & 0 & 4+\frac{20}{3}L_b \\ 0 & 0 & 0 & 0 & 0 & 0 \\ 0 & 0 & 0 & 0 & 0 & 0 \end{pmatrix}, \tag{5.14}$$

where $L_b \equiv \ln \frac{m_b(\mu_b)^2}{\mu_b^2}$, where $m_b(\mu_b)$ is the $\overline{\text{MS}}$-mass. The $\mathcal{O}(\tilde{\alpha}_s^2)$ determination of the CC block involves the insertion of current-current type diagrams dressed with gluons that have a bottom quark self-energy, see the first diagram of fig. 5.2. After the appropriate inclusion of the effective theory renormalization and wave-function renormalization of the external quark fields, one obtains

$$M_{CC}^{(b,2)} = \begin{pmatrix} \frac{17}{27} + \frac{8}{9}L_b + \frac{2}{3}L_b^2 & -\frac{79}{18} + \frac{10}{3}L_b - 2L_b^2 \\ \frac{-79}{81} + \frac{20}{27}L_b - \frac{4}{9}L_b^2 & 0 \end{pmatrix}, \tag{5.15}$$

which is a new result for the operator basis (4.54). It agrees with the results of Ref. [44] after the relevant change of operator basis has been performed. No penguin type insertions of current-current operators exist at the two-loop level and the corresponding matrix elements

$$M_{PC}^{(b,2)} = 0_{4\times 2} \tag{5.16}$$

vanish at this order.

The threshold corrections of the penguin operators can be written as

$$M_{PP}^{(b,2)} = \begin{pmatrix} 0 & b_{34} & b_{35} & b_{36} \\ b_{43} & b_{44} & b_{45} & b_{46} \\ 0 & b_{54} & b_{55} & b_{56} \\ b_{63} & b_{64} & b_{65} & b_{66} \end{pmatrix}, \tag{5.17}$$

where the matrix entries are

$$b_{43} = \frac{443}{54} + \frac{10}{9}L_b + \frac{10}{3}L_b^2, \qquad b_{63} = -\frac{85}{108} - \frac{L_b}{9} - \frac{L_b^2}{3}, \tag{5.18}$$

$$b_{34} = \frac{886}{243} + \frac{184}{81}L_b + \frac{40}{27}L_b^2, \qquad b_{44} = \frac{589}{162} + \frac{370}{81}L_b + \frac{37}{54}L_b^2, \tag{5.19}$$

$$b_{54} = -\frac{85}{243} - \frac{4}{81}L_b - \frac{4}{27}L_b^2, \qquad b_{64} = -\frac{425}{648} - \frac{5}{54}L_b - \frac{5}{18}L_b^2, \tag{5.20}$$

$$b_{35} = -\frac{452}{27} - \frac{80}{9}L_b, \qquad b_{45} = \frac{565}{27} - \frac{740}{9}L_b + \frac{100}{3}L_b^2, \tag{5.21}$$

$$b_{55} = \frac{38}{27} + \frac{8}{9}L_b, \qquad b_{65} = -\frac{383}{54} + \frac{74}{9}L_b - \frac{10}{3}L_b^2, \tag{5.22}$$

$$b_{36} = \frac{6874}{243} + \frac{88}{81}L_b + \frac{328}{27}L_b^2, \qquad b_{46} = -\frac{2651}{162} - \frac{5030}{81}L_b - \frac{220}{27}L_b^2, \tag{5.23}$$

$$b_{56} = -\frac{826}{243} + \frac{128}{81}L_b - \frac{40}{27}L_b^2, \qquad b_{66} = -\frac{467}{162} + \frac{266}{27}L_b - \frac{23}{18}L_b^2. \tag{5.24}$$

The PP block has been obtained before to $\mathcal{O}(\alpha_s^2)$.

Finally, we note that $C_1^{u(n_f)} = C_1^{(n_f)}$ and $C_2^{u(n_f)} = C_2^{(n_f)}$ for $n_f \geq 4$. If this were not the case (for example, due to new-physics contributions), the relevant matching equation could then be represented by a 2×2 matrix multiplication

$$\vec{C}^{u(4)}(\mu_b) = M_{CC}^{(b)}(m_b/\mu_b)\vec{C}^{u(5)}(\mu_b), \tag{5.25}$$

where $\vec{C}^{u(n_f)} = (C_1^{u(n_f)}, C_2^{u(n_f)})^T$ comprises of the C_i^u Wilson coefficients in the four and five flavour theory.

Yet, current lattice results are only available in the $n_f = 3$-flavour theory. Hence the resulting Wilson coefficients $\vec{C}(\mu_b)$ are then evolved down to the charm-quark scale using the RGE,

$$\vec{C}(\mu_c) = \hat{U}(\mu_c, \mu_b)\hat{M}(\mu_b/m_b)\vec{C}(\mu_b). \tag{5.26}$$

Once the relevant hadronic matrix elements become available in an $n_f = 4$-flavour theory, one may omit this step; this will be discussed further below in section 6.7.1.

Charm threshold

At this scale, $\mu_c = \mathcal{O}(m_c)$, the matching equation for the charm quark is now evaluated. However, at very low-energy scales the value of $\tilde{\alpha}_s(\mu)$ is larger and the renormalization group improved perturbation theory might not converge if compared to higher scales. We will comment on this after having shown our results. Here we match the four-flavour theory onto the three-flavour theory and find the new threshold corrections $\hat{M}(\mu_c)$. Writing the Wilson coefficients in the 3-flavour theories

$$\vec{C}^{(3)} = (C_3^{(3)}, C_4^{(3)}, C_5^{(3)}, C_6^{(3)})^T \,, \tag{5.27}$$

we can express the matching equation

$$\vec{C}^{(3)}(\mu_c) = M^{(c)}(m_c/\mu_c)\vec{C}^{(4)}(\mu_c) \tag{5.28}$$

in terms of a matrix multiplication. The matrix $M^{(c)}$ has the general block-form

$$M^{(c)} = \begin{pmatrix} M_{PC}^{(c)} & M_{PP}^{(c)} \end{pmatrix} . \tag{5.29}$$

Expanding

$$M^{(c)} = M^{(c,0)} + \tilde{\alpha}_s^{(3)}(\mu_c)M^{(c,1)} + [\tilde{\alpha}_s^{(3)}(\mu_c)]^2 M^{(c,2)} + \mathcal{O}(\alpha_s^3), \tag{5.30}$$

one finds the tree level matching conditions

$$M_{PC}^{(c,0)} = \mathbf{0}_{4\times 2} \quad \text{and} \quad M_{PP}^{(c,0)} = \mathbf{1}_{4\times 4} \,. \tag{5.31}$$

The one-loop and two-loop matching of the penguin operators can be inferred from the bottom scale matching by the replacement $L_b \to L_c \equiv \ln \frac{m_c(\mu_c)^2}{\mu_c^2}$. We find explicitly

$$M_{PP}^{(c,1)} = \begin{pmatrix} 0 & 0 & 0 & 0 \\ 0 & \frac{2}{3}L_c & 0 & 4 + \frac{20}{3}L_c \\ 0 & 0 & 0 & 0 \\ 0 & 0 & 0 & 0 \end{pmatrix} \tag{5.32}$$

at one-loop and relate the two-loop matching matrix to $M_{PP}^{(b,2)}$ as

$$M_{PP}^{(c,2)} = M_{PP}^{(b,2)}\Big|_{L_b \to L_c} . \tag{5.33}$$

The current-current operators in the 4-flavour theory contain a charm-quark. Removing this charm quark generates matching corrections that can be absorbed in a redefinition of the penguin Wilson coefficients. To find these corrections we calculate the insertions of current-current operators into a QCD penguin diagrams at one-loop. The resulting matching matrix

$$M_{PC}^{(c,1)} = \begin{pmatrix} 0 & 0 \\ -\frac{1}{9}(1+L_c) & \frac{2}{3}(1+L_c) \\ 0 & 0 \\ 0 & 0 \end{pmatrix} \tag{5.34}$$

receives only a contribution to C_4 in the effective theory at $\mathcal{O}(\tilde{\alpha}_s)$. At the next order both penguin and box-type diagrams contribute and we find

$$M_{PC}^{(c,2)} = \begin{pmatrix} -\frac{797}{1458} - \frac{766}{243}L_c - \frac{10}{81}L_c^2 & \frac{554}{243} - \frac{88}{81}L_c + \frac{20}{27}L_c^2 \\ -\frac{371}{1944} - \frac{283}{486}L_c + \frac{109}{162}L_c^2 & \frac{275}{81} + \frac{40}{81}L_c - \frac{28}{27}L_c^2 \\ -\frac{125}{2916} + \frac{73}{243}L_c + \frac{1}{81}L_c^2 & -\frac{59}{243} + \frac{16}{81}L_c - \frac{2}{27}L_c^2 \\ \frac{295}{3888} - \frac{5}{81}L_c + \frac{5}{216}L_c^2 & -\frac{295}{648} + \frac{10}{27}L_c - \frac{5}{36}L_c^2 \end{pmatrix}. \tag{5.35}$$

Below the charm threshold the GIM mechanism is absent. This implies in particular that the Wilson coefficients C_1^u and C_2^u are no longer trivially related to C_1 and C_2. In addition, all Wilson coefficients

$$\vec{C}^{u(3)} = (C_1^{u(3)}, C_2^{u(3)}, C_3^{u(3)}, C_4^{u(3)}, C_5^{u(3)}, C_6^{u(3)}) \tag{5.36}$$

receive non-zero matching contributions at two-loop level. The Wilson coefficients of the three-flavour theory satisfy the matching relation as

$$\vec{C}^{u(3)} = M^{u(c)}\vec{C}^{u(4)}\,, \tag{5.37}$$

where the matching matrix is parametrized as

$$M^{u(c)} = \begin{pmatrix} M_{UU}^{(c)} \\ M_{PU}^{(c)} \end{pmatrix}, \tag{5.38}$$

and it can be perturbatively expanded in terms of the strong coupling constant,

$$M^{u(c)} = M^{u(c,0)} + \tilde{\alpha}_s^{(3)}(\mu_c)M^{u(c,1)} + [\tilde{\alpha}_s^{(3)}(\mu_c)]^2 M^{u(c,2)} + \mathcal{O}(\tilde{\alpha}_s^3). \tag{5.39}$$

The matching of the current-current operators is trivially related to the matching at the bottom scale as

$$M_{UU}^{(c)} = M_{CC}^{(b)}\Big|_{L_b \to L_c} \tag{5.40}$$

to all orders in QCD. To extract the other entries of the matching matrix we recall that the current-current operators $\mathcal{O}_1^u$ and $\mathcal{O}_2^u$ involve the charm quark with an opposite sign to the operators $\mathcal{O}_1$ and $\mathcal{O}_2$. Hence we find the relation

$$M_{PU}^{(c)} = -M_{PC}^{(c)} \tag{5.41}$$

that holds at least up to the order $\mathcal{O}(\tilde{\alpha}_s^2)$.

Finally, we incorporate these results and perform the renormalization group evolution down to the scales where the hadronic matrix elements are computed,

$$\vec{C}(\mu_{\rm L}) = \hat{U}(\mu_{\rm L}, \mu_c)\hat{M}(\mu_c)\vec{C}(\mu_c). \tag{5.42}$$

This RGE will be discussed separately in Section 5.4.

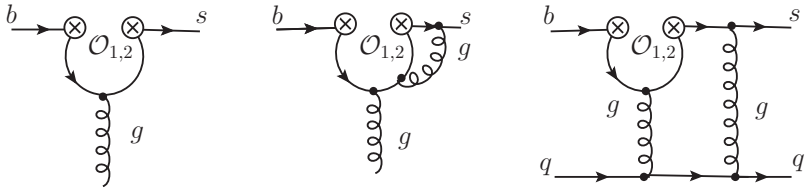

Figure 5.1: 1PI diagrams mixing the current-current operators into QCD-penguin operators

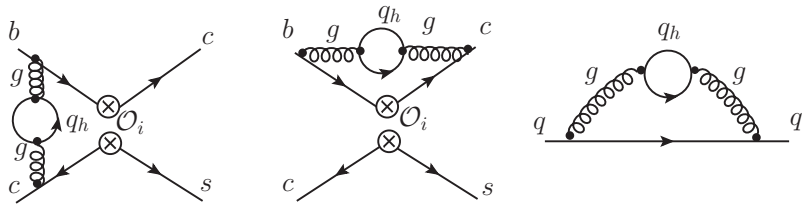

Figure 5.2: 1PI diagrams mixing into current-current operators

5.3.1 Details of the matching calculation

This section provides more details about the matching calculations. We would like to describe here how the cancellation of the divergences takes place and the role of the threshold corrections. We will begin our discussion with the latter, in particular, our aim is to disentangle the expressions of the $\delta\hat{r}$ matrices, which appear in the matching equations (4.52), and comment on how they are specialized to the cases of $d \to sg$ and $d \to sq\bar{q}$. The general forms of these matrices up to two loops are given below,

$$\begin{aligned}
\delta\hat{r}^{(1)}_{ik} &= \delta\hat{F}^{(1),\Gamma}_{ik} + \delta\hat{Z}^{(1)}_{ik} + \left[\delta Z^{(1)}_{f,k} + \delta z^{(1)}_{\Gamma}\right]\delta_{ik}, \\
\delta\hat{r}^{(2)}_{ik} &= \delta\hat{F}^{(2),\Gamma}_{ik} + \delta\hat{Z}^{(2)}_{ik} + \left[\delta Z^{(2)}_{f,k} + \delta z^{(2)}_{\Gamma}\right]\delta_{ik} - \zeta^{(1)}_{\xi} Z^{(1)}_{f,k}\delta_{ik} \\
&\quad + \delta\left(Z^{(1)}_{f,i}\hat{F}^{(1),\Gamma}_{ik}\right) + \delta\left(\hat{Z}^{(1)}_{ij}\hat{F}^{(1),\Gamma}_{jk}\right) + \delta\left(z^{(1)}_{\Gamma}\hat{F}^{(1),\Gamma}_{ik}\right) \\
&\quad + \delta\left(\hat{Z}^{(1)}_{ik}Z^{(1)}_{f,k}\right) + \delta\left(z^{(1)}_{\Gamma}\hat{Z}^{(1)}_{ik}\right) + \delta\left(z^{(1)}_{\Gamma}Z^{(1)}_{f,k}\right)\delta_{ik}.
\end{aligned} \tag{5.43}$$

Here the matrix $\hat{F}^{(l),\Gamma}_{ik}$ (with l the loop order, and Γ referring to the initial and final states) is the loop contribution obtained when a given operator is inserted into an effective vertex. In the case we discuss this corresponds to the insertion of the current-current operators: $\mathcal{O}_1$ and $\mathcal{O}_2$. It is important to mention here that the one-loop diagrams with inserted counter-terms which subtract the divergences of the sub-graphs, and the overall counter-terms are also included in that function. To clarify the this statement, we could express the QCD-renormalized matrix elements as a function of $\hat{F}^{(l),\Gamma}_{ik}$ in a mathematical form:

$$\langle\mathcal{O}_i\rangle^{(l)}_{\text{QCD-reno}} = \hat{F}^{(l),\Gamma}_{ik}\langle\mathcal{O}_k\rangle^{(0)}. \tag{5.44}$$

Moreover, the matrix $\hat{Z}^{(l)}_{ik}$ and the term $Z^{(l)}_{f,k}$ in eq. (5.43) stand for the mixing matrix and the renormalization of the field. In Section 4.2, we denoted the latter by Z_ψ, here we use the subscript f since some operators have extra terms (m_s, additional g_s or e factors) in their definition, for this reason we keep a more general label. Furthermore, the factor z_Γ refers to the wave function renormalization, see eq. (4.9). Finally, one has to understand the terms δA, where A can be any of the combinations appearing above, as the discontinuity between effective field theory of n_f+1 and that of n_f-flavours, see the relation in (4.51).

The next point is to analyse what occurs in the matching. For the case of current-current into current-current operators, we receive the first contribution at two-loops, thus the $\hat{F}^{(1),\Gamma}_{ik}$ term vanishes. Moreover, the physical processes considered, which are denoted by Γ, correspond to the decay $d \to sq\bar{q}$. In section 4.4.3 we saw that the fermion field redefinition, which appears when a heavy mode is integrated out as a dynamical degree of freedom, occurs for the first time at two-loops. Consequently, the

term $\delta z_{\Gamma}^{(1)}$ also does not contribute. At two loops, we have:

$$\delta\hat{r}_{ik}^{(2)} = \delta\hat{F}_{ik}^{(2),\Gamma} + \delta\hat{Z}_{ik}^{(2)} + \left[\delta Z_{f,k}^{(2)} + \delta z_{\Gamma}^{(2)}\right]\delta_{ik} + \delta\left(\hat{Z}_{ik}^{(1)} Z_{f,k}^{(1)}\right) - \zeta_{\xi}^{(1)} Z_{f,k}^{(1)}\delta_{ik} \tag{5.45}$$

The term multiplied by the threshold corrections of the gauge parameter, $\zeta_{\xi}^{(1)}$, will be cancelled by the contribution $-\zeta_{g^2}^{(1)} Z_{f,k}^{(1)}\delta_{ik}$, which is contained in the last term of equation (4.52). The latter appears due to express the coupling of the complete theory in terms of the coupling of the effective field theory. In addition, $-\zeta_{g^2}^{(1)}\hat{Z}_{ik}^{(1)}$ cancels the $\log(\mu_f)$ of $\delta\hat{F}_{ik}^{(2),\Gamma}$. It is important to note that the epsilon terms of $\zeta_{g^2}^{(1)}$ must also be also included, otherwise the previous statement will not be satisfied. Furthermore, it is essential to include the term $\delta z_{\Gamma}^{(2)}$ to obtain a correct result when $\mathcal{O}_2$ is inserted in the first diagram of fig. 5.2, since otherwise we would obtain a non-zero value, which is inconsistent.

When the current-current operators are inserted into the penguin diagrams ($i \neq k$), the situation changes. Indeed, at one-loop the term multiplied by δ_{ik} in the first equation of (5.43) do not contribute, and therefore, we have the following expression for $\delta\hat{r}_{ik}^{(1)}$,

$$\delta\hat{r}_{ik}^{(1)} = \delta\hat{F}_{ik}^{(1),\Gamma} + \delta\hat{Z}_{ik}^{(1)}. \tag{5.46}$$

On the other hand, the two-loop term is given by

$$\begin{aligned}\delta\hat{r}_{ik}^{(2)} = {} & \delta\hat{F}_{ik}^{(2),\Gamma} + \delta\hat{Z}_{ik}^{(2)} + \delta\left(z_{\Gamma}^{(1)}\hat{Z}_{ik}^{(1)}\right) + \delta\left(z_{\Gamma}^{(1)}\hat{F}_{ik}^{(1),\Gamma}\right) \\ & + \delta\left(Z_{f,i}^{(1)}\hat{F}_{ik}^{(1),\Gamma}\right) + \delta\left(\hat{Z}_{ij}^{(1)}\hat{F}_{jk}^{(1),\Gamma}\right) + \delta\left(\hat{Z}_{ik}^{(1)} Z_{f,k}^{(1)}\right).\end{aligned} \tag{5.47}$$

The last two terms of the first line in the previous equation will be cancelled by $-\zeta_{g^2}^{(1)} Z_{ik}^{(1)}$ and by $-\zeta_{g^2}^{(1)}\hat{F}_{ik}^{(1),\Gamma}$, respectively.

It is worth mentioning here that the threshold corrections coming from the gauge parameter might play an important role in the matching calculation at three loops, and therefore they must be included for a consistent analysis.

5.4 Renormalization Group Invariant Elements

Our new contributions will be used to improve the theoretical prediction of the observable ε'/ε. To derive the phenomenological formula for this observable some Fierz identities between operators are used, which reduce the dependence on the hadronic parameters, as we will see in more detail in the next chapter. Yet these relations are in general not valid beyond LO, indeed they receive $\mathcal{O}(\tilde{\alpha}_s)$ corrections; more information on this will be given in section 6.3. Moreover, some subtleties arise in the calculation of non-perturbative hadronic matrix elements. They cannot be computed in the MS-scheme. In fact, these elements are obtained in a different scheme and then perturbatively converted to the $\overline{\text{MS}}$-scheme, which is at least as complicated as the calculation of the Wilson coefficients and must be done for every intermediate scheme. Hence, it is highly desirable to define an interface that is both non-perturbatively defined and easy to convert to the $\overline{\text{MS}}$-scheme. We take inspiration from the Renormalization Group Invariant (RGI) parameters $\hat{m}$ and $\hat{B}_K$ which successfully accomplish this, and introduce a renormalization scheme that has the benefit of separating the scale and scheme dependence of the matching contribution, the Wilson coefficients, and the hadronic matrix elements for all the different scales involved in the RGE running to low-energy regimes. Moreover this new interface preserves the Fierz identities of eq. (6.5) to all orders.

The basics of our formalism are based on the fact that the evolution matrix presented in equation (4.114) depends on two different scales, with $\mu \ll \mu_0$. Thus, for pure QCD this matrix can be factorized into two parts,

$$\begin{aligned} \hat{U}^{\frac{1}{2}}(\mu) &= \hat{K}(\mu)\hat{V}\text{diag}[\tilde{\alpha}_s(\mu)]^{-a_i}\hat{V}^{-1}, \\ \hat{U}^{-\frac{1}{2}}(\mu_0) &= \hat{V}\text{diag}[\tilde{\alpha}_s(\mu_0)]^{a_i}\hat{V}^{-1}\hat{K}^{-1}(\mu_0) \end{aligned} \tag{5.48}$$

that contain the contributions of the different scales. Remember that the matrix $\hat{K}$ and its inverse were given in equations (4.117) and (4.118), and in the pure QCD case $\tilde{\alpha}_e(\mu)$ is set to zero. From this factorization we find that the following object appears in the intermediate stages in our calculations:

$$\left[\hat{U}^{-\frac{1}{2}}(\mu)\right]_{n_f}\left[\hat{M}(\mu)\right]_{n_f,n_f+1}\left[\hat{U}^{\frac{1}{2}}(\mu)\right]_{n_f+1}. \tag{5.49}$$

Moreover at the electroweak scale we have

$$\hat{C}_i^{(5)} = \hat{U}_{ij}^{-\frac{1}{2}}(\mu_W)C_j^{(5)}(\mu_W), \tag{5.50}$$

where the term in the left-hand side of the equation above is also scheme and scale independent. Proceeding in this way, the pure QCD evolution to the charm-quark

scale can be parametrized as

$$\hat{C}_i^{(3)} = \hat{\mathcal{M}}_{ik}^c \hat{\mathcal{M}}_{kj}^b \hat{C}_j^{(5)}, \tag{5.51}$$

where we use the "calligraphic-hat" notation for the term given in eq. (5.49), and only hat for the Wilson coefficients. The remaining evolution piece with dependence $\mu_{\rm L}$ (lattice scale) will be absorbed in the operators,

$$\langle \pi\pi|\hat{\mathcal{O}}_i|K\rangle = \langle \pi\pi|\mathcal{O}_l|K\rangle(\mu_{\rm L})\hat{U}_{li}^{\frac{1}{2}}(\mu_{\rm L}). \tag{5.52}$$

5.5 Analytical check of scale independence

As the RGE matrix elements and Wilson coefficients are scheme and scale independent a complete cancellation of the $\ln \mu$ dependence has to occur. This section will explain this cancellation in detail, since it is an important check of our results. Several important expansions have to be performed in this evaluation. The first step to consider is the RGE solution for the strong coupling constant and expand it up to second order in $\tilde{\alpha}_s$ for a general number of flavours by,

$$\begin{aligned}\tilde{\alpha}_s^{(n_f)}(\mu) = \tilde{\alpha}_s^{(n_f)}(m_f) - [\tilde{\alpha}_s^{(n_f)}(m_f)]^2\ 2\beta_{00}^s \log\left(\frac{\mu}{m_q(\mu_f)}\right) \\ - [\tilde{\alpha}_s^{(n_f)}(m_f)]^3 \left[2\beta_{10}^s \log\left(\frac{\mu}{m_q(\mu_f)}\right) - 4(\beta_{00}^s)^2 \log^2\left(\frac{\mu}{m_q(\mu_f)}\right)\right]\end{aligned} \tag{5.53}$$

where there is also a n_f dependence in the beta function terms,

$$\beta_{00}^s = \frac{1}{4}\left(11 - \frac{2}{3}n_f\right), \text{and} \quad \beta_{10}^s = \frac{1}{16}\left(102 - \frac{38}{3}n_f\right). \tag{5.54}$$

The complete solution for the $\tilde{\alpha}_s$ RGE can be found in [68] including an elegant derivation of the combined QED and QCD running of the strong and electromagnetic coupling constants. In addition, the quark masses also depend on the considered energy scale, μ, and the number of active quark flavours: $m_q^{(n_f)}(\mu)$; and their behaviour at low-energy scales are governed by the ADM function γ_m through the RGE equation (3.41). The expanded LO solution up to first order in $\tilde{\alpha}_s$ reads

$$m_q^{(n_f)}(\mu) = m_q^{(n_f)}(m_f)\left[1 + \tilde{\alpha}_s^{(n_f)}(m_f)\gamma_m^{(n_f)} \ln\left(\frac{\mu}{m_f}\right)\right]. \tag{5.55}$$

The previous expressions are necessary for the running and the decoupling of $\tilde{\alpha}_s$ and for the quark masses. With these two important ingredients we can focus on the object of eq. (5.49). Observe that it depends on both $\tilde{\alpha}_s^{(n_f)}(\mu)$ and on $\tilde{\alpha}_s^{(n_f+1)}(\mu)$. By means of the results (5.53) and (5.55), we can take care of the large logarithms; expressing the $\tilde{\alpha}_s^{(n_f+1)}(m_f)$ in terms of $\tilde{\alpha}_s^{(n_f)}(m_f)$, we observe that the scale dependence appearing in

the evolution down to the n_f-flavour theory (third term in eq. (5.49)) and that emerging in the evolution up to this theory (first term in eq. (5.49)) are cancelled by the $\ln(\mu_q)$ from the light-quark matching, $\hat{M}(\mu_q)$. Therefore, this object is individually scale- and scheme-independent. This implies certain consistency conditions on the elements of the matching matrix, which we derive below.

Let us look deeper at scale and scheme cancellations. For convenience, we multiply the left-hand side of the equation (5.49) by $[\hat{U}^{\frac{1}{2}}(m_q)]_{n_f}$ and the right-hand side by the term $[\hat{U}^{-\frac{1}{2}}(m_q)]_{n_f+1}$, where m_q is the fixed quark mass: $m_q \equiv m_q(m_q)$, that is,

$$\left[\hat{U}^{-1}(m_q,\mu)\right]_{n_f}\left[\hat{M}(\mu)\right]_{n_f,n_f+1}\left[\hat{U}(\mu,m_q)\right]_{n_f+1}. \tag{5.56}$$

In what follows, we proceed following the previous steps mentioned and consider the following expansion for the evolution matrix,

$$\begin{aligned}\hat{U}(\mu,m_q) = \hat{1} &+ \tilde{\alpha_s}^{(n_f)}(m_q)\left[\hat{U}_0^{(1)} + \hat{U}_1^{(1)}\ln\left(\frac{\mu}{m_q}\right)\right] \\ &+ [\tilde{\alpha_s}^{(n_f)}(m_q)]^2\left[\hat{U}_0^{(2)} + \hat{U}_1^{(2)}\ln\left(\frac{\mu}{m_q}\right) + \hat{U}_1^{(2)}\ln^2\left(\frac{\mu}{m_q}\right)\right],\end{aligned} \tag{5.57}$$

where the subscript of $\hat{U}$ refers to the power of the logarithm, and the corresponding coefficients are given as consistency conditions of the RGE and read at NNLO,

$$\begin{aligned}\hat{U}_1^{(1)} &= \hat{\gamma}_{n_f}^{(0)T}, \\ \hat{U}_1^{(2)} &= \hat{\gamma}_{n_f}^{(1)T} + \left(\hat{\gamma}_{n_f}^{(0)T} - 2\beta_{00}^s\hat{1}\right)\hat{U}_0^{(1)}, \\ \hat{U}_2^{(2)} &= \frac{1}{2}[\hat{\gamma}_{n_f}^{(0)T}]^2 - \beta_{00}^s\hat{\gamma}_{n_f}^{(0)T}.\end{aligned} \tag{5.58}$$

The initial conditions of the RGE also require $\hat{U}(m_q,m_q) = \hat{1}$ and one obtains that both $\hat{U}_0^{(1)}$ and $\hat{U}_0^{(2)}$ vanish. In the equations (5.58) we have omitted the index s for the ADM matrices to simplify the notation. In addition, the matching matrix can be expanded in terms of the logarithmic terms as

$$\begin{aligned}\hat{M}(\mu) = \hat{1} &+ \tilde{\alpha}_s^{(n_f)}(\mu)\left[\hat{M}_0^{(1)} + \hat{M}_1^{(1)}\ln\left(\frac{\mu}{m_q(\mu)}\right)\right] \\ &+ [\tilde{\alpha}_s^{(n_f)}(\mu)]^2\left[\hat{M}_0^{(2)} + \hat{M}_1^{(2)}\ln\left(\frac{\mu}{m_q(\mu)}\right) + \hat{M}_2^{(2)}\ln^2\left(\frac{\mu}{m_q(\mu)}\right)\right].\end{aligned} \tag{5.59}$$

From (5.56) and making use of the previous expansions (5.58) and (5.59) we arrive at the following analytical expressions,

$$\hat{M}_1^{(1)} + \hat{\gamma}_{n_f+1}^{(0)T} - \hat{\gamma}_{n_f}^{(0)T} = 0, \tag{5.60}$$

$$\hat{M}_1^{(2)} - 2\beta_{00}^s \hat{M}_0^{(1)} + \hat{\gamma}_m^{(0)T} \hat{M}_1^{(1)} - \hat{\gamma}_{n_f}^{(0)T} \hat{M}_0^{(1)} + \hat{M}_0^{(1)} \hat{\gamma}_{n_f+1}^{(0)T} - \hat{\gamma}_{n_f}^{(1)T} + \hat{\gamma}_{n_f+1}^{(1)T} = 0, \tag{5.61}$$

$$\begin{aligned} &\hat{M}_2^{(2)} - 2\beta_{00}^s \hat{M}_1^{(1)} - \hat{\gamma}_{n_f}^{(0)T} \hat{M}_1^{(1)} + \hat{M}_1^{(1)} \hat{\gamma}_{n_f+1}^{(0)T} + \frac{1}{2}\left[\hat{\gamma}_{n_f}^{(0)T}\right]^2 + \frac{1}{2}\left[\hat{\gamma}_{n_f+1}^{(0)T}\right]^2 \\ &+ \beta_{00}^{s(n_f)} \hat{\gamma}_{n_f}^{(0)T} + \beta_{00}^{s(n_f+1)} \hat{\gamma}_{n_f+1}^{(0)T} - \hat{\gamma}_{n_f}^{(0)T} \hat{\gamma}_{n_f+1}^{(0)T} = 0, \end{aligned} \tag{5.62}$$

that we used to check the $\ln \mu$ cancellation explicitly. It is worth pointing out that the log cancellation works order by order, and it has been checked at each matching scale.

5.6 Formalism for NNLO numerics

The hat objects only exhibit a residual scale dependence that is expected to reduce order by order and that is of the size of higher order corrections. Hence one can then estimate higher order effects by varying the matching scale μ_q while not expanding the expression in $\tilde{\alpha}_s(\mu)$. These effects will be studied in more detail in the coming section. In what follows, we expand the expressions for the matching matrix up to NNLO accuracy as

$$\hat{\mathcal{M}} = \hat{\mathcal{M}}_{\rm LO} + \hat{\mathcal{M}}_{\rm NLO} + \hat{\mathcal{M}}_{\rm NNLO}, \tag{5.63}$$

where the explicit form can be written if we factor out the leading order evolution kernel as

$$\hat{\mathcal{M}} = [\hat{U}^{(0)-1/2}]_{n_f} \left(\hat{1} + [\hat{\mathcal{M}}^{(1)}]_{n_f,n_f+1} + [\hat{\mathcal{M}}^{(2)}]_{n_f,n_f+1}\right) [\hat{U}^{(0)1/2}]_{n_f+1} \tag{5.64}$$

where the expression that contributes at NLO is given by

$$\hat{\mathcal{M}}^{(1)} = \tilde{\alpha}_s^{(n_f+1)}(\mu)[\hat{J}_s^{(1)}]_{n_f+1} + \tilde{\alpha}_s^{(n_f)}(\mu)\left([\hat{M}^{(1)}(\mu)]_{n_f,n_f+1} - [\hat{J}_s^{(1)}]_{n_f}\right). \tag{5.65}$$

The expressions that incorporate the two-loop matching corrections and the results from the three-loop anomalous dimensions read:

$$\begin{aligned} \hat{\mathcal{M}}^{(2)} &= [\tilde{\alpha}_s^{(n_f+1)}(\mu)]^2 [\hat{J}_s^{(2)}]_{n_f+1} \\ &+ [\tilde{\alpha}_s^{(n_f)}(\mu)]^2 \left([\hat{M}^{(2)}(\mu)]_{n_f,n_f+1} - [\hat{J}_s^{(2)}]_{n_f} + [\hat{J}_s^{(1)}]_{n_f}[\hat{J}_s^{(1)}]_{n_f}\right) \\ &+ \tilde{\alpha}_s^{(n_f+1)}(\mu)\tilde{\alpha}_s^{(n_f)}(\mu)\left([\hat{M}^{(1)}(\mu)]_{n_f,n_f+1}[\hat{J}_s^{(1)}]_{n_f+1} - [\hat{J}_s^{(1)}]_{n_f}[\hat{J}_s^{(1)}]_{n_f+1}\right). \end{aligned} \tag{5.66}$$

In a similar manner we can expand the Wilson coefficients in eq. (5.50) as

$$\hat{C}^{(n_f)} = \hat{C}^{(n_f)}_{\rm LO} + \hat{C}^{(n_f)}_{\rm NLO} + \hat{C}^{(n_f)}_{\rm NNLO} \tag{5.67}$$

to find the resulting expression for the Wilson coefficient (5.51) in the theory with three active flavours:

$$\begin{aligned}\hat{C}^{(3)} = {} & \hat{\mathcal{M}}^{(c)}_{\rm LO}\hat{\mathcal{M}}^{(b)}_{\rm LO}\hat{C}^{(5)}_{\rm LO} \\ & + \hat{\mathcal{M}}^{(c)}_{\rm NLO}\hat{\mathcal{M}}^{(b)}_{\rm LO}\hat{C}^{(5)}_{\rm LO} + \hat{\mathcal{M}}^{(c)}_{\rm LO}\hat{\mathcal{M}}^{(b)}_{\rm NLO}\hat{C}^{(5)}_{\rm LO} + \hat{\mathcal{M}}^{(c)}_{\rm LO}\hat{\mathcal{M}}^{(b)}_{\rm LO}\hat{C}^{(5)}_{\rm NLO} \\ & + \hat{\mathcal{M}}^{(c)}_{\rm NNLO}\hat{\mathcal{M}}^{(b)}_{\rm LO}\hat{C}^{(5)}_{\rm LO} + \hat{\mathcal{M}}^{(c)}_{\rm LO}\hat{\mathcal{M}}^{(b)}_{\rm NNLO}\hat{C}^{(5)}_{\rm LO} + \hat{\mathcal{M}}^{(c)}_{\rm LO}\hat{\mathcal{M}}^{(b)}_{\rm LO}\hat{C}^{(5)}_{\rm NNLO} \\ & + \hat{\mathcal{M}}^{(c)}_{\rm NLO}\hat{\mathcal{M}}^{(b)}_{\rm NLO}\hat{C}^{(5)}_{\rm LO} + \hat{\mathcal{M}}^{(c)}_{\rm NLO}\hat{\mathcal{M}}^{(b)}_{\rm LO}\hat{C}^{(5)}_{\rm NLO} + \hat{\mathcal{M}}^{(c)}_{\rm LO}\hat{\mathcal{M}}^{(b)}_{\rm NLO}\hat{C}^{(5)}_{\rm NLO}.\end{aligned} \tag{5.68}$$

Each term in this sum of products can be numerically evaluated for explicit values of $\alpha_s^{(3)}(\mu_c)$, $\alpha_s^{(4)}(\mu_c)$, $\alpha_s^{(4)}(\mu_b)$, $\alpha_s^{(5)}(\mu_b)$, $\alpha_s^{(5)}(\mu_t)$, $m_c(\mu_c)$, $m_b(\mu_b)$ and $m_t(\mu_t)$. After the determination of these quantities, we determine the Wilson coefficients through the simple matrix and vector calculation as shown in the above formula.

5.7 Numerical size of the NNLO QCD corrections

In this section we present the residual scale dependence for the renormalization group invariant Wilson coefficients in the modern basis, see section 4.6. In addition these results are transformed to a linear combination corresponding to the modern basis in chiral form ($V \pm A$). This transformation is equivalent to a simple rotation in four dimensions

$$Q_i = \sum_j \hat{R}_{ij}\tilde{\mathcal{O}}^u_j, \quad Q^c_i = \sum_j \hat{R}_{ij}\mathcal{O}_j \tag{5.69}$$

where the explicit expression for $\hat{R}$ can be extracted form the literature and the new results we presented in this thesis. Moreover the Q_i operators are traditionally defined using vector (V) and axial-vector (A) currents:

$$Q_1 \overset{(d=4)}{=} (\bar{s}_i\gamma^\mu u_j)_{V-A}(\bar{u}_j\gamma_\mu d_i)_{V-A}\,, \qquad Q_2 \overset{(d=4)}{=} (\bar{s}_i\gamma^\mu u_i)_{V-A}(\bar{u}_j\gamma_\mu d_j)_{V-A}\,, \tag{5.70}$$

$$Q_3 \overset{(d=4)}{=} (\bar{s}d)_{V-A}\sum_q(\bar{q}q)_{V-A}\,, \qquad Q_4 \overset{(d=4)}{=} (\bar{s}_i d_j)_{V-A}\sum_q(\bar{q}_j q_i)_{V-A}\,, \tag{5.71}$$

$$Q_5 \overset{(d=4)}{=} (\bar{s}d)_{V-A}\sum_q(\bar{q}q)_{V+A}\,, \qquad Q_6 \overset{(d=4)}{=} (\bar{s}_i d_j)_{V-A}\sum_q(\bar{q}_j q_i)_{V+A}\,, \tag{5.72}$$

$$Q_7 \overset{(d=4)}{=} \frac{3}{2}(\bar{s}d)_{V-A}\sum_q e_q\,(\bar{q}q)_{V+A}\,, \qquad Q_8 \overset{(d=4)}{=} \frac{3}{2}(\bar{s}_i d_j)_{V-A}\sum_q e_q\,(\bar{q}_j q_i)_{V+A}\,, \tag{5.73}$$

$$Q_9 \overset{(d=4)}{=} \frac{3}{2}(\bar{s}d)_{V-A}\sum_q e_q\,(\bar{q}q)_{V-A}\,, \qquad Q_{10} \overset{(d=4)}{=} \frac{3}{2}(\bar{s}_i d_j)_{V-A}\sum_q e_q\,(\bar{q}_j q_i)_{V-A}\,. \tag{5.74}$$

Here e_q denotes the electric quark charges and the sum over q extends over all active quark flavours. Finally, $(\bar{s}d)_{V\pm A} \equiv \bar{s}_\alpha \gamma_\mu (1 \pm \gamma_5) d_\alpha$. Moreover we have $\mathcal{O}_i = Q_i$, for $i \in \{7\gamma, 8g, b1, b2\}$. The linear transformation of equation (5.69) fixes the scheme for the effective Lagrangian

$$\mathcal{L}_{\text{eff}} = -\frac{G_F}{\sqrt{2}} V_{ud} V_{us}^* \left(\sum_i (z_i + \tau y_i) Q_i - (1-\tau) \sum_{i=1}^{2} z_i^c Q_i^c \right) \tag{5.75}$$

in d-dimensions and no additional finite renormalization is needed for the change of basis. The Wilson coefficients are then related via $\hat{z}_i(\mu) = R_{ji}^{-1} \hat{C}_j^u(\mu)$ and $\hat{y}_i(\mu) = \hat{R}_{ji}^{-1} \hat{C}_j(\mu)$ at every renormalization scale μ.

The short-distance terms in both bases are functions of the $\overline{\text{MS}}$ masses $m_t(\mu_t)$, $m_b(\mu_b)$ and $m_c(\mu_c)$, the strong coupling constant $\alpha_s^{(f)}(\mu)$, where $f = 3, 4$ or 5 and $\mu = \mu_W, \mu_b$ or μ_c, and the pole mass of the W boson. In our numerical analysis we use `RunDec` [69] to determine the above parameters at the appropriate scale as a function of the input parameters listed in Table 5.1. The calculation of the top $\overline{\text{MS}}$ mass value $m_t(m_t)$ involves only QCD corrections such that higher order electroweak corrections will cancel in the ratio m_t/M_W.

	value range	comment
M_W	80.403 GeV	from [70]
M_Z	91.1876 GeV	from [70]
$\alpha_s(M_Z)$	0.1181 ± 0.0011	from [70]
$m_t(m_t)$	(163.4 ± 2.0) GeV	calculated from pole mass value [70]
$m_b(m_b)$	(4.18 ± 0.3) GeV	from [70]
$m_c(m_c)$	(1.280 ± 0.025) GeV	from [70]
μ_t	120 GeV	if not varied
μ_b	5 GeV	if not varied
μ_c	1.5 GeV	if not varied
$\text{Im}\lambda_t$	$(1.4 \pm 0.1) \times 10^{-4}$	see text
G_F	1.1663787×10^{-5} GeV^{-2}	from [70]
V_{us}	0.2248(6)	from [70]
$\hat{\Omega}_{\text{eff}}$	$(14.8 \pm 8.0) \times 10^{-2}$	from [71]

Table 5.1: Input parameters, grouped into: input for perturbative calculation, central values of renormalisation scales employed, parametric input, isospin breaking corrections.

While each Wilson coefficients $\hat{y}_i$ and $\hat{z}_i$ are scheme and scale invariant, their numerical values will exhibit a residual dependence on the matching scales μ_W, μ_b and μ_c. This residual matching scale is a numerical artifact of the resummation of large logarithms and should reduce order by order in perturbation theory. We will estimate the size of higher order corrections by varying the matching scales μ_c, μ_b and μ_W in the ranges $[1, 3]$GeV, $[2.5, 10]$GeV and $[60, 240]$GeV respectively, while setting the other parameters to their respective central values given in Table 5.1. Furthermore,

the solution of the renormalisation group running of the strong coupling constants can be implemented in different manners that lead to a different prediction of the α_s at a given scale μ. This is another artifact of the perturbative expansion and should reduce order by order in perturbation theory. In `RunDec` three different methods of the renormalisation group running are implemented. One method is the numerical solution of the renormalisation group equation. The other two methods use the scale parameter $\Lambda_{\overline{\rm MS}}$ that is either determined by an explicit solution or the interative solution of the renormalistion group equation [69]. This determination agrees very well at LO in perturbation theory and any differences are numerical artifacts at this order. The resulting scale dependence will be given as dotted lines in the plot. At NLO the solutions of the renormalisation group equations exhibit differences that are of NNLO in the strong coupling constant. These measure the uncertainty due to NNLO corrections and are shown as dashed, dashed dotted and dashed dotted dotted lines in the respective scale variation plots. The numerical differences are reduced through the inclusion of NNLO corrections. Since at this order there are only minor differences in the scale dependence we will show all three scale variations as plain lines.

5.7.1 Residual scale dependence of the Wilson coefficients

The LO, NLO and NNLO central values of $\hat{y}_3$ to $\hat{y}_6$ are given Table 5.2, where one can also find the uncertainty band associated with the variation of the matching scales μ_c, μ_b and μ_t. The uncertainty band encloses the results for a given variation of a matching scale, while fixing the other scale parameters to their central values. The results of the variation of the scales μ_c, μ_b and μ_t are given in Figures 5.3, 5.4 and 5.5 respectively. While there is a significant shift in the scale dependence when going from LO to NLO, the NNLO shift is quite modest at the $\mathcal{O}(\tilde{\alpha}_s^2)$. In particular, one can observe that the NNLO scale variation is within the NLO uncertainty band for all QCD penguin coefficients $\hat{y}_i$. The largest relative scale variation can be observed in the dependence on the matching scale μ_c of the coefficients $\hat{y}_5$, which exhibits a relatively large uncertainty of $\mathcal{O}(8\%)$ for this Wilson coefficient. This can be explained by the significant suppression of $\hat{y}_5$ compared to the other coefficients. The largest coefficient $\hat{y}_6$, which plays the most important role in ε'/ε, has on the other hand only a very mild scale uncertainty of $\mathcal{O}(2\%)$ even if all residual uncertainties are taken into account.

On the other hand, the central values and the error bands for the short-distance contributions parametrized by the coefficients $\hat{z}_i$ are given in Table 5.3. The largest coefficients correspond to the current-current terms $\hat{z}_-$ and $\hat{z}_+$. For the latter no significant shift appears between the different orders. This artificially small scale dependence is due to the fact that the ADM of the current-current operators have no explicit dependence on quark-loops at leading order. Moreover, the uncertainty for $\hat{z}_4$ is notoriously reduced by the inclusion of the NNLO corrections at the scale μ_c. Also it is worth pointing out that the error bands increase their values at lower-energy scales for all

	central value	μ_c	μ_b	μ_t	
$\hat{y}_3^{\rm LO}$	3.733	$^{+0.563}_{-0.824}$	$^{+0.038}_{-0.041}$	$^{+0.444}_{-0.765}$	$\times 10^{-2}$
$\hat{y}_3^{\rm NLO}$	4.622	$^{+0.387}_{-0.397}$	$^{+0.164}_{-0.1}$	$^{+0.27}_{-0.246}$	$\times 10^{-2}$
$\hat{y}_3^{\rm NNLO}$	4.56	$^{+0.006}_{-0.099}$	$^{+0.007}_{-0.019}$	$^{+0.044}_{-0.055}$	$\times 10^{-2}$
$\hat{y}_4^{\rm LO}$	-4.455	$^{+1.122}_{-0.829}$	$^{+0.084}_{-0.075}$	$^{+0.786}_{-0.434}$	$\times 10^{-2}$
$\hat{y}_4^{\rm NLO}$	-5.949	$^{+0.817}_{-0.489}$	$^{+0.189}_{-0.312}$	$^{+0.308}_{-0.41}$	$\times 10^{-2}$
$\hat{y}_4^{\rm NNLO}$	-5.874	$^{+0.146}_{-0.014}$	$^{+0.037}_{-0.022}$	$^{+0.054}_{-0.053}$	$\times 10^{-2}$
$\hat{y}_5^{\rm LO}$	5.117	$^{+1.568}_{-1.842}$	$^{+0.204}_{-0.238}$	$^{+0.102}_{-0.387}$	$\times 10^{-3}$
$\hat{y}_5^{\rm NLO}$	7.687	$^{+0.608}_{-1.735}$	$^{+0.703}_{-0.639}$	$^{+0.911}_{-0.7}$	$\times 10^{-3}$
$\hat{y}_5^{\rm NNLO}$	7.17	$^{+0.455}_{-0.621}$	$^{+0.075}_{-0.068}$	$^{+0.216}_{-0.087}$	$\times 10^{-3}$
$\hat{y}_6^{\rm LO}$	-1.424	$^{+0.275}_{-0.18}$	$^{+0.003}_{-0.005}$	$^{+0.344}_{-0.215}$	$\times 10^{-1}$
$\hat{y}_6^{\rm NLO}$	-1.631	$^{+0.083}_{-0.029}$	$^{+0.055}_{-0.034}$	$^{+0.083}_{-0.053}$	$\times 10^{-1}$
$\hat{y}_6^{\rm NNLO}$	-1.605	$^{+0.028}_{-0.004}$	$^{+0.011}_{-0.005}$	$^{+0.015}_{-0.011}$	$\times 10^{-1}$

Table 5.2: Central values and error bands for the RGI Wilson coefficients $\hat{y}_i$.

	central value	μ_c	μ_b	μ_t	
$\hat{z}_+^{\rm LO}$	5.988	$^{+0.026}_{-0.019}$	$^{+0.017}_{-0.021}$	$^{+0.264}_{-0.142}$	$\times 10^{-1}$
$\hat{z}_+^{\rm NLO}$	6.087	$^{+0.042}_{-0.048}$	$^{+0.035}_{-0.054}$	$^{+0.057}_{-0.083}$	$\times 10^{-1}$
$\hat{z}_+^{\rm NNLO}$	6.154	$^{+0.008}_{-0.004}$	$^{+0.005}_{-0.004}$	$^{+0.012}_{-0.013}$	$\times 10^{-1}$
$\hat{z}_-^{\rm LO}$	2.789	$^{+0.018}_{-0.024}$	$^{+0.02}_{-0.016}$	$^{+0.137}_{-0.23}$	$\times 10^{0}$
$\hat{z}_-^{\rm NLO}$	2.663	$^{+0.042}_{-0.039}$	$^{+0.05}_{-0.031}$	$^{+0.063}_{-0.05}$	$\times 10^{0}$
$\hat{z}_-^{\rm NNLO}$	2.613	$^{+0.008}_{-0.005}$	$^{+0.004}_{-0.005}$	$^{+0.007}_{-0.008}$	$\times 10^{0}$
$\hat{z}_3^{\rm LO}$	3.243	$^{+0.783}_{-0.543}$	$^{+0.085}_{-0.083}$	$^{+0.1}_{-0.165}$	$\times 10^{-2}$
$\hat{z}_3^{\rm NLO}$	3.282	$^{+0.648}_{-0.436}$	$^{+0.281}_{-0.281}$	$^{+0.434}_{-0.349}$	$\times 10^{-2}$
$\hat{z}_3^{\rm NNLO}$	3.193	$^{+0.117}_{-0.027}$	$^{+0.029}_{-0.029}$	$^{+0.077}_{-0.066}$	$\times 10^{-2}$
$\hat{z}_4^{\rm LO}$	-6.486	$^{+0.823}_{-1.086}$	$^{+0.129}_{-0.133}$	$^{+0.337}_{-0.204}$	$\times 10^{-2}$
$\hat{z}_4^{\rm NLO}$	-6.102	$^{+0.592}_{-1.145}$	$^{+0.467}_{-0.485}$	$^{+0.483}_{-0.588}$	$\times 10^{-2}$
$\hat{z}_4^{\rm NNLO}$	-5.93	$^{+0.041}_{-0.179}$	$^{+0.052}_{-0.046}$	$^{+0.074}_{-0.077}$	$\times 10^{-2}$
$\hat{z}_5^{\rm LO}$	1.729	$^{+0.186}_{-0.164}$	$^{+0.027}_{-0.027}$	$^{+0.055}_{-0.091}$	$\times 10^{-2}$
$\hat{z}_5^{\rm NLO}$	1.496	$^{+0.221}_{-0.081}$	$^{+0.108}_{-0.093}$	$^{+0.137}_{-0.145}$	$\times 10^{-2}$
$\hat{z}_5^{\rm NNLO}$	1.49	$^{+0.059}_{-0.046}$	$^{+0.007}_{-0.012}$	$^{+0.02}_{-0.029}$	$\times 10^{-2}$
$\hat{z}_6^{\rm LO}$	-9.33	$^{+1.64}_{-2.505}$	$^{+0.253}_{-0.26}$	$^{+0.474}_{-0.287}$	$\times 10^{-2}$
$\hat{z}_6^{\rm NLO}$	0.543	$^{+0.805}_{-1.559}$	$^{+0.808}_{-0.884}$	$^{+0.835}_{-0.919}$	$\times 10^{-2}$
$\hat{z}_6^{\rm NNLO}$	1.376	$^{+0.15}_{-0.189}$	$^{+0.099}_{-0.078}$	$^{+0.081}_{-0.09}$	$\times 10^{-2}$

Table 5.3: Central values and error bands for the RGI Wilson coefficients $\hat{z}_i$.

Wilson coefficients. Their residual scale dependence can be found in figures 5.6, 5.7 and 5.8. While the NNLO scale variation of μ_c is within the NLO uncertainty band for the $\hat{z}_3$ to $\hat{z}_6$ coefficients, see. fig. 5.6, there is no overlap of the NLO and NNLO bands for the current-current Wilson coefficients $\hat{z}_-$ and $\hat{z}_+$ (first two plots of fig. 5.6). The explanation for this is as follows: these types of coefficients are generated by the exchange of a W-boson at high-energy scale. But the value of the strong coupling at this energy scale has been fixed for the evaluation of the μ_c residual scale dependence of the corresponding value at the top mass $\tilde{\alpha}_s(m_t)$. From the graphs, when the scale variation of μ_t is analysed, one observes that the NLO and NNLO lines would start to overlap very close to the value of the W mass, that is, at $\mu_t \sim 80\,\text{GeV}$.

Finally the most important statement extracted from the inspection of the scale variation of the Wilson coefficients $\hat{y}_i$ and $\hat{z}_i$ it is that our analysis suggests a good convergence of the perturbation theory.

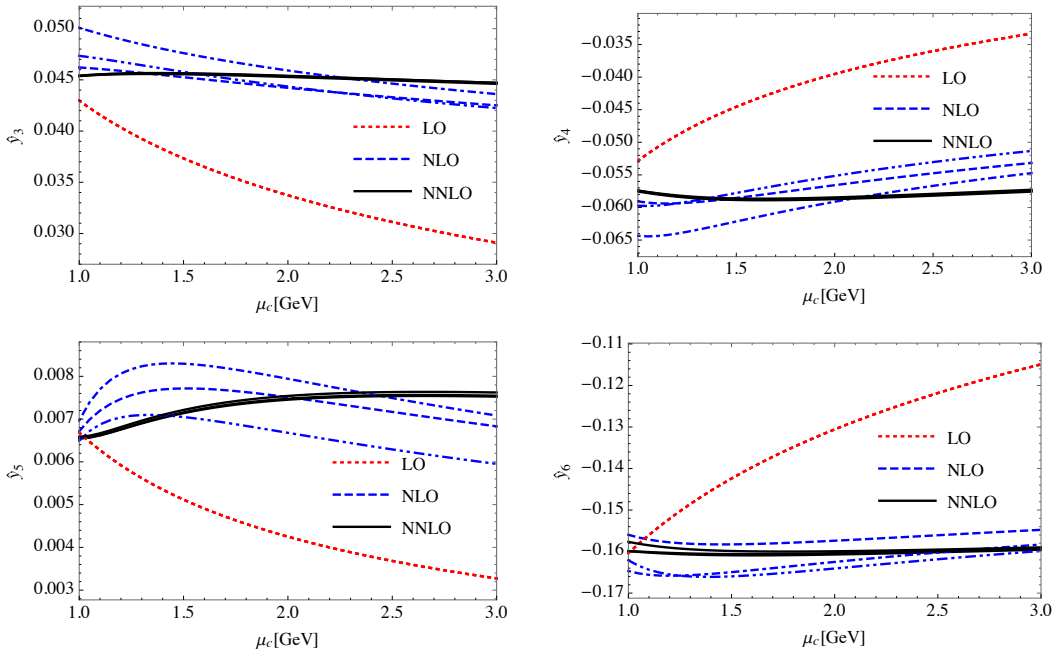

Figure 5.3: Renormalization group invariant Wilson coefficients in the modern basis as a function of the μ_c dependent scale.

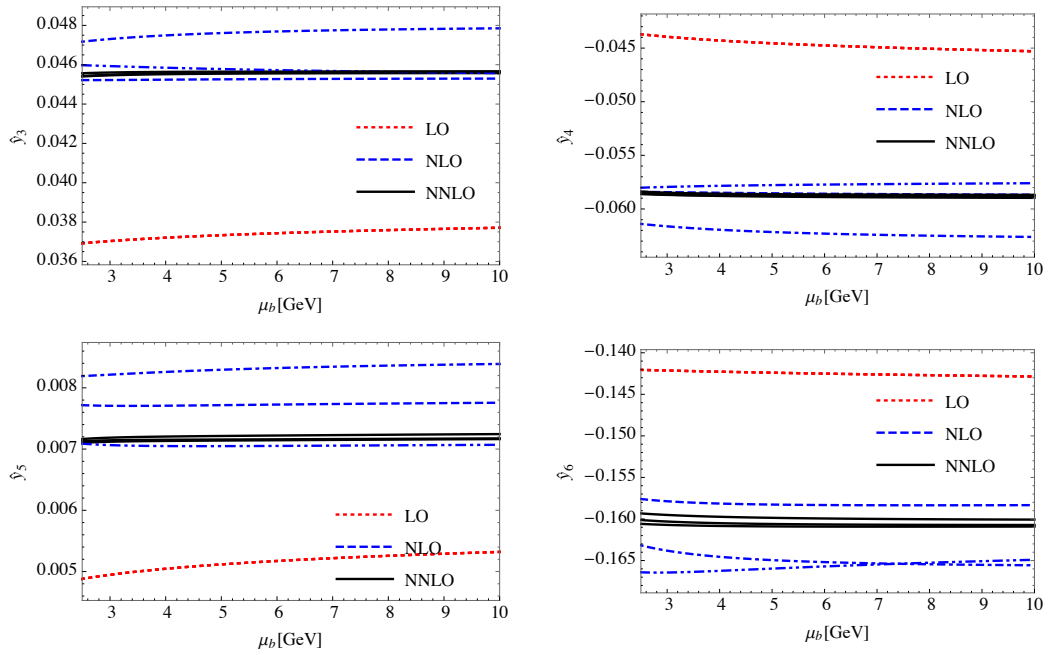

Figure 5.4: Renormalization group invariant Wilson coefficients in the modern basis as a function of the μ_b dependent scale.

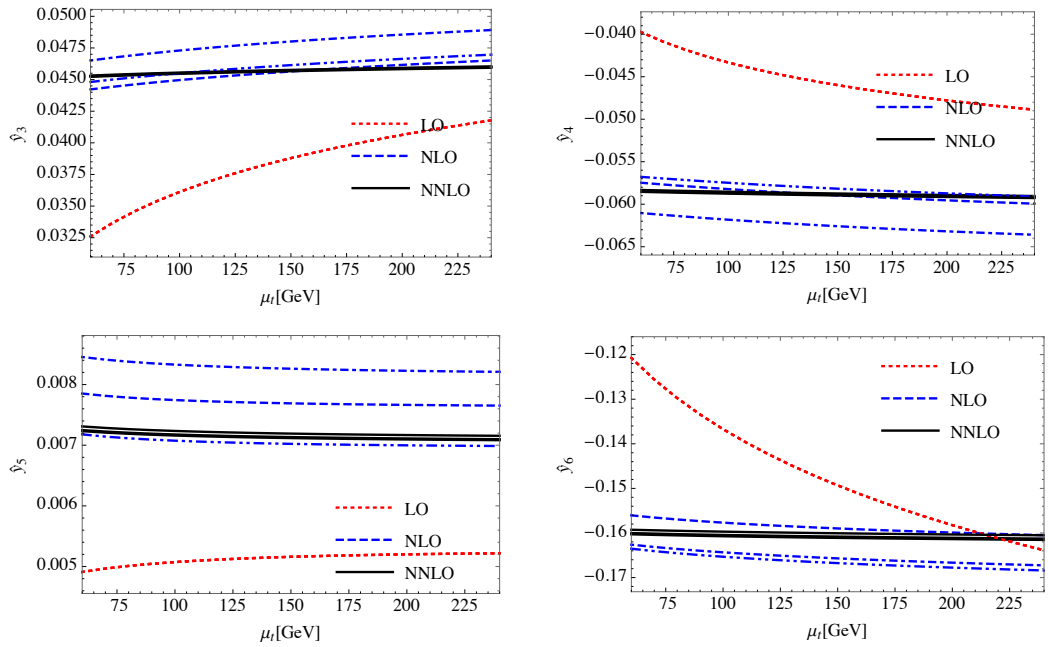

Figure 5.5: Renormalization group invariant Wilson coefficients in the modern basis as a function of the μ_t dependent scale.

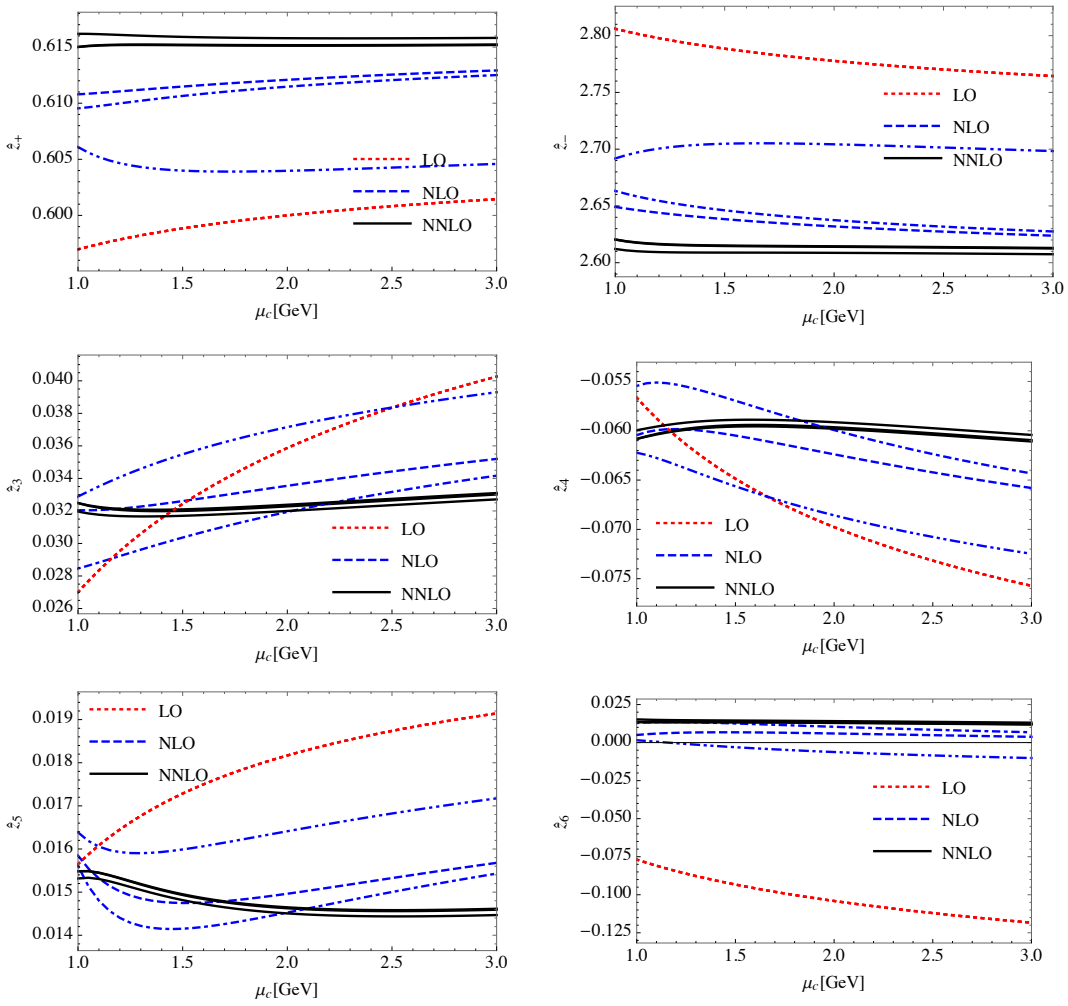

Figure 5.6: Renormalization group invariant Wilson coefficients in the modern basis as a function of the μ_c dependent scale.

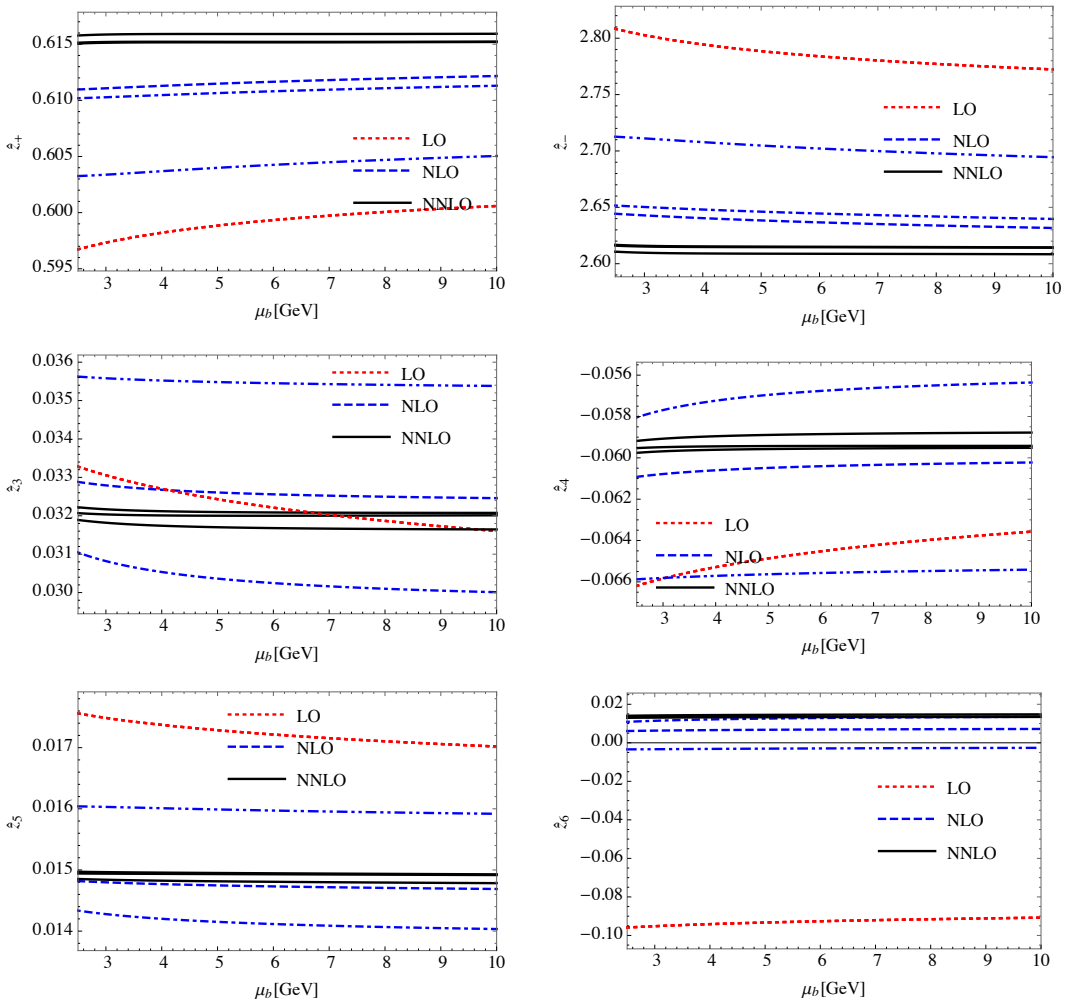

Figure 5.7: Renormalization group invariant Wilson coefficients in the modern basis as a function of the μ_b dependent scale.

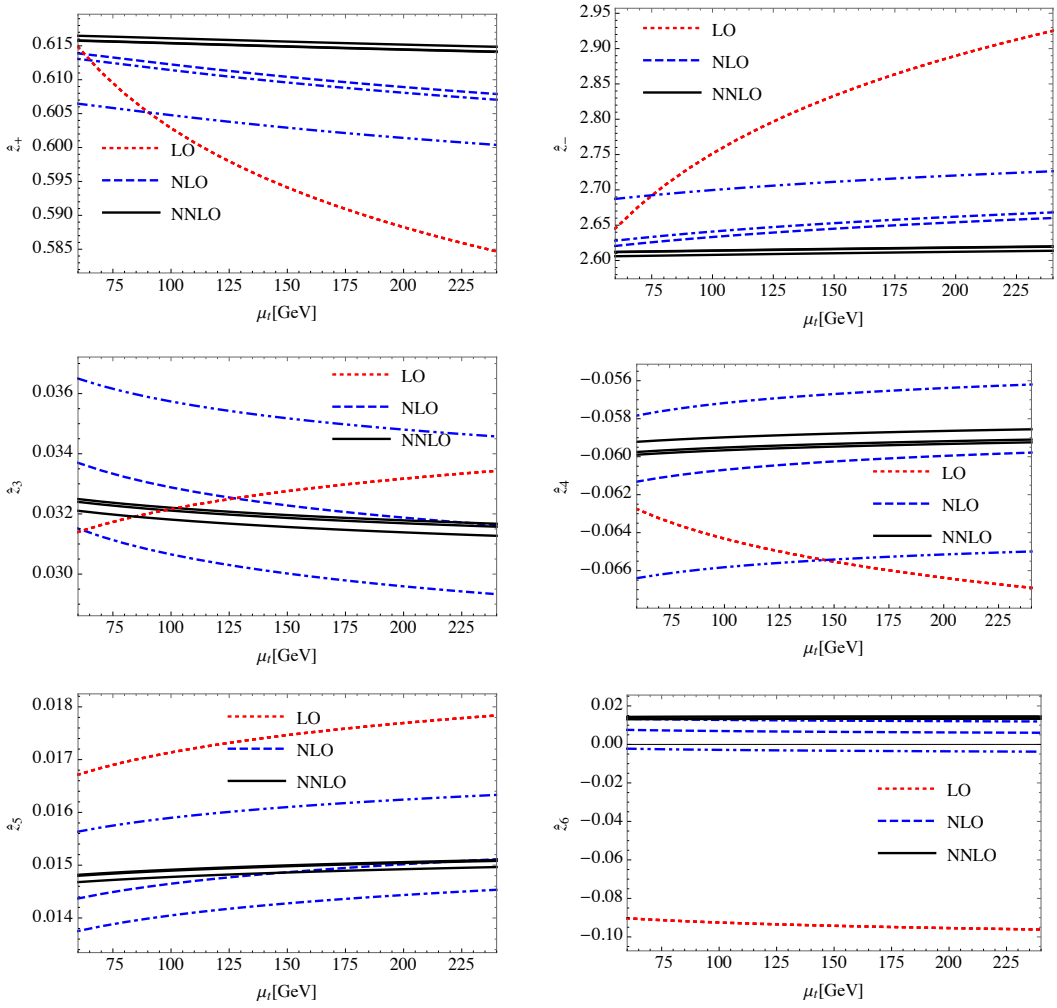

Figure 5.8: Renormalization group invariant Wilson coefficients in the modern basis as a function of the μ_t dependent scale.

Chapter 6

Observables

The results we presented in the previous sections can be used to evaluate some observables such as the $\Delta I = 1/2$ rule and the ratio $\varepsilon^{'}/\varepsilon$. The inclusion of our calculations will improve the theoretical prediction of these quantities. In the first section of this chapter we will introduce the motivation to study the latter observable in a sophisticated way. The next section covers the phenomenological description of direct CP-violation within the SM. In section 6.4 we discuss in detail the inputs from the non-perturbative sector and we prove that the Fierz identities are satisfied by the RGI-operators at all orders in perturbation theory. The following section covers the numerical analysis for CP-conserving decays and $\varepsilon^{'}/\varepsilon$. The effects of the NNLO QCD corrections are discussed in detail. Section 6.6 states the limitations of the formula used for the analysis of the latter observable. Finally, in the last section, we discuss possible strategies to address the aforementioned limitations.

6.1 Direct CP-Violation in Kaon Decays

CP violation (CPV) is one of the most fascinating phenomena of high energy physics and it is a natural place to search for physics beyond the SM. Within this framework complex Yukawa-type interactions of the quark fields with the Higgs doublet generate one CP-violating phase in the quark sector and at most three phases in the lepton sector. Yet, not enough CPV is present in this model to explain the matter-antimatter asymmetry in the Universe. New sources of CPV could modify the standard model expectations for direct and indirect CP violation of hadronic decays such as $K \to \pi\pi$. For these decays the standard model prediction of CP violation contains an additional flavour suppression due to the smallness of some CKM factors. This mechanism is typically not present in models of new physics. Therefore kaon mesons could shed some light on this curious puzzle. In fact high precision CP-violating observables offer an exciting possibility to disentangle the presence of new physics.

During the past 50 years there has been significant progress in understanding this phenomenon. One of the most important experimental results in the field since its discovery was the observation of direct CP violation parametrized by the ratio ε'/ε and measured by a long series of precision counting experiments. The world average based on the recent results of NA48 [72] and KTeV [73] collaborations stands at

$$\left(\frac{\varepsilon'}{\varepsilon}\right)_{\text{exp}} = (16.6 \pm 2.3) \times 10^{-4}. \tag{6.1}$$

The theoretical estimation of this observable is notoriously difficult due to the presence of the strong interactions and confinement at low energy scales. In recent years a huge effort has been made by the Lattice community and the QCD matrix elements can now be determined [6,7]. This achievement opens the possibility for a precision theory prediction of this ratio. Moreover the use of EFT facilitates the calculations through the separation of the perturbative regime (Wilson coefficients) and the non-perturbative sector (matrix elements). The latter are still the main source of uncertainty for the determination of ε'/ε. The last analysis of this ratio at NLO within the SM [8] has shown a 2.9 σ tension between the theoretical prediction and the experimental data,

$$\left(\frac{\varepsilon'}{\varepsilon}\right)_{\text{SM}} = (1.9 \pm 4.5) \times 10^{-4}. \tag{6.2}$$

This inconsistency could have several sources, one of which could be the missing contribution of new particles in the theory prediction. However a reliable SM prediction is essential to disentangle possible NP effects from the SM background. In the near future there will be further improvements to the non-perturbative sector via Lattice QCD that will make NNLO accuracy crucial. For this reason we present here a NNLO analysis for this observable. Additionally we emphasise the need for a more complete expression and formalism for ε'/ε.

6.2 ε'/ε within the Standard Model

All relevant matrix elements for the analysis of ε'/ε are currently evaluated on the lattice only in the isospin limit ($\tilde{\alpha}_e = 0$, degenerate masses), and the Standard Model prediction is based on the following expression

$$\frac{\varepsilon'}{\varepsilon} = -i\frac{\omega_+}{\sqrt{2}|\varepsilon_K|}e^{i(\delta_2-\delta_0-\phi_{\varepsilon_K})}\left[\frac{\text{Im}\text{A}_0}{\text{Re}\text{A}_0}(1-\hat{\Omega}_{\text{eff}}) - \frac{1}{a}\frac{\text{Im}\text{A}_2}{\text{Re}\text{A}_2}\right], \tag{6.3}$$

with ω_+ determined from the charged decay mode. $A_I \equiv \langle(\pi\pi)_I|\mathcal{H}_{\text{eff}}|K\rangle$ $(I = 0, 2)$ are the amplitudes for the two isospin states, and $\delta_{0,2}$ denote the isospin strong phase-shifts. These as well as the phase ϕ_{ε_K} and the magnitude $|\varepsilon_K|$ of ε_K, which parametrizes indirect CP-violation, are all determined from experimental data. Moreover, the coef-

ficients a and $\hat{\Omega}_{\text{eff}}$ are a partial parametrization of corrections to the isospin limit [71]. The latter coefficient describes the corrections to the isospin zero amplitude

$$\text{ImA}_0 = (\text{ImA}_0)^{\text{QCDP}} + b\,(\text{ImA}_0)^{\text{EWP}}, \qquad b = \frac{1}{a\,(1-\hat{\Omega}_{\text{eff}})}\,, \tag{6.4}$$

while its numerical value $\hat{\Omega}_{\text{eff}} = (14.8 \pm 8.0) \times 10^{-2}$ [8] is based on a chiral perturbation theory calculation [71, 74, 75].

For a theoretical prediction of direct CP-violation within the SM the real and imaginary parts of the (strong-)isospin amplitudes should be determined. The current-current operators give the dominant contribution to the real part of the isospin amplitude, while the imaginary part of the amplitudes is given by the QCD and electroweak penguins. The formalism used to determine these important pieces is based on reference [61]. They work under the hypothesis that the amplitudes ReA_0 and ReA_2 originate already at tree-level within the SM. Therefore these two quantities are expected to be only marginally affected by NP contributions. Moreover, the use of Fierz identities which relate current-current and $(V-A)\times(V-A)$ type QCD and eletroweak penguin operators allows them to reduce the hadronic uncertainty in the standard model prediction. In the following, we will extend this formalism to incorporate the non-zero z_i coefficients with $i > 2$, and consistently adapt it to incorporate higher order corrections by working with the renormalization group invariant quantities. In addition, we will extend the formalism to four active flavours in Section 6.7.1.

6.3 3-flavour theory

There are three exact operator identities in the 3-flavour theory. In terms of $Q_\pm = \frac{1}{2}(Q_2 \pm Q_1)$, and in a Fierz-symmetric scheme, they read

$$\begin{aligned} 0 &= -Q_4 + Q_3 + 2\,Q_-\,, \\ 0 &= -Q_9 + \frac{3}{2}(Q_+ - Q_-) - \frac{1}{2}Q_3\,, \\ 0 &= -Q_{10} + \frac{3}{2}Q_+ + \frac{1}{2}(Q_- - Q_3)\,. \end{aligned} \tag{6.5}$$

While these identities are violated in dimensional regularization in general, these relations hold to all orders for our hatted quantities. This can be understood as follows: each linear combination of operators in eq. (6.5) forms a Fierz-evanescent operator in the three flavour theory. At leading order the Fierz identities are preserved and the Fierz-evanescent operators cannot mix into physical operators at this order. At higher orders the appearance of $J_{n_f}(\mu)$ ensures that the product $\left[J_{n_f}(\mu)\right]^{-1}_{kj} C_j^{(n_f)}(\mu)$ exhibits only leading order running. Hence the Fierz evanescent matrix elements cannot mix into the physical operators and the relations (6.5) hold to all orders in perturbation theory for the matrix elements $\langle\pi\pi|\hat{Q}_i|K\rangle$ in the three-flavour theory. These Fierz iden-

tities are employed in the derivation of the phenomenological expression for ε'/ε. This will be discussed in more detail below.

The operators Q_-, Q_3, Q_5, Q_6 are pure $I = 1/2$ operators, hence in the isospin limit their matrix elements for $I = 2$ vanish: $\langle Q_-\rangle_2 = \langle Q_3\rangle_2 = \langle Q_5\rangle_2 = \langle Q_6\rangle_2 = 0$. As a result, in the isospin limit they do not contribute to A_2 and we find for the real part of the amplitudes

$$\begin{aligned}
\mathrm{ReA}_2 &= \frac{G_F}{\sqrt{2}}\lambda_u\left[(\hat{z}_+ + \frac{3}{2}[\hat{z}_9+\hat{z}_{10}])\langle\hat{Q}_+\rangle_2 + \hat{z}_7\langle\hat{Q}_7\rangle_2 + \hat{z}_8\langle\hat{Q}_8\rangle_2\right],\\
\mathrm{ReA}_0 &= \frac{G_F}{\sqrt{2}}\lambda_u\left[(\hat{z}_+ + \frac{3}{2}[\hat{z}_9+\hat{z}_{10}])\langle\hat{Q}_+\rangle_0 + (\hat{z}_- + \frac{1}{2}[4\hat{z}_4 - 3\hat{z}_9 + \hat{z}_{10}])\langle\hat{Q}_-\rangle_0\right.\\
&\quad\left.+\frac{1}{2}(2\hat{z}_3 + 2\hat{z}_4 - \hat{z}_9 - \hat{z}_{10})\langle\hat{Q}_3\rangle_0 + \hat{z}_5\langle\hat{Q}_5\rangle_0 + \hat{z}_6\langle\hat{Q}_6\rangle_0 + \hat{z}_7\langle\hat{Q}_7\rangle_0 + \hat{z}_8\langle\hat{Q}_8\rangle_0\right],
\end{aligned} \tag{6.6}$$

where $\lambda_u = V_{ud}V_{us}^*$ and we explicitly keep the small penguin contribution. Similarly, the imaginary parts of the amplitudes read

$$\begin{aligned}
\mathrm{ImA}_2 &= \frac{G_F}{\sqrt{2}}\lambda_u\,\mathrm{Im}\tau\left[\frac{3}{2}(\hat{y}_9+\hat{y}_{10})\langle\hat{Q}_+\rangle_2 + \hat{y}_7\langle\hat{Q}_7\rangle_2 + \hat{y}_8\langle\hat{Q}_8\rangle_2\right],\\
\mathrm{ImA}_0 &= \frac{G_F}{\sqrt{2}}\lambda_u\,\mathrm{Im}\tau\left[\frac{3}{2}b(\hat{y}_9+\hat{y}_{10})\langle\hat{Q}_+\rangle_0 + (2\,\hat{y}_4 - \frac{b}{2}[3\hat{y}_9 - \hat{y}_{10}])\langle\hat{Q}_-\rangle_0\right.\\
&\quad\left.+(\hat{y}_3+\hat{y}_4 - \frac{b}{2}[\hat{y}_9+\hat{y}_{10}])\langle\hat{Q}_3\rangle_0 + \hat{y}_5\langle\hat{Q}_5\rangle_0 + \hat{y}_6\langle\hat{Q}_6\rangle_0 + b\hat{y}_7\langle\hat{Q}_7\rangle_0 + b\hat{y}_8\langle\hat{Q}_8\rangle_0\right].
\end{aligned} \tag{6.7}$$

In the ratio of isospin amplitudes, note that the same $(V-A)\times(V-A)$ operators appear in the numerators and the denominators. This suggests that we split the numerator into $(V-A)\times(V-A)$ and $(V-A)\times(V+A)$ pieces. Whereas the first type are dominated by short distance (Wilson coefficients) due to a cancellation of the matrix elements, the contributions coming from the $(V-A)\times(V+A)$ operators are very sensitive to long-distance effects (hadronic matrix elements). To minimize the non-perturbative uncertainties, one can extract the denominators from CP-averaged $K\to\pi\pi$ decay rates to remove the dependence on the $(V-A)\times(V-A)$ operators. For the isospin 2 amplitude we obtain

$$\frac{\mathrm{ImA}_2}{\mathrm{ReA}_2} = \mathrm{Im}\tau\left[\frac{3}{2}\frac{\hat{y}_9+\hat{y}_{10}}{\hat{z}_+}(1+\delta z_2) + \frac{G_F}{\sqrt{2}}\lambda_u(\hat{y}_8 + p_{72}y_7)\frac{\langle\hat{Q}_8\rangle_2}{\mathrm{ReA}_2}\right], \tag{6.8}$$

where we performed an expansion in the small penguin contribution

$$\delta z_2 = -\frac{3}{2}\frac{(\hat{z}_9+\hat{z}_{10})}{\hat{z}_+} - \frac{G_F}{\sqrt{2}}\lambda_u\frac{\langle\hat{Q}_8\rangle_2}{\mathrm{ReA}_2}(p_{72}\hat{z}_7 + \hat{z}_8) \tag{6.9}$$

and defined

$$p_{72} = \frac{\langle \hat{Q}_7 \rangle_2}{\langle \hat{Q}_8 \rangle_2} \,. \tag{6.10}$$

Note that the first term in (6.8) is completely free of hadronic matrix elements. This is because data have not been used for the denominator of this part of the ratio. In case of having used ReA_0 and ReA_2 from data also in the $(V-A)\times(V-A)$ part a dependence on (mainly) the matrix element of the operator Q_4 and its Wilson coefficients would be introduced, and this should be avoided. Indeed, this is the main reason why the prediction of [8] is more accurate than that of RBC and UKQCD, and leads to a more pronounced tension with the data, in spite of employing the same non-perturbative matrix elements.

Extending this formalism to the isospin-zero ratio, we have

$$\begin{aligned} \frac{\mathrm{ImA}_0}{\mathrm{ReA}_0} = \mathrm{Im}\tau \Bigg[& \frac{(2\,\hat{y}_4 - \frac{b}{2}[3\hat{y}_9 - \hat{y}_{10}])}{\hat{z}_-(1+\hat{q})} + \frac{\frac{3b}{2}[\hat{y}_9 + \hat{y}_{10}]\hat{q}}{\hat{z}_+(1+\hat{q})} + \frac{\left(\hat{y}_3 + \hat{y}_4 - \frac{b}{2}[\hat{y}_9 + \hat{y}_{10}]\right)}{\hat{z}_-(1+\hat{q})} p_3 \\ & + \frac{\mathrm{G_F}}{\sqrt{2}} \frac{\lambda_\mathrm{u}}{\mathrm{ReA}_0} \left([\hat{y}_6 + p_5 \hat{y}_5 + p_{8g} \hat{y}_{8g}] \langle \hat{Q}_6 \rangle_0 + b[\hat{y}_8 + p_{70} \hat{y}_7 + p_{70\gamma} \hat{y}_{7\gamma}] \langle \hat{Q}_8 \rangle_0 \right) \Bigg] , \end{aligned} \tag{6.11}$$

where we again expanded in the small penguin contribution

$$\begin{aligned} \delta z_0 = & \frac{(-2\hat{z}_3 - 2\hat{z}_4 + \hat{z}_9 + \hat{z}_{10})}{2(\hat{q}+1)\hat{z}_-} p_3 - \frac{4\hat{z}_4 - 3\hat{z}_9 + \hat{z}_{10}}{2(\hat{q}+1)\hat{z}_-} - \frac{3\hat{q}\,(\hat{z}_9 + \hat{z}_{10})}{2(\hat{q}+1)\hat{z}_+} \\ & - \frac{\mathrm{G_F}}{\sqrt{2}} \frac{\lambda_\mathrm{u}}{\mathrm{ReA}_0} \left[(p_5 \hat{z}_5 + \hat{z}_6) \langle \hat{Q}_6 \rangle_0 + (p_7 \hat{z}_7 + \hat{z}_8) \langle \hat{Q}_8 \rangle_0 \right] , \end{aligned} \tag{6.12}$$

and defined the following ratios of matrix elements

$$\hat{p}_3 = \frac{\langle \hat{Q}_3 \rangle_0}{\langle \hat{Q}_- \rangle_0},\ \hat{p}_5 = \frac{\langle \hat{Q}_5 \rangle_0}{\langle \hat{Q}_6 \rangle_0},\ \hat{p}_{8g} = \frac{\langle \hat{Q}_{8g} \rangle_0}{\langle \hat{Q}_6 \rangle_0},\ \hat{p}_{70} = \frac{\langle \hat{Q}_7 \rangle_0}{\langle \hat{Q}_8 \rangle_0},\ \hat{p}_{70\gamma} = \frac{\langle \hat{Q}_{7\gamma} \rangle_0}{\langle \hat{Q}_8 \rangle_0}, \tag{6.13}$$

where the first two ratios are colour-suppressed, but still important enough to be included for a proper analysis of direct-CP violation. Moreover, the weakly scale-dependent parameter $\hat{q}$, which appears in the expressions (6.11) and (6.12), is defined in terms of the current-current Wilson coefficients and operators:

$$\hat{q} = \hat{z}_+ \langle \hat{Q}_+ \rangle_0 / \hat{z}_- \langle \hat{Q}_- \rangle_0 . \tag{6.14}$$

The small ratio z_+/z_- implies that only modest accuracy is needed for the hadronic matrix elements entering the isospin-zero ratio through $\hat{q}$. As a result, the prediction for ε'/ε involves predominantly two hadronic matrix elements (often parametrised in terms of parameters $B_6^{(1/2)}$ and $B_8^{(3/2)}$, refer to section 5.2 of reference [61]), as well as perturbative Wilson coefficients $\hat{z}_{1,2}$ and $\hat{y}_{6,8}$. Our new calculation essentially removes the perturbative uncertainty on $\hat{y}_6$. The uncertainties on $\hat{z}_{1,2}$ are already tiny, leaving $\hat{y}_8$ and an improved treatment of isospin-breaking corrections as the main objectives

for the future.

6.4 Non-perturbative sector: Input from Lattice QCD

We will start our discussion by presenting the relevant non-perturbative matrix elements $\langle Q_i \rangle_0$ and $\langle Q_i \rangle_2$ required to evaluate the isospin $I = 0$ and isospin $I = 2$ ratios respectively. On the lattice the complete isospin $I = 2$ matrix elements have been presented in Ref. [5, 6], while the isospin $I = 0$ results are given in Ref. [7]. In this respective Lattice evaluation, the matrix elements are renormalized non-perturbatively in the RI-SMOM renormalization scheme and then matched to the traditional operator basis in the continuum $\overline{\text{MS}}$ renormalisation scheme using NDR. The relevant transformation matrix can be derived from Table XI and Eqs. (54), (56), (60) and (65) of Ref. [76]. By choosing the basis of the RI-SMOM operators as

$$\langle \vec{Q} \rangle^{\text{RISMOM}} = \begin{pmatrix} \langle Q_1 \rangle_0^{\text{RISMOM}} \\ \langle Q_2 \rangle_0^{\text{RISMOM}} \\ \langle Q_3 \rangle_0^{\text{RISMOM}} \\ \langle Q_5 \rangle_0^{\text{RISMOM}} \\ \langle Q_6 \rangle_0^{\text{RISMOM}} \\ \langle Q_7 \rangle_0^{\text{RISMOM}} \\ \langle Q_8 \rangle_0^{\text{RISMOM}} \end{pmatrix} , \tag{6.15}$$

we represent the transformation to the $\overline{\text{MS}}$ scheme as

$$\langle \vec{Q}' \rangle_0 = \left(\bar{T}^{(0)} + \frac{\alpha_s(\mu_{\text{Lattice}})}{4\pi} \bar{T}^{(1)} \right) \langle \vec{Q} \rangle_0^{\text{RISMOM}} , \tag{6.16}$$

where the Lattice scale is fixed to $\mu_{\text{Lattice}} = 1.531\text{GeV}$ [7]. The explicit form of the leading-order transformation reads

$$\bar{T}^{(0)} = \begin{pmatrix} \frac{1}{5} & 1 & 0 & 0 & 0 & 0 & 0 \\ \frac{1}{5} & 0 & 1 & 0 & 0 & 0 & 0 \\ 0 & 3 & 2 & 0 & 0 & 0 & 0 \\ 0 & 2 & 3 & 0 & 0 & 0 & 0 \\ 0 & 0 & 0 & 1 & 0 & 0 & 0 \\ 0 & 0 & 0 & 0 & 1 & 0 & 0 \\ 0 & 0 & 0 & 0 & 0 & 1 & 0 \\ 0 & 0 & 0 & 0 & 0 & 0 & 1 \\ \frac{3}{10} & 0 & -1 & 0 & 0 & 0 & 0 \\ \frac{3}{10} & -1 & 0 & 0 & 0 & 0 & 0 \end{pmatrix} , \tag{6.17}$$

while we find at next-to-leading order

$$\bar{T}^{(1)} = \begin{pmatrix} -0.090964 & 2.62741 & 4.91777 & 0 & 0 & 0 & 0 \\ -0.090964 & -4.50446 & -8.69111 & 0.07407 & -0.22222 & 0 & 0 \\ 0 & -1.12669 & -2.62891 & 0.14814 & -0.44444 & 0 & 0 \\ 0 & -9.25856 & -18.5711 & 0.555543 & -1.66666 & 0 & 0 \\ 0 & 0 & 0 & 0.04319 & -0.12957 & 0 & 0 \\ 0 & -1.66667 & -3.88889 & -0.05815 & -0.17106 & 0 & 0 \\ 0 & 0 & 0 & 0 & 0 & 0.04319 & -0.12957 \\ 0 & 0 & 0 & 0 & 0 & -0.61371 & 1.49561 \\ -0.136446 & 4.50446 & 8.69111 & -0.07407 & 0.22222 & 0 & 0 \\ -0.136446 & -2.62741 & -4.91777 & 0 & 0 & 0 & 0 \end{pmatrix}. \tag{6.18}$$

In addition to the direct Lattice evaluation, a combination of the Lattice results and Large N estimations for the non-perturbative matrix elements were used in a previous analysis of ε'/ε [8]. To compare our results to this analysis, we will fit the RI-SMOM renormalised matrix elements to the central values given in Ref. [8]. In this fit we transform a general set of RI-SMOM matrix elements to the $\overline{\text{MS}}$ at $\mu_{\text{Lattice}} = 1.531\,\text{GeV}$ and run the resulting matrix-elements to 1.3 GeV at NLO using the anomalous dimensions in the traditional basis. At this scale we require that

$$\begin{aligned} 0 &= \langle Q_3' \rangle_0 (1.3\text{GeV}), \\ 0 &= \langle Q_5' \rangle_0 (1.3\text{GeV}), \\ 0.05 &= \frac{z_+'(1.3\text{GeV}) \langle Q_+' \rangle_0 (1.3\text{GeV})}{z_-'(1.3\text{GeV}) \langle Q_-' \rangle_0 (1.3\text{GeV})}, \\ -0.3302 &= \text{GeV}^{-3} \langle Q_6' \rangle_0 (1.3\text{GeV}), \end{aligned} \tag{6.19}$$

which fixes all but one matrix element.[1] The last matrix element would not contribute to the analysis of ε'/ε if the corresponding matrix elements are used at this fixed values at $\mu = 1.3\,\text{GeV}$. This follows from our 3-flavour formalism of ε'/ε, where the matrix element cancels for the $(V-A)\times(V-A)$ contribution, while data is used for the real part of the amplitude for the $(V-A)\times(V+A)$ contribution. Yet, the non-perturbative parameters still exhibit a small renormalisation group running and the operator identities used in our 3-flavour formalism are broken by small one-loop corrections. Hence we fix the final RI-SMOM paramter to $\langle Q_1 \rangle_0^{\text{RI-SMOM}} = -0.0815$ and get a reasonable agreement within the non-perturbative uncertainty. The explicit values used in the RI-SMOM scheme are given in Table 6.1, where the largest discrepancy is in the parameter $\langle Q_5 \rangle_0^{\text{RI-SMOM}}$. This is due to the choice of Ref. [8] which sets $\langle Q_5' \rangle_0$

[1] The choice of the parameter $B_6^{(1/2)} = 0.57$, which is to a good approximation scale independent, fixes the last line in Eq. (6.19) through the relation $\langle Q_6' \rangle_0 (1.3\text{GeV}) = -\sqrt{6} \left(\frac{m_K^2}{m_s(1.3\text{GeV}) + m_d(1.3\text{GeV})} \right)^2 (F_K - F_\pi) B_6^{(1/2)}$.

	Lattice	Lattice & Large N
$\langle Q_1\rangle_0^{\text{RI-SMOM}}\,\text{GeV}^{-3}$	$-0.0675(1109)(128)$	-0.0815
$\langle Q_2\rangle_0^{\text{RI-SMOM}}\,\text{GeV}^{-3}$	$-0.165(27)(30)$	-0.1557
$\langle Q_3\rangle_0^{\text{RI-SMOM}}\,\text{GeV}^{-3}$	$0.212(52)(40)$	0.2327
$\langle Q_5\rangle_0^{\text{RI-SMOM}}\,\text{GeV}^{-3}$	$-0.193(62)(37)$	-0.0144
$\langle Q_6\rangle_0^{\text{RI-SMOM}}\,\text{GeV}^{-3}$	$-0.366(103)(70)$	-0.3485

Table 6.1: Current-current and QCD-Penguin $I = 0$ matrix elements, renormalised in the RI-SMOM scheme. The first column represents the results given in Table SII of Ref. [7], where the first and second error show the statistical and systematic uncertainties. The second column represents the central values of the RI-SMOM renormalised matrix elements that are fixed to reproduce the choice of $\overline{\text{MS}}$-renormalised matrix elements of Ref. [8].

to zero at the renormalization scale $\mu = 1.3$ GeV.

Using the central values of the lattice inputs in Table 6.1 we obtain the RGI renormalised matrix elements

$$\begin{pmatrix}\langle\hat{Q}_1\rangle\\ \langle\hat{Q}_2\rangle\\ \langle\hat{Q}_3\rangle\\ \langle\hat{Q}_4\rangle\\ \langle\hat{Q}_5\rangle\\ \langle\hat{Q}_6\rangle\end{pmatrix}\text{GeV}^{-3} = \begin{pmatrix}-0.0969\\ 0.1387\\ 0.0717\\ 0.3073\\ -0.1297\\ -0.1349\end{pmatrix} + \frac{\alpha_s^{(3)}(\mu_{\text{Lattice}})}{4\pi}\begin{pmatrix}1.199\\ -0.439\\ 2.842\\ 1.204\\ 0.928\\ -1.218\end{pmatrix} + \left(\frac{\alpha_s^{(3)}(\mu_{\text{Lattice}})}{4\pi}\right)^2\begin{pmatrix}8.7\\ 4.81\\ -20.08\\ -24.94\\ 21.32\\ 4.58\end{pmatrix}. \tag{6.20}$$

If we instead also incorporate the Large N motivated matrix elements listed in the second column of Table 6.1 and denote by $\langle\hat{Q}_i\rangle^{(N)}$ the resulting expressions in the $\overline{\text{MS}}$ scheme we find

$$\begin{pmatrix}\langle\hat{Q}_1\rangle^{(N)}\\ \langle\hat{Q}_2\rangle^{(N)}\\ \langle\hat{Q}_3\rangle^{(N)}\\ \langle\hat{Q}_4\rangle^{(N)}\\ \langle\hat{Q}_5\rangle^{(N)}\\ \langle\hat{Q}_6\rangle^{(N)}\end{pmatrix}\text{GeV}^{-3} = \begin{pmatrix}-0.0936\\ 0.1548\\ 0.1315\\ 0.3799\\ 0.0666\\ -0.1281\end{pmatrix} + \frac{\alpha_s^{(3)}(\mu_{\text{Lattice}})}{4\pi}\begin{pmatrix}1.32\\ -0.534\\ 3.039\\ 1.185\\ 0.385\\ -1.001\end{pmatrix} + \left(\frac{\alpha_s^{(3)}(\mu_{\text{Lattice}})}{4\pi}\right)^2\begin{pmatrix}8.45\\ 3.91\\ -21.89\\ -32.7\\ 16.61\\ 3.9\end{pmatrix}. \tag{6.21}$$

In both expressions, the scale is fixed to $\mu_{\text{Lattice}} = 1.531$ GeV and we have kept the product of the two NLO contributions in the α_s^2 term. There is only a residual scale dependence through the determination of $\alpha_s^{(3)}(1.531\text{ GeV})$ from $\alpha_s^{(5)}(M_Z)$. Finally, let us note that we explicitly checked that the resulting matrix elements fulfill the tree-level Fierz identities as required.

RGI scheme	$\hat{q}$	$\hat{p}_3$	$\hat{p}_5$	$\langle\hat{Q}_6\rangle_0$
a) Lattice	0.078	1.628	0.645	-0.159GeV^3
b) Lattice & Large N	0.099	2.248	-0.542	-0.147GeV^3
Primed scheme at $\mu = 1.3$GeV	q'	p'_3	p'_5	$\langle Q'_6\rangle_0$
c) Input used in Ref. [8]	0.05	0	0	-0.3302GeV^3

Table 6.2: Central values of the non-perturbative QCD parameters in the RGI scheme and for the traditional basis, i.e. the primed scheme, at $\mu = 1.3\,\text{GeV}$. They are either directly determined from Lattice QCD inputs or from a combination of Lattice and Large N inputs as explained in the text.

Using these expressions and the NLO value of $\alpha_s^{(3)}(1.531\text{ GeV}) = 0.336$, that is obtained via the numerical evaluation of the renormalisation group equations, we compute the relevant ratios of non-perturbative matrix elements and present them in Table 6.2.

The matrix element inputs for the decay into isospin $I = 0$ amplitudes are listed in Table 6.1. The isospin $I = 2$ matrix elements of QCD penguins vanish. The relevant matrix-element for the current-current operators in the so-called RI-SMOM $(\not{q}, \not{q})$ scheme are directly related to the matrix element

$$M^{K^+}_{(27,1)} = 0.0506(13)(26) \tag{6.22}$$

computed on the Lattice [6] at a renormalisation scale of 3 GeV, where the first and second numbers in brackets represent the statistical and systematic uncertainty respectively. The RGI renormalised matrix elements are again computed in two steps. First the RI-SMOM matrix elements

$$\langle Q_1\rangle_2^{\text{RI-SMOM}} = \langle Q_2\rangle_2^{\text{RI-SMOM}} = \frac{1}{5} M^{K^+}_{(27,1)} \tag{6.23}$$

are transformed to the $\overline{\text{MS}}$ scheme in the traditional basis using eqs. (6.16)–(6.18) at the renormalisation scale $[\mu_{\text{Lattice}}]_{I=2} = 3\,\text{GeV}$, where $\alpha_s(3\text{ GeV}) = 0.245$. Next the matrix elements are transformed to the RGI scheme using the NLO anomalous dimensions in the traditional basis. The resulting central values for the matrix elements are given in Table 6.3.

	Lattice
$\langle \hat{Q}_+ \rangle_0 \, \mathrm{GeV}^{-3}$	0.0315(567)
$\langle \hat{Q}_- \rangle_0 \, \mathrm{GeV}^{-3}$	0.0939(188)
$\langle \hat{Q}_3 \rangle_0 \, \mathrm{GeV}^{-3}$	0.153(238)
$\langle \hat{Q}_4 \rangle_0 \, \mathrm{GeV}^{-3}$	0.341(247)
$\langle \hat{Q}_5 \rangle_0 \, \mathrm{GeV}^{-3}$	−0.102(82)
$\langle \hat{Q}_6 \rangle_0 \, \mathrm{GeV}^{-3}$	−0.159(59)
$\langle \hat{Q}_+ \rangle_2 \, \mathrm{GeV}^{-3}$	0.0137(8)

Table 6.3: Values of the RGI renormalized matrix elements relevant for the analysis of $\mathrm{Re}A_0$, $\mathrm{Re}A_2$ and $\mathrm{Re}A_0/\mathrm{Re}A_2$. The isospin $I = 2$ and $I = 0$ matrix elements are computed using the central RI-SMOM values of the Lattice determinations quoted in Ref. [6] and Ref. [7] respectively. The matrix elements $\langle \hat{Q}_i \rangle_2$, where $i = -, 3, \ldots, 6$, vanish in the isospin limit. The numbers in brackets denote the non-perturbative uncertainties.

6.5 Numerical significance of the NNLO QCD corrections

In this section, we present the numerical analysis of the CP-conserving parts ReA_0 and ReA_2, which play an important role in the determination of the $\Delta I = 1/2$ rule. Moreover, we update the SM prediction for the observable ε'/ε in the three-flavour theory including our pure QCD NNLO new results, and the advanced formalism introduced in Section 5.4.

6.5.1 NNLO corrections to the $\Delta I = 1/2$ rule

The enhancement of the Kaon decay into an isospin $I = 2$ two pion final state versus the decay into an isospin $I = 0$ final state has been an important and long-standing puzzle in particle physics. The experimental numbers for the respective isospin decay modes,

$$\mathrm{Re}A_0 = 33.22(1) \times 10^{-8}\mathrm{GeV}\,, \qquad \mathrm{Re}A_2 = 1.479(3) \times 10^{-8}\mathrm{GeV}\,, \tag{6.24}$$

exhibit the enhancement factor

$$\frac{\mathrm{ReA}_0}{\mathrm{ReA}_2} = 22.46. \tag{6.25}$$

Data seem to prefer non-leptonic kaon decays with transitions $\Delta I = 1/2$ over those where their isospin changes by a factor $\Delta I = 3/2$. This fact is known by the name of the $\Delta I = 1/2$ rule, and is still an enigma. Although CP-conserving decays involve tree-level contributions and therefore are expected to be governed by SM dynamics, the presence of hadrons convolute their theoretical evaluation due to the non-perturbative behaviour at very low energy scales. We aim to perform a phenomenological analysis of the observables ReA_0 and ReA_2 including our NNLO QCD contributions and evaluate the convergence of perturbation theory.

The suppression of the hadronic matrix element of the isospin 2 final state [77, 78] gives the largest contribution to the $\Delta I = 1/2$ rule. Yet the renormalisation group running of the Wilson coefficients $\hat{z}_+$ and $\hat{z}_-$ on its own results in enhancement of the ratio by a factor of three. The real parts of the decay amplitudes are given in eq. (6.6) in the three flavour theory. Here the current-current operators give the leading contribution, with a sub-leading contribution of the QCD penguins to ReA_0. The Wilson coefficients of the electroweak penguins have a further $\mathcal{O}(\alpha)$ suppression and will be neglected in the following analysis of ReA_0, ReA_2 and $\mathrm{ReA}_0 \,/\, \mathrm{ReA}_2$. Using the parametric input for G_F and V_{us} of Table 5.1, the central values for the matrix elements of Table 6.3 and our results for the Wilson coefficients $\hat{z}_{+,-,3,\ldots,6}$, we can determine the perturbative corrections to the real part of the decay amplitudes.

For the decay into an isospin $I = 2$ state we find at LO, NLO and NNLO

$$\begin{aligned} \mathrm{Re}A_2|_{\mathrm{SM\ LO}} &= 1.482^{+0.066}_{-0.035} \times 10^{-8}\,\mathrm{GeV}\,, \\ \mathrm{Re}A_2|_{\mathrm{SM\ NLO}} &= 1.505^{+0.020}_{-0.027} \times 10^{-8}\,\mathrm{GeV}\,, \\ \mathrm{Re}A_2|_{\mathrm{SM\ NNLO}} &= 1.522^{+0.004}_{-0.004} \times 10^{-8}\,\mathrm{GeV}\,, \end{aligned} \tag{6.26}$$

where the combined perturbative uncertainty determined through the respective matching scale variation and different α_s determinations are shown as subscripts and superscripts. From the plot of the real part of the isospin $I = 2$ amplitude in Figure 6.1, we observe only a mild scale dependence at leading order. This is consistent with the scale dependence of the Wilson coefficients $\hat{z}_+$ and $\hat{z}_-$ in Figure 5.6. At NLO accuracy the dependence on the implementation of the α_s renormalisation group running gives a more significant scale dependence. This scale dependence is to a very good approximation removed completely at NNLO, where there is only a mild dependence on the implementation of the α_s running. While the residual μ_c uncertainty provides a good estimate of higher order uncertainties, it might also underestimate uncertainties when the scale variation is accidentally small. Still, the current non-perturbative uncertainty is now significantly larger than the perturbative uncertainty. Using our NNLO determination we find

$$\mathrm{ReA}_2|_{\mathrm{SM}} = 1.526(87)(17) \times 10^{-8}\,\mathrm{GeV}\,, \tag{6.27}$$

where the first term in brackets represents the non-perturbative error and the second brackets possible effects of NNNLO corrections. Due to the smallness of the residual scale variation we estimated the latter uncertainty through the shift of the central value at NLO and NNLO. The experimental value agrees well with the standard model prediction within the given theory uncertainty.

We proceed for the isospin $I = 0$ decay in a similar manner. At LO, NLO and NNLO we have

$$\begin{aligned} \mathrm{Re}A_0|_{\mathrm{SM\ LO}} &= 50.0^{+2.2}_{-3.7} \times 10^{-8}\,\mathrm{GeV}\,, \\ \mathrm{Re}A_0|_{\mathrm{SM\ NLO}} &= 45.4^{+1.5}_{-1.3} \times 10^{-8}\,\mathrm{GeV}\,, \\ \mathrm{Re}A_0|_{\mathrm{SM\ NNLO}} &= 44.4^{+0.2}_{-0.2} \times 10^{-8}\,\mathrm{GeV}\,, \end{aligned} \tag{6.28}$$

and note again the the small residual scale dependence at NNLO. The non-perturbative uncertainties are determined by independently varying the RI-SMOM Matrix elements of Table 6.1 and computing the resulting RGI matrix-elements $\langle \hat{Q}_i \rangle$. We find

$$\mathrm{ReA}_0|_{\mathrm{SM}} = 44.4(11.0)(1.0) \times 10^{-8}\,\mathrm{GeV}\,, \tag{6.29}$$

where again the first number in brackets represents the non-perturbative uncertainty while the second number in brackets is our estimation of potential higher order cor-

rections. Here the non-perturbative uncertainty is dominated by the uncertainty in the matrix element $\langle Q_3 \rangle^{\text{RI-SMOM}}$. Given the non-perturbative uncertainty we find that the standard model theory prediction is consistent at the order of $\mathcal{O}(\tilde{\alpha}_s^2)$ with the experimental data, eq. (6.24).

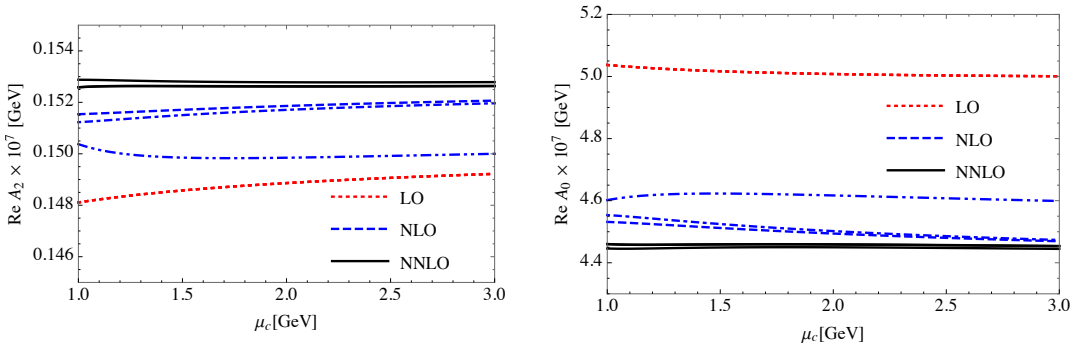

Figure 6.1: Residual scale dependence of ReA_2 and ReA_0 using the central values for the RGI renormalised matrix elements of Table 6.3. The scale variation is due to the residual scale dependence of the Wilson coefficients $\hat{z}_+$, $\hat{z}_-$ and $\hat{z}_3$–$\hat{z}_6$ and measures part of the remaining perturbative uncertainty. The different lines at LO, NLO and NNLO correspond to different solutions of the renormalisation group equations as explained in the text. Their variation provides an additional measure of the remaining perturbative uncertainty.

Finally we present our results for the ratio $\text{ReA}_0 \,/\, \text{ReA}_2$. At LO, NLO and NNLO we have

$$\begin{aligned} \text{Re}A_0/\text{Re}A_2|_{\text{SM LO}} &= 33.8^{+2.4}_{-3.8}\,, \\ \text{Re}A_0/\text{Re}A_2|_{\text{SM NLO}} &= 30.2^{+1.6}_{-1.3}\,, \\ \text{Re}A_0/\text{Re}A_2|_{\text{SM NNLO}} &= 29.2^{+0.2}_{-0.2}\,. \end{aligned} \tag{6.30}$$

Even if our NNLO prediction is larger than the experimental value given in eq. (6.25), the perturbative corrections shift our theory prediction closer to the experimental result. Taking the non-perturbative uncertainty into account, the theory prediction is again consistent with the experimental value

$$\left.\frac{\text{ReA}_0}{\text{ReA}_2}\right|_{\text{SM}} = 29.2(7.4)(1.0)\,, \tag{6.31}$$

where we again show the non-perturbative uncertainty and the higher order uncertainty determined from the shift between NLO and NNLO.

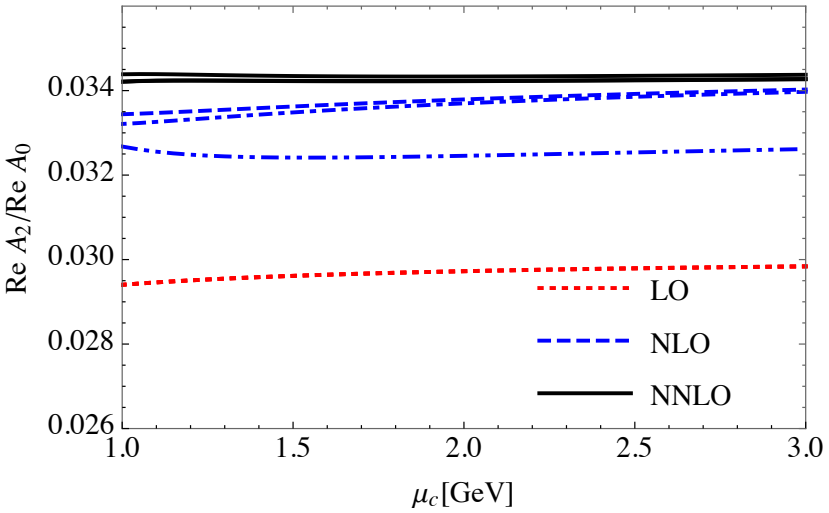

Figure 6.2: Residual scale dependence of $\mathrm{ReA}_0 \,/\, \mathrm{ReA}_2$ using the central values for the RGI renormalised matrix elements of Table 6.3. The scale variation is due to the residual scale dependence of the Wilson coefficients $\hat{z}_+$, $\hat{z}_-$ and $\hat{z}_3$–$\hat{z}_6$ and measures part of the remaining perturbative uncertainty. The different lines at LO, NLO and NNLO correspond to different solutions of the renormalisation group equations as explained in the text. Their variation provides an additional measure of the remaining perturbative uncertainty.

The main conclusion here would be that an improvement on the lattice results would lead to a precise determination for the observables ReA_0 and ReA_2. Even though the decay modes are generated through tree-level processes in the standard model, CP-conserving decay modes could be used in the future to constrain new physics using an increased theoretical precision. In addition, the improved theory prediction will be important to arrive at a quantitative understanding of the dynamics behind the $\Delta I = 1/2$ rule. This will also be an important ingredient in a better control of the theory prediction of CP violating decay modes such as ε'/ε.

6.5.2 NNLO corrections to the ratio ε'/ε

For a consistent evaluation of this physical quantity the ratios ImA_0 / ReA_0 and ImA_2 / ReA_2 have to be determined. In the absence of QED corrections the isospin $I = 2$ ratio would vanish, and the isospin-zero part would receive corrections only from QCD and current-current operators. This pure QCD calculation gives the dominant contribution to the observable ε'/ε, even though the QED part is important through its contribution to the isospin $I = 2$ ratio. Incorporating the recent Lattice determination of the isospin zero matrix elements, we can analyse the effect of our results on the ImA_0 / ReA_0 contribution to ε'/ε in the isospin limit. In what follows we will study the impact of the NNLO QCD corrections on the theory prediction of ε'/ε. These new contributions should reduce the perturbative uncertainties in the leading order of this quantity.

Let us first consider the impact of our higher order corrections to this CP violating observable. Keeping the values of the isospin $I = 2$ amplitudes fixed to the values of the analysis of Ref. [8] we perform the scale variation in the Wilson coefficients that contribute to the isospin $I = 0$ amplitude ratio. The resulting dependence on the matching scale μ_c is shown in Figure 6.3, where we have fixed the non-perturbative parameters in the RGI scheme to the one determined from the central values of the Lattice evaluations, i.e. parameter set a) of table 6.2. The plot exhibits a nice reduction of the residual scale dependence order by order in perturbation theory, where the perturbative corrections are nicely estimated through the respective scale variations. For the LO, NLO and NNLO treatment of the isospin $I = 0$ contribution we then find

$$\begin{aligned}
\varepsilon'/\varepsilon\big|_{\text{SM I=0 LO}} &= 1.7^{+2.4}_{-3.7} \times 10^{-4}\,, \\
\varepsilon'/\varepsilon\big|_{\text{SM I=0 NLO}} &= 1.5^{+1.5}_{-1.3} \times 10^{-4}\,, \\
\varepsilon'/\varepsilon\big|_{\text{SM I=0 NNLO}} &= 1.3^{+0.14}_{-0.18} \times 10^{-4}\,,
\end{aligned}$$

where the perturbative uncertainties stemming from current-current and QCD penguin operators are reduced to around 12% at NNLO level. This removes the largest part of the perturbative uncertainty in this quantity and also strengthens the approach to treat the charm quark contribution perturbatively. After incorporating the NNLO corrections to the isospin $I = 0$ we find that the uncertainties in the isospin $I = 2$

decay mode will dominate the perturbative error. Following the procedures of Ref. [8] we estimate an associated uncertainty of $\pm 0.8 \times 10^{-4}$ to the standard model prediction of ε'/ε from the electroweak penguins.

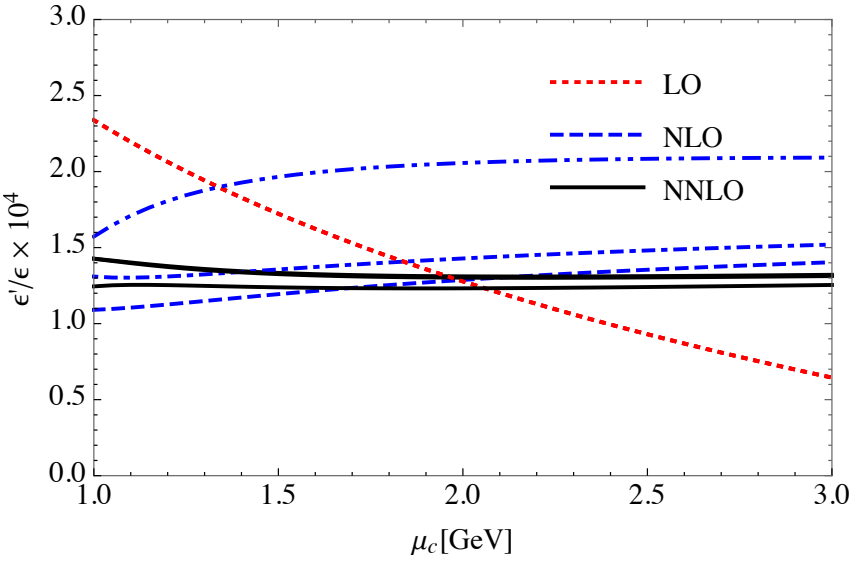

Figure 6.3: Residual scale dependence of ϵ'/ϵ using non-perturbative parameter set a) at LO, NLO and NNLO. The scale variation is due to the residual scale dependence of the Wilson coefficients $\hat{y}_3$–$\hat{y}_6$, $\hat{z}_+$, $\hat{z}_-$ and $\hat{z}_3$–$\hat{z}_6$ and measures part of the remaining perturbative uncertainty. The different lines at LO, NLO and NNLO correspond to different solutions of the renormalisation group equations as explained in the text. Their variation provides an additional measure of the remaining perturbative uncertainty.

To estimate the non-perturbative uncertainties we consider the full correlation of our input parameters of table 6.2 with the errors of the lattice parameters given in table 6.1. We find for our NNLO value that the uncertainties in the matrix elements $\langle Q_i \rangle^{\text{RI-SMOM}}$ results in an error of $\pm 0.3 \times 10^{-4}$, $\pm 0.7 \times 10^{-4}$, $\pm 1.0 \times 10^{-4}$, $\pm 0.2 \times 10^{-4}$ and $\pm 4.1 \times 10^{-4}$ for $i = 1, 2, 3, 5$ and $i = 6$ respectively. Here the largest contribution to the error stems from the uncertainty in the hadronic matrix element $\langle Q_6 \rangle^{\text{RI-SMOM}}$. Combining all uncertainties in squares we find

$$\left.\frac{\varepsilon'}{\varepsilon}\right|_{\text{SM}} = (1.3 \pm 4.4) \times 10^{-4}\,, \tag{6.32}$$

where we also added the contribution from iso-spin breaking and electroweak penguins to the error estimation. Our updated analysis results in a 3σ discrepancy if compared to the experimental value $(\varepsilon'/\varepsilon)_{\text{exp}} = 16.6(2.3) \times 10^{-4}$ [72, 73].

Finally we would like to compare our results to previous phenomenological analyses. Traditionally, the Wilson coefficients were combined with the matrix elments in the traditional basis at $\mu \simeq 1.3\,\text{GeV}$. Yet, the use of the operator relations as in our formalism is formally not valid beyond leading order, but might be phenomenologically acceptable given the smallness of certain matrix elements. To check this we evaluate the QCD penguin Wilson coefficients in the traditional basis at $\mu = 1.3\,\text{GeV}$ and combine them with the choice of non-perturbative input parameters used in Ref. [8] (parameter set c) of Table 6.2). The resulting scale dependence is shown in figure 6.4.

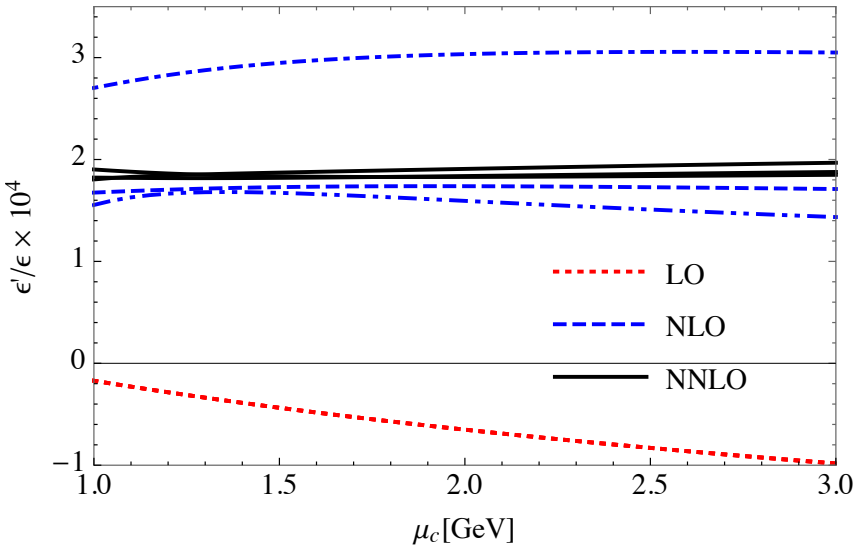

Figure 6.4: Residual scale dependence of ϵ'/ϵ using non-perturbative parameter set c) at LO, NLO and NNLO as performed in Ref. [8]. The scale variation is due to the residual scale dependence of the Wilson coefficients y'_3–y'_6, z'_+, z'_- and z'_3–z'_6 and measures part of the remaining perturbative uncertainty. The different lines at LO, NLO and NNLO correspond to different solutions of the renormalisation group equations as explained in the text. Their variation provides an additional measure of the remaining perturbative uncertainty. Not all higher order corrections are included as a consequence of the analysis procedure.

The shift in the central value compared to our NNLO value has two origins. One origin of the shift is due to the inconsistency in the treatment of higher order corrections, the other is due to a different choice of input parameters. To disentangle the latter we also show the scale dependence of a ε'/ε analysis using the RGI matrix elements and Wilson coefficients in figure 6.5, but hadronic input that is consistent with the choices used in the plot of figure 6.4. In this case, the theoretical estimation of Direct CP-violation stands for

$$\left.\frac{\varepsilon'}{\varepsilon}\right|_{\rm SM} = (1.33 \pm 4.26) \times 10^{-4}, \tag{6.33}$$

where the error is dominated by the non-perturbative sector.

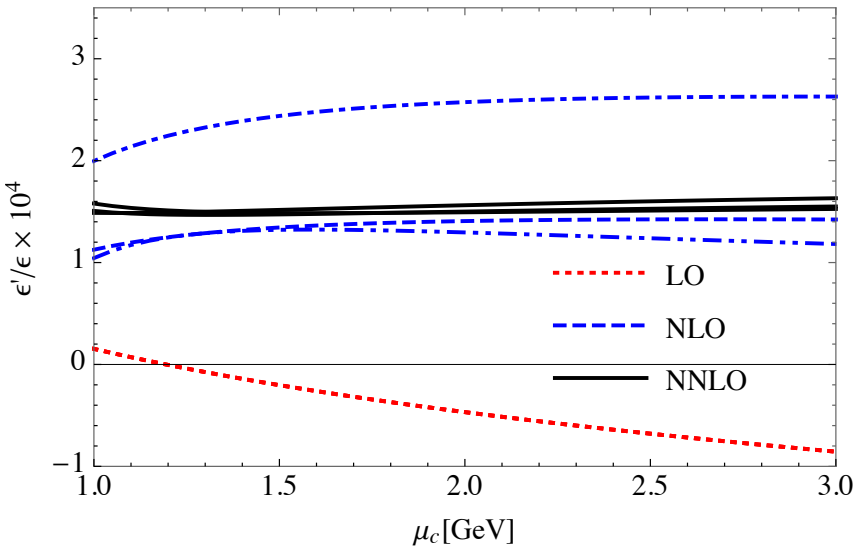

Figure 6.5: Residual scale dependence of ϵ'/ϵ using non-perturbative parameter set b) at LO, NLO and NNLO. The scale variation is due to the residual scale dependence of the Wilson coefficients $\hat{y}_3$–$\hat{y}_6$, $\hat{z}_+$, $\hat{z}_-$ and $\hat{z}_3$–$\hat{z}_6$ and measures part of the remaining perturbative uncertainty. The different lines at LO, NLO and NNLO correspond to different solutions of the renormalisation group equations as explained in the text. Their variation provides an additional measure of the remaining perturbative uncertainty.

6.6 Limitations of the phenomenological analysis

Even though the previous formalism leads to an estimation for ε'/ε several subtleties are still present in the analysis of this interesting observable. To derive equation (6.3) one expresses the pion states in terms of the isospin ones. The two-isospin values allowed in s-wave are $I = 0$ and $I = 2$. Within this limit, the strong phases factor out and are related to the $\pi\pi$ scattering phase shifts (Watson's theorem). This statement is only valid when isospin is conserved, that is, when there are no electromagnetic effects, $\tilde{\alpha}_e = 0$, and the masses of the quarks are degenerate, $m_u = m_d = m_q$. But in reality, pions are not exact $I = 1$ states, and moreover electromagnetic effects cannot be neglected when charged particles are present. Indeed, the experimental measurements (hence theoretical expressions) depend on phase space cuts on additional soft photons. Consequently, the isospin limit is not very good. In fact, it receives at $\mathcal{O}(10\%)$ corrections, which have been parametrised by the factor $\hat{\Omega}_{\text{eff}}$, together with a particular scheme for ω, which defines ω_+. The parameter $a \approx 1.017$ is also an attempt to include a class of higher-order isospin-breaking effects. While the latter factors introduce isospin-breaking effects, the phases $\delta_{0,2}$ are still defined in the isospin limit, even if they are no longer the true strong phases of the amplitudes.

On the other hand, the definition of the isospin limit is also not self-consistent as the electroweak Wilson coefficients have scale dependence that is due to electromagnetism, and this does not cancel against the scale dependence of an isospin-symmetric evaluation of the matrix elements. In practice, one matches a QCD×QED evolution to a pure QCD lattice calculation at some scale ($\mu = m_c$). This can only be resolved by including electromagnetism into the matrix elements, which introduces an IR problem.

6.7 Future improvements

The following sections try to give an insight of the different subtleties and limitations of the current phenomenological analysis for direct CP-violation. The formalism explained in section 6.3 is extended to the four flavour case incorporating the charm quark as a dynamical degree of freedom. In addition, we present a new formula in terms of the charge and neutral pion states which can be connected with the experimental analysis. The isospin-breaking effects due to the difference on the quark masses for the up-type and down-type quarks are discussed. Moreover the inclusion of the photon emission and therefore electroweak effects is reviewed in the last part of this section.

6.7.1 Four flavour formalism

The practical evaluation of the hadronic matrix elements involves a theory with three light quarks u, d, s. To control possible non-perturbative effects of virtual charm quarks, it would be desirable to calculate the matrix elements in a theory with four or even five flavours. In the future, non-perturbative calculations with a dynamical charm quark will likely become available, allowing to work based on a weak Lagrangian in a theory with $n_f > 3$ flavours. In the meantime, we can use our NNLO results to provide an estimation of the four-flavour matrix elements. In what follows, we will consider a formulation of the amplitude ratios in a four-flavour theory, prior to have discussed how the Fierz identities change.

The four flavour theory contains two extra operators Q_1^c and Q_2^c, or in the modern basis $\mathcal{O}_1^c$ and $\mathcal{O}_2^c$. In the isospin limit, they contribute only to A_0. In this case the operator relations are modified by the contribution of these operators. In any Fierz-symmetric scheme they read

$$\begin{aligned} Q_4 &= Q_3 + 2Q_- + 2Q_-^c, \\ Q_9 &= \frac{3}{2}(Q_1 + Q_1^c) - \frac{1}{2}Q_3 = \frac{3}{2}(Q_+ - Q_- + Q_1^c) - \frac{1}{2}Q_3, \\ Q_{10} &= \frac{3}{2}(Q_2 + Q_2^c) - \frac{1}{2}Q_4 = \frac{3}{2}(Q_+ + Q_+^c) - \frac{1}{2}(Q_- + Q_-^c - Q_3), \end{aligned} \tag{6.34}$$

where the last equality involves the use of the first equation. The $n_f = 3$ relations are recovered by dropping the Q_i^c operators, and the charm components inside the penguin operators Q_3 and Q_4. In a Fierz-nonsymmetric scheme, each relation has extra penguin terms on the r.h.s that involve explicit powers of $\tilde{\alpha}_s$. These terms include the $(V-A)\times(V+A)$ penguin operators. As explained previously our formalism satisfies the relations of eq. (6.34) to all orders in perturbation theory. This fact is one of the advantages of the hatted quantities. From the equations above and using that Q_-^u and all charm and penguin operators are pure $\Delta I = 2$, there is only one independent non-zero $I = 2$ matrix element in the left-handed sector:

$$\langle Q_-^u \rangle_2 = \langle Q_{1,2}^c \rangle_2 = \langle Q_{1,2,3,4,5,6} \rangle_2 = 0, \tag{6.35}$$

$$\langle Q_9 \rangle_2 = \langle Q_{10} \rangle_2 = \langle Q_+ \rangle_2. \tag{6.36}$$

As a result, the expression for the $(V-A)\times(V-A)$ part of $\mathrm{Im}\mathrm{A}_2 \,/\, \mathrm{Re}\mathrm{A}_2$ is unchanged and still free from hadronic uncertainties, except that the Wilson coefficients need to be evaluated in the $n_f = 4$-flavour theory. On the other hand, the isospin-zero part

becomes

$$\mathrm{ReA}_0 = \frac{\mathrm{G_F}}{\sqrt{2}}\lambda_\mathrm{u}\,\hat{z}_-\langle\hat{Q}_- - \hat{Q}^c_-\rangle_0(1+\tilde{q}) + \mathcal{O}(\mathrm{Re}\,\tau), \tag{6.37}$$

$$\mathrm{ImA}_0 = \frac{\mathrm{G_F}}{\sqrt{2}}\lambda_\mathrm{u}\,\mathrm{Im}\,\tau\,\langle\hat{Q}_- - \hat{Q}^c_-\rangle_0\Big[(2\,\hat{y}_4 - \frac{1}{2}[3\hat{y}_9 - \hat{y}_{10}])(1+2\,\hat{q}^c_-) - \hat{z}_-\hat{q}^c_- \tag{6.38}$$

$$+[\frac{3}{2}(\hat{y}_9+\hat{y}_{10})\frac{\hat{z}_-}{\hat{z}_+}(1+\hat{q}^c_+) - \hat{z}_-\hat{q}^c_+]\tilde{q} + (\hat{y}_3+\hat{y}_4 - \frac{1}{2}[\hat{y}_9+\hat{y}_{10}])\tilde{p}_3\Big] \tag{6.39}$$

$$+\ \frac{\mathrm{G_F}}{\sqrt{2}}\lambda_\mathrm{u}\,\mathrm{Im}\,\tau\,\Big[\langle\hat{Q}_6\rangle_0(\hat{y}_6 + \tilde{p}_5\hat{y}_5 + \hat{y}_{8g}\tilde{p}_{8g}) + \langle\hat{Q}_8\rangle_0(\hat{y}_8 + \tilde{p}_{70}\hat{y}_7 + \tilde{p}_{70\gamma}\hat{y}_{7\gamma})\Big]\,, \tag{6.40}$$

where we have defined

$$\tilde{q} = \frac{\hat{z}_+\langle\hat{Q}_+ - \hat{Q}^c_+\rangle_0}{\hat{z}_-\langle\hat{Q}_- - \hat{Q}^c_-\rangle_0}, \quad \hat{q}^c_- = \frac{\langle\hat{Q}^c_-\rangle_0}{\langle\hat{Q}_- - \hat{Q}^c_-\rangle_0}, \quad \hat{q}^c_+ = \frac{\langle\hat{Q}^c_+\rangle_0}{\langle\hat{Q}_+ - \hat{Q}^c_+\rangle_0}, \quad \tilde{p}_3 = \frac{\langle\hat{Q}_3\rangle_0}{\langle\hat{Q}_- - \hat{Q}^c_-\rangle_0}. \tag{6.41}$$

Here $\tilde{q}$ generalises $\hat{q}$ of the 3-flavour theory. It should numerically be very similar, and fully scale and scheme independent. $\tilde{p}_3$ generalises $\hat{p}_3$ in the 3-flavour theory, while the symbols $\hat{p}_5$, $\hat{p}_{70}$, $\hat{p}_{70\gamma}$ and $\hat{p}_{8g}$ are unchanged (apart from being evaluated in the $n_f = 4$ theory). q^c_-, q^c_+, parameterise operator matrix elements not present in the $n_f = 3$ theory.

The resulting generalisation of the $I = 0$ amplitude ratio is

$$\begin{aligned}\frac{\mathrm{Im}A_0}{\mathrm{Re}A_0} \;=\; \mathrm{Im}\tau\Bigg[&\frac{(2\,\hat{y}_4 - \frac{1}{2}[3\hat{y}_9 - \hat{y}_{10}])}{z_-}\frac{(1+2\,q^c_-)}{(1+\tilde{q})} - \frac{\hat{q}^c_-}{1+\tilde{q}} \\ &+\frac{3}{2}\frac{[\hat{y}_9+\hat{y}_{10}]}{z_+}\frac{(1+\hat{q}^c_+)}{(1+\tilde{q})}\tilde{q} - \frac{q^c_+\tilde{q}}{1+\tilde{q}} + \frac{\big(\hat{y}_3+\hat{y}_4 - \frac{1}{2}[\hat{y}_9+\hat{y}_{10}]\big)}{z_-(1+\tilde{q})}\tilde{p}_3 \\ &+\frac{G_F V_{ud}V^*_{us}}{\sqrt{2}\,\mathrm{Re}A_0}\Big(\langle\hat{Q}_6\rangle_0\Big(\hat{y}_6 + \hat{p}_5\hat{y}_5 + \hat{p}_{8g}\hat{y}_{8g}\Big) + \langle\hat{Q}_8\rangle_0\Big(\hat{y}_8 + \hat{p}_{70}\hat{y}_7 + \hat{p}_{70\gamma}\hat{y}_{7\gamma}\Big)\Big)\Bigg]\,.\end{aligned} \tag{6.42}$$

In the future, isospin breaking effects might be estimated on the lattice. Hence we refrain from including them in the four-flavour formalism; but the equations might still be useful.

6.7.2 ε'/ε formula for charge eigenstate particles

We aim to present here a more consistent expression for ε'/ε describing the actual measurements. For this purpose we express the old formalism in terms of the charge eigenstates: $|\pi^+\pi^-\rangle$ and $|\pi^0\pi^0\rangle$. The contribution of final states with one or more soft-photons will be discussed in detail in the next section.

The starting point of our derivation is the "experimental" definition of ε' and ε parameters, which connects them to the measured quantities η_{+-} and η_{00} (extracted from $K \to \pi\pi$ time-dependent decay),

$$\varepsilon \equiv \frac{2\eta_{+-} + \eta_{00}}{3}, \quad \text{and} \quad \varepsilon' \equiv \frac{\eta_{+-} - \eta_{00}}{3}. \tag{6.43}$$

For an arbitrary decay channel f the η parameters are defined as,

$$\eta_f = |\eta_f| e^{i\phi_f} \equiv \frac{\langle f|\mathrm{H}_W|K_L\rangle}{\langle f|\mathrm{H}_W|K_S\rangle} r. \tag{6.44}$$

Here, the factor r parametrises the rephasing-invariance. This r term has to depend on the phases of the states $|K_S\rangle$ and $|K_L\rangle$ to cancel out the phase-convention dependence of the ratio: $\langle f|\mathrm{H}_W|K_L\rangle/\langle f|\mathrm{H}_W|K_S\rangle$. Under this condition the phase ϕ_f is physical. We assume CPT symmetry throughout, then the only freedom is the phase of r. Adopting the partial phase convention $\langle K_0|K_L\rangle = \langle K_0|K_S\rangle$, the parameter r takes the value $r = 1$. We use this particular parametrization. Additionally, we follow the PDG convention for the definition of K_L and K_S states, and we expand to leading order in $\mathrm{Re}\tau$, $(p-q)/(p+q)$ and $\mathrm{Im}\tau$. Furthermore, we work to leading order in the weak effective Hamiltonian. We split the weak (CP-odd) phases according to the CKM factors,

$$\mathrm{H}_W = V_{ud}V_{us}^*(H_W^T + \tau H_W^P), \tag{6.45}$$

obtaining the following general expression for η_{+-} and η_{00},

$$\eta_f = \frac{p-q}{p+q} + i\mathrm{Im}\tau R_f, \tag{6.46}$$

where

$$R_f = \frac{\langle f|\mathrm{H}_W^P|K^0\rangle}{\langle f|\mathrm{H}_W^T|K^0\rangle}, \tag{6.47}$$

are rephasing-invariant quantities, and H_W^P and H_W^T refer to penguin and tree contributions, respectively. The latter are CP-even terms, that do not change when K_0 is replaced by $\overline{K}_0$. We introduce equation (6.46) into the experimental definition for ε'

and ε, see eq. (6.43), which leads to

$$\begin{aligned}\varepsilon' &= i\frac{\mathrm{Im}\tau}{3}(R_{\pi^+\pi^-} - R_{\pi^0\pi^0}),\\ \varepsilon &= \frac{p-q}{p+q} + i\frac{\mathrm{Im}\tau}{3}(2R_{\pi^+\pi^-} + R_{\pi^0\pi^0}).\end{aligned} \tag{6.48}$$

Note that the expression for ε' does not depend on the factors p and q. However, the one for ε suffers from that dependence. Hence, we use the experimental definition of ε' and set ε to its experimentally determined value: ε_K. In this manner, our expression in terms of the charge states does not involve any dependence on p and q,

$$\frac{\varepsilon'}{\varepsilon} = \frac{i}{3}\frac{\mathrm{Im}\tau}{\varepsilon_K}(R_{\pi^+\pi^-} - R_{\pi^0\pi^0}). \tag{6.49}$$

In this derivation no use of the $\Delta I = 1/2$ rule has been made and no isospin limit has been assumed. This can be recovered by using the isospin decomposition of the two-pion states. In the isospin limit, the charged and neutral two pion states are related to the isospin $I = 0$ and $I = 2$ states as

$$\begin{aligned}\langle\pi^+\pi^-| &= \sqrt{\frac{1}{3}}\langle(\pi\pi)_{I=2}| + \sqrt{\frac{2}{3}}\langle(\pi\pi)_{I=0}|,\\ \langle\pi^0\pi^0| &= \sqrt{\frac{2}{3}}\langle(\pi\pi)_{I=2}| - \sqrt{\frac{1}{3}}\langle(\pi\pi)_{I=0}|.\end{aligned} \tag{6.50}$$

In the isospin limit our R_f factors reduce to

$$\begin{aligned}[R_{\pi^+\pi^-}]_{\mathrm{iso}} &= \frac{1}{\mathrm{Im}\tau}\frac{\mathrm{ImA_0}}{\mathrm{ReA_0}} + \frac{1}{\mathrm{Im}\tau}\frac{1}{\sqrt{2}}\frac{\mathrm{ReA_2}}{\mathrm{ReA_0}}e^{i(\delta_2-\delta_0)}\left[\frac{\mathrm{ImA_2}}{\mathrm{ReA_2}} - \frac{\mathrm{ImA_0}}{\mathrm{ReA_0}}\right],\\ [R_{\pi^0\pi^0}]_{\mathrm{iso}} &= \frac{1}{\mathrm{Im}\tau}\frac{\mathrm{ImA_0}}{\mathrm{ReA_0}} - \frac{2}{\mathrm{Im}\tau}\frac{1}{\sqrt{2}}\frac{\mathrm{ReA_2}}{\mathrm{ReA_0}}e^{i(\delta_2-\delta_0)}\left[\frac{\mathrm{ImA_2}}{\mathrm{ReA_2}} - \frac{\mathrm{ImA_0}}{\mathrm{ReA_0}}\right],\end{aligned} \tag{6.51}$$

where A_I are the CP-conserving amplitudes. The ratio $1/\omega = \mathrm{ReA_2}\,/\,\mathrm{ReA_0}$ is known to be small ($\omega \sim 22$). Consequently, only linear terms of $1/\omega$ have been kept in the equations above. Using these results in the expression (6.48), we recover the isospin limit formula for ε' and ε,

$$\begin{aligned}\varepsilon' &= \frac{i}{\sqrt{2}}e^{i(\delta_2-\delta_0)}\frac{\mathrm{ReA_2}}{\mathrm{ReA_0}}\left[\frac{\mathrm{ImA_2}}{\mathrm{ReA_2}} - \frac{\mathrm{ImA_0}}{\mathrm{ReA_0}}\right],\\ \varepsilon &= \frac{p-q}{p+q} + i\frac{\mathrm{ImA_0}}{\mathrm{ReA_0}} = \tilde{\varepsilon} + i\frac{\mathrm{ImA_0}}{\mathrm{ReA_0}}.\end{aligned} \tag{6.52}$$

In the following we consider the isospin breaking effects due to the difference of the quark masses. The R_f ratio of equation (6.47) contains a piece which preserves isospin symmetry and another one which breaks this property. Considering that the latter is very small, we can split the previous matrix elements in terms of their isospin limit part and the isospin breaking effects,

$$R_f = \frac{\langle f|\mathrm{H}_W^P|K^0\rangle_{\mathrm{iso}} + \delta A_f^P}{\langle f|\mathrm{H}_W^T|K^0\rangle_{\mathrm{iso}} + \delta A_f^T}. \tag{6.53}$$

To simplify the analysis we will consider the case of only current-current and pure QCD-penguin operators. Therefore the ImA_2 factor will vanish since no electroweak operators are considered here. Proceeding in the same way as before where the pion states are expressed in terms of the isospin states by means of equation (6.50), at the leading order of our isospin expansion, we then expand in the ratio $\mathrm{ReA}_2\,/\,\mathrm{ReA}_0$ and the isospin breaking corrections and arrive at the following expressions for the R_{+-} and R_{00} terms:

$$R_{\pi^+\pi^-} = \frac{1}{\mathrm{Im}\tau}\frac{\mathrm{ImA}_0}{\mathrm{ReA}_0}\left[1 - \frac{1}{\sqrt{2}}\frac{\mathrm{ReA}_2}{\mathrm{ReA}_0}e^{i(\delta_2-\delta_0)} + \frac{1}{\sqrt{2}}\delta A_{+-}^{\mathrm{strong}}e^{-i\delta_0}\right], \tag{6.54}$$

$$R_{\pi^0\pi^0} = \frac{1}{\mathrm{Im}\tau}\frac{\mathrm{ImA}_0}{\mathrm{ReA}_0}\left[1 + \sqrt{2}\frac{\mathrm{ReA}_2}{\mathrm{ReA}_0}e^{i(\delta_2-\delta_0)} + \delta A_{00}^{\mathrm{strong}}e^{-i\delta_0}\right]. \tag{6.55}$$

Here $\delta A_f^{\mathrm{strong}}$ parametrizes the total isospin breaking effect given by

$$\begin{aligned}\delta A_{+-}^{\mathrm{strong}} &= \left(\mathrm{Im}\tau\frac{\delta A_{+-}^P}{\mathrm{ImA}_0} - \frac{\delta A_{+-}^T}{\mathrm{ReA}_0}\right),\\ \delta A_{00}^{\mathrm{strong}} &= \left(\frac{\delta A_{00}^T}{\mathrm{ReA}_0} - \mathrm{Im}\tau\frac{\delta A_{00}^P}{\mathrm{ImA}_0}\right),\end{aligned} \tag{6.56}$$

where only isospin breaking effects from the strong sector have been included and where terms of quadratic order in isospin breaking and $\mathrm{ReA}_2\,/\,\mathrm{ReA}_0 \times \delta A_f^P$ have been neglected. If we set the isospin correction terms to zero and for the case of no presence of electroweak operators ($\mathrm{ImA}_2 = 0$), we reproduce the isospin limit expressions (6.51) for the R_f terms with $f = +-, 00$,

$$\frac{\varepsilon'}{\varepsilon} = -\frac{i}{\sqrt{2}}\frac{1}{\varepsilon_K}\frac{\mathrm{ImA}_0}{\mathrm{ReA}_0}\left[\frac{\mathrm{ReA}_2}{\mathrm{ReA}_0}e^{i(\delta_2-\delta_0)} + \left(\delta A_{+-}^{\mathrm{strong}} - \sqrt{2}\delta A_{00}^{\mathrm{strong}}\right)e^{-i\delta_0}\right]. \tag{6.57}$$

Comparing with the expression (6.3) when no electroweak penguin operators are considered we get

$$\hat{\Omega}_{\mathrm{eff}}^{\mathrm{strong}} = \frac{\mathrm{ReA}_0}{\mathrm{ReA}_2}\left(\delta A_{00}^{\mathrm{strong}} - \sqrt{2}\delta A_{+-}^{\mathrm{strong}}\right)e^{-i\delta_2}\,. \tag{6.58}$$

Notice that the resulting strong isospin breaking effects are enhanced by the $\Delta I = 1/2$ rule. This enhancement has been observed before in the literature [71], yet our derivation relies on our new formalism of expressing ε'/ε in terms of the charged decay ratios R_{+-} and R_{00}. Modern techniques of Lattice QCD should be able to determine the iso-spin breaking effects directly by evaluating the matrix elements of the respective quantities $\delta A_{00}^{\text{strong}}$ and $\delta A_{+-}^{\text{strong}}$.

6.7.3 Photon emission

In addition to isospin-breaking effects from quark mass differences, which are fully captured by the formalism considered here, a complete treatment also has to deal with electromagnetic effects, since experiments cannot distinguish the states $|\pi^+\pi^-\rangle$ and $|\pi^+\pi^-\rangle + |n\gamma\rangle$ when the photons emitted are soft (with energy much smaller than the experimental resolution). Thus, the experimental measurements always include sum over $|\pi^+\pi^-\rangle$ and $|\pi^+\pi^-\rangle + |n\gamma\rangle$ final states. For instance, the NA48 experiment [72] imposes certain cuts on the dipion mass (in the charged case) and on the admissible collections of photon showers (in the neutral case). In this section we try to present a theory expression valid for any realistic photon energy cut.

When charged external particles are involved one has to deal with universal infra-red effects originated by virtual photons attached to the charged particles. These contributions are independent of the original state, and they lead to IR divergent Green's functions. These IR singularities have to be cancelled by considering the effect of soft real photons in the external states, which would be described by diagrams with direct photon emission. If this is taken into account the decay rate can be expanded at $\mathcal{O}(\alpha_e)$, as

$$\Gamma(K_i \to \pi\pi + n\gamma) = \Gamma^{(0)}(K_i \to \pi\pi) + \Gamma^{(1)}(K_i \to \pi\pi) + \int d\Gamma^{(1)}(K_i \to \pi\pi\gamma), \quad (6.59)$$

where K_i is K_L or K_S and $\pi\pi$ is $\pi^+\pi^-$ or $\pi^0\pi^0$. IR divergences cancel in the sum, however the second and third term require IR regularisation to be calculated separately. If we assume that the real emission is well approximated by the leading-order result multiplied by a universal correction factor,

$$\int d\Gamma^{(1)}(K_i \to \pi\pi\gamma) = C \cdot \Gamma^{(0)}(K_i \to \pi\pi)$$

we can write, and expand the K_S/K_L ratio as

$$\begin{aligned}
\frac{\Gamma(K_L \to \pi\pi + n\gamma)}{\Gamma(K_S \to \pi\pi + n\gamma)} &\approx \frac{\Gamma^{(0)}(K_L \to \pi\pi)(1+C) + \Gamma^{(1)}(K_L \to \pi\pi)}{\Gamma^{(0)}(K_S \to \pi\pi)(1+C) + \Gamma^{(1)}(K_S \to \pi\pi)} \\
&= \frac{\Gamma^{(0)}(K_L \to \pi\pi)}{\Gamma^{(0)}(K_S \to \pi\pi)} \times \left(1 + \frac{\Gamma^{(1)}(K_L \to \pi\pi)}{\Gamma^{(0)}(K_L \to \pi\pi)} - \frac{\Gamma^{(1)}(K_S \to \pi\pi)}{\Gamma^{(0)}(K_S \to \pi\pi)}\right) \\
&\quad + \mathcal{O}(\tilde{\alpha}_e^2). \qquad (6.60)
\end{aligned}$$

The first factor on the second line is just the $\mathcal{O}(\alpha_e^0)$ result for which we know the expression already. The two correction terms in the parentheses need to be expanded out in terms of ratios of the form

$$\frac{\langle \pi\pi|Q_i|K^0\rangle^{(1)}_{\text{reg}}}{\langle \pi\pi|Q_i|K^0\rangle}.$$

These expressions generally require IR regularisation. However, we know that the difference of the two terms in parentheses is IR finite. Our future aim would be to group together (ratios of) hadronic matrix elements into combinations that are hopefully both simple and IR-finite. Eventually Lattice could estimate electromagnetic effects, and these calculation would be defined completely independently of any particular IR regularisation employed by them.

Chapter 7

Conclusions

In this thesis, we have discussed the pure QCD corrections to two important observables in Kaon physics: the $\Delta I = 2$ rule and the ratio ε'/ε, which parametrizes direct CP-violation. More precisely, we have computed the NNLO QCD corrections in the four- and three-flavour theories for current-current and QCD-penguin operators. We give a detailed explanation of several subtleties associated with the matching calculations. Moreover a new formalism that connects calculations performed in different operator bases has been introduced by defining the RGI-scheme objects. We have also computed the scheme change for the electroweak operators at NLO and presented the ADM for a general number of flavours in the modern basis. Finally our new results are applied to the theory prediction of hadronic kaon decays: $\Delta I = 1/2$ and ε'/ε to check the perturbative convergence. The SM prediction for the latter is updated at NNLO, where an improved formula in terms of the RGI-quantities has been used. This new expression includes the sub-leading effects by correcting the application of Fierz relations in the phenomenological formula for ε'/ε in our formalism. The impact of our new contributions leads to a reduction of the perturbative uncertainties. Indeed they are completely eliminated for pure QCD-corrections. Moreover in the analysis one can observe a very good convergence of the perturbation theory at low-energy scales. Improving the accuracy of the SM predictions is crucial for identifying the origin of the discrepancy between experimental data and theory predictions, and the results of this thesis make significant progress in this direction.

Bibliography

[1] S. L. Glashow. Partial Symmetries of Weak Interactions. *Nucl. Phys.*, 22:579–588, 1961.

[2] Steven Weinberg. A Model of Leptons. *Phys. Rev. Lett.*, 19:1264–1266, 1967.

[3] Abdus Salam. Weak and Electromagnetic Interactions. *Conf. Proc.*, C680519:367–377, 1968.

[4] A. D. Sakharov. Violation of CP Invariance, c Asymmetry, and Baryon Asymmetry of the Universe. *Pisma Zh. Eksp. Teor. Fiz.*, 5:32–35, 1967. [Usp. Fiz. Nauk161,61(1991)].

[5] T. Blum et al. Lattice determination of the $K \to (\pi\pi)_{I=2}$ Decay Amplitude A_2. *Phys. Rev.*, D86:074513, 2012.

[6] T. Blum et al. $K \to \pi\pi$ $\Delta I = 3/2$ decay amplitude in the continuum limit. *Phys. Rev.*, D91(7):074502, 2015.

[7] Z. Bai et al. Standard Model Prediction for Direct CP Violation in $K \to \pi\pi$ Decay. *Phys. Rev. Lett.*, 115(21):212001, 2015.

[8] Andrzej J. Buras, Martin Gorbahn, Sebastian Jager, and Matthias Jamin. Improved anatomy of ε'/ε in the Standard Model. *JHEP*, 11:202, 2015.

[9] F. Englert and R. Brout. Broken Symmetry and the Mass of Gauge Vector Mesons. *Phys. Rev. Lett.*, 13:321–323, 1964.

[10] Peter W. Higgs. Broken Symmetries and the Masses of Gauge Bosons. *Phys. Rev. Lett.*, 13:508–509, 1964.

[11] G. S. Guralnik, C. R. Hagen, and T. W. B. Kibble. Global Conservation Laws and Massless Particles. *Phys. Rev. Lett.*, 13:585–587, 1964.

[12] Peter W. Higgs. Spontaneous Symmetry Breakdown without Massless Bosons. *Phys. Rev.*, 145:1156–1163, 1966.

[13] Steven Weinberg. *The Quantum theory of fields. Vol. 1: Foundations*. Cambridge University Press, 2005.

[14] Michael E. Peskin and Daniel V. Schroeder. *An Introduction to quantum field theory*. Addison-Wesley, Reading, USA, 1995.

[15] John C. Collins. *Renormalization*, volume 26 of *Cambridge Monographs on Mathematical Physics*. Cambridge University Press, Cambridge, 1986.

[16] David J. Gross and Frank Wilczek. Ultraviolet Behavior of Nonabelian Gauge Theories. *Phys. Rev. Lett.*, 30:1343–1346, 1973.

[17] H. David Politzer. Reliable Perturbative Results for Strong Interactions? *Phys. Rev. Lett.*, 30:1346–1349, 1973.

[18] H. Lehmann, K. Symanzik, and W. Zimmermann. On the formulation of quantized field theories. *Nuovo Cim.*, 1:205–225, 1955.

[19] L. D. Faddeev and V. N. Popov. Feynman Diagrams for the Yang-Mills Field. *Phys. Lett.*, 25B:29–30, 1967.

[20] C. Becchi, A. Rouet, and R. Stora. Renormalization of the Abelian Higgs-Kibble Model. *Commun. Math. Phys.*, 42:127–162, 1975.

[21] J. C. Taylor. Ward Identities and Charge Renormalization of the Yang-Mills Field. *Nucl. Phys.*, B33:436–444, 1971.

[22] A. A. Slavnov. Ward Identities in Gauge Theories. *Theor. Math. Phys.*, 10:99–107, 1972. [Teor. Mat. Fiz.10,153(1972)].

[23] L. F. Abbott. Introduction to the Background Field Method. *Acta Phys. Polon.*, B13:33, 1982.

[24] Gerard 't Hooft and M. J. G. Veltman. Regularization and Renormalization of Gauge Fields. *Nucl. Phys.*, B44:189–213, 1972.

[25] C. G. Bollini and J. J. Giambiagi. Dimensional Renormalization: The Number of Dimensions as a Regularizing Parameter. *Nuovo Cim.*, B12:20–26, 1972.

[26] Andrzej J. Buras. Weak Hamiltonian, CP violation and rare decays. In *Probing the standard model of particle interactions. Proceedings, Summer School in Theoretical Physics, NATO Advanced Study Institute, 68th session, Les Houches, France, July 28-September 5, 1997. Pt. 1, 2*, pages 281–539, 1998.

[27] Thomas Hahn. Generating Feynman diagrams and amplitudes with FeynArts 3. *Comput. Phys. Commun.*, 140:418–431, 2001.

[28] Andrei I. Davydychev and J. B. Tausk. Two loop selfenergy diagrams with different masses and the momentum expansion. *Nucl. Phys.*, B397:123–142, 1993.

[29] K. G. Chetyrkin, A. L. Kataev, and F. V. Tkachov. New Approach to Evaluation of Multiloop Feynman Integrals: The Gegenbauer Polynomial x Space Technique. *Nucl. Phys.*, B174:345–377, 1980.

[30] William A. Bardeen, A. J. Buras, D. W. Duke, and T. Muta. Deep Inelastic Scattering Beyond the Leading Order in Asymptotically Free Gauge Theories. *Phys. Rev.*, D18:3998, 1978.

[31] Konstantin G. Chetyrkin, Mikolaj Misiak, and Manfred Munz. Weak radiative B meson decay beyond leading logarithms. *Phys. Lett.*, B400:206–219, 1997. [Erratum: Phys. Lett.B425,414(1998)].

[32] Konstantin G. Chetyrkin, Mikolaj Misiak, and Manfred Munz. Beta functions and anomalous dimensions up to three loops. *Nucl. Phys.*, B518:473–494, 1998.

[33] Martin Gorbahn. *QCD and QED anomalous dimension matrix for weak decays at NNLO*. PhD thesis, Munich, Tech. U., 2003.

[34] Ernest C. G. Stueckelberg and Andre Petermann. The normalization group in quantum theory. *Helv. Phys. Acta*, 24:317–319, 1951.

[35] H. Simma. Equations of motion for effective Lagrangians and penguins in rare B decays. *Z. Phys.*, C61:67–82, 1994.

[36] Wolfhart Zimmermann. Composite operators in the perturbation theory of renormalizable interactions. *Annals Phys.*, 77:536–569, 1973. [Lect. Notes Phys.558,244(2000)].

[37] Andrzej J. Buras and Peter H. Weisz. QCD Nonleading Corrections to Weak Decays in Dimensional Regularization and 't Hooft-Veltman Schemes. *Nucl. Phys.*, B333:66–99, 1990.

[38] K. Symanzik. Infrared singularities and small distance behavior analysis. *Commun. Math. Phys.*, 34:7–36, 1973.

[39] Thomas Appelquist and J. Carazzone. Infrared Singularities and Massive Fields. *Phys. Rev.*, D11:2856, 1975.

[40] Edward Witten. Heavy Quark Contributions to Deep Inelastic Scattering. *Nucl. Phys.*, B104:445–476, 1976.

[41] Burt A. Ovrut and Howard J. Schnitzer. Gauge Theory and Effective Lagrangian. *Nucl. Phys.*, B189:509–534, 1981.

[42] Werner Bernreuther and Werner Wetzel. Decoupling of Heavy Quarks in the Minimal Subtraction Scheme. *Nucl. Phys.*, B197:228–236, 1982. [Erratum: Nucl. Phys.B513,758(1998)].

[43] Robert D. C. Miller and Bruce H. J. McKellar. Effective Theories With Broken Flavor Symmetry. *Phys. Rev.*, D26:878, 1982.

[44] A. J. Buras, M. Gorbahn, U. Haisch, and U. Nierste. The Rare decay $K^+ \to \pi^+ \nu\bar{\nu}$ at the next-to-next-to-leading order in QCD. *Phys. Rev. Lett.*, 95:261805, 2005.

[45] Konstantin G. Chetyrkin, Mikolaj Misiak, and Manfred Munz. $|\Delta F| = 1$ non-leptonic effective Hamiltonian in a simpler scheme. *Nucl. Phys.*, B520:279–297, 1998.

[46] Martin Gorbahn and Ulrich Haisch. Effective Hamiltonian for non-leptonic $|\Delta F| = 1$ decays at NNLO in QCD. *Nucl. Phys.*, B713:291–332, 2005.

[47] Christoph Bobeth, Mikolaj Misiak, and Jorg Urban. Photonic penguins at two loops and m_t dependence of $BR[B \to X_s l^+ l^-]$. *Nucl. Phys.*, B574:291–330, 2000.

[48] Christoph Bobeth, Paolo Gambino, Martin Gorbahn, and Ulrich Haisch. Complete NNLO QCD analysis of $\bar{B} \to X_s \ell^+ \ell^-$ and higher order electroweak effects. *JHEP*, 04:071, 2004.

[49] H. Kluberg-Stern and J. B. Zuber. Ward Identities and Some Clues to the Renormalization of Gauge Invariant Operators. *Phys. Rev.*, D12:467–481, 1975.

[50] H. Kluberg-Stern and J. B. Zuber. Renormalization of Nonabelian Gauge Theories in a Background Field Gauge. II. Gauge Invariant Operators. *Phys. Rev.*, D12:3159–3180, 1975.

[51] Stefano Bertolini, Marco Fabbrichesi, and Emidio Gabrielli. The Relevance of the dipole Penguin operators in ε'/ε. *Phys. Lett.*, B327:136–144, 1994.

[52] Benjamin Grinstein, Roxanne P. Springer, and Mark B. Wise. Effective Hamiltonian for Weak Radiative B Meson Decay. *Phys. Lett.*, B202:138–144, 1988.

[53] Gerhard Buchalla, Andrzej J. Buras, and Michaela K. Harlander. The Anatomy of ε'/ε in the Standard Model. *Nucl. Phys.*, B337:313–362, 1990.

[54] Michael J. Dugan and Benjamin Grinstein. On the vanishing of evanescent operators. *Phys. Lett.*, B256:239–244, 1991.

[55] Stefan Herrlich and Ulrich Nierste. Evanescent operators, scheme dependences and double insertions. *Nucl. Phys.*, B455:39–58, 1995.

[56] Andrzej J. Buras, Matthias Jamin, M. E. Lautenbacher, and Peter H. Weisz. Effective Hamiltonians for $\Delta S = 1$ and $\Delta B = 1$ nonleptonic decays beyond the leading logarithmic approximation. *Nucl. Phys.*, B370:69–104, 1992. [Addendum: Nucl. Phys.B375,501(1992)].

[57] Marco Ciuchini, E. Franco, G. Martinelli, and L. Reina. The $\Delta S = 1$ effective Hamiltonian including next-to-leading order QCD and QED corrections. *Nucl. Phys.*, B415:403–462, 1994.

[58] Andrzej J. Buras, Matthias Jamin, Markus E. Lautenbacher, and Peter H. Weisz. Two loop anomalous dimension matrix for $\Delta S = 1$ weak nonleptonic decays I: $\mathcal{O}(\alpha_s^2)$. *Nucl. Phys.*, B400:37–74, 1993.

[59] Andrzej J. Buras, Matthias Jamin, and Markus E. Lautenbacher. Two loop anomalous dimension matrix for $\Delta S = 1$ weak nonleptonic decays II: $\mathcal{O}(\alpha_s^2)$. *Nucl. Phys.*, B400:75–102, 1993.

[60] Marco Ciuchini, E. Franco, G. Martinelli, and L. Reina. ϵ'/ϵ at the Next-to-leading order in QCD and QED. *Phys. Lett.*, B301:263–271, 1993.

[61] Andrzej J. Buras, Matthias Jamin, and Markus E. Lautenbacher. The Anatomy of ϵ'/ϵ beyond leading logarithms with improved hadronic matrix elements. *Nucl. Phys.*, B408:209–285, 1993.

[62] M. Beneke, T. Feldmann, and D. Seidel. Systematic approach to exclusive $B \to Vl^+l^-$, $V\gamma$ decays. *Nucl. Phys.*, B612:25–58, 2001.

[63] Teppei Kitahara, Ulrich Nierste, and Paul Tremper. Singularity-free next-to-leading order $\Delta S = 1$ renormalization group evolution and ϵ'_K/ϵ_K in the Standard Model and beyond. *JHEP*, 12:078, 2016.

[64] M. Cerdà-Sevilla, M. Gorbahn, S. Jager, and A. Kokulu. Towards NNLO accuracy for ε'/ε. *J. Phys. Conf. Ser.*, 800(1):012008, 2017.

[65] Andrzej J. Buras, Paolo Gambino, and Ulrich A. Haisch. Electroweak penguin contributions to nonleptonic $\Delta F = 1$ decays at NNLO. *Nucl. Phys.*, B570:117–154, 2000.

[66] Joachim Brod and Martin Gorbahn. ϵ_K at Next-to-Next-to-Leading Order: The Charm-Top-Quark Contribution. *Phys. Rev.*, D82:094026, 2010.

[67] S. L. Glashow, J. Iliopoulos, and L. Maiani. Weak Interactions with Lepton-Hadron Symmetry. *Phys. Rev.*, D2:1285–1292, 1970.

[68] Tobias Huber, Enrico Lunghi, Mikolaj Misiak, and Daniel Wyler. Electromagnetic logarithms in $\bar{B} \to X_s l^+ l^-$. *Nucl. Phys.*, B740:105–137, 2006.

[69] K. G. Chetyrkin, Johann H. Kuhn, and M. Steinhauser. RunDec: A Mathematica package for running and decoupling of the strong coupling and quark masses. *Comput. Phys. Commun.*, 133:43–65, 2000.

[70] C. Patrignani et al. Review of Particle Physics. *Chin. Phys.*, C40(10):100001, 2016.

[71] V. Cirigliano, G. Ecker, H. Neufeld, and A. Pich. Isospin breaking in $K \to \pi\pi$ decays. *Eur. Phys. J.*, C33:369–396, 2004.

[72] J. R. Batley et al. A Precision measurement of direct CP violation in the decay of neutral kaons into two pions. *Phys. Lett.*, B544:97–112, 2002.

[73] A. Alavi-Harati et al. Measurements of direct CP violation, CPT symmetry, and other parameters in the neutral kaon system. *Phys. Rev.*, D67:012005, 2003. [Erratum: Phys. Rev.D70,079904(2004)].

[74] V. Cirigliano, A. Pich, G. Ecker, and H. Neufeld. Isospin violation in ε'. *Phys. Rev. Lett.*, 91:162001, 2003.

[75] Vincenzo Cirigliano, Gerhard Ecker, Helmut Neufeld, Antonio Pich, and Jorge Portoles. Kaon Decays in the Standard Model. *Rev. Mod. Phys.*, 84:399, 2012.

[76] Christoph Lehner and Christian Sturm. Matching factors for $\Delta S = 1$ four-quark operators in RI/SMOM schemes. *Phys. Rev.*, D84:014001, 2011.

[77] William A. Bardeen, A. J. Buras, and J. M. Gerard. A Consistent Analysis of the $\Delta I = 1/2$ Rule for K Decays. *Phys. Lett.*, B192:138–144, 1987.

[78] Andrzej J. Buras, Jean-Marc Gérard, and William A. Bardeen. Large N Approach to Kaon Decays and Mixing 28 Years Later: $\Delta I = 1/2$ Rule, $\hat{B}_K$ and ΔM_K. *Eur. Phys. J.*, C74:2871, 2014.